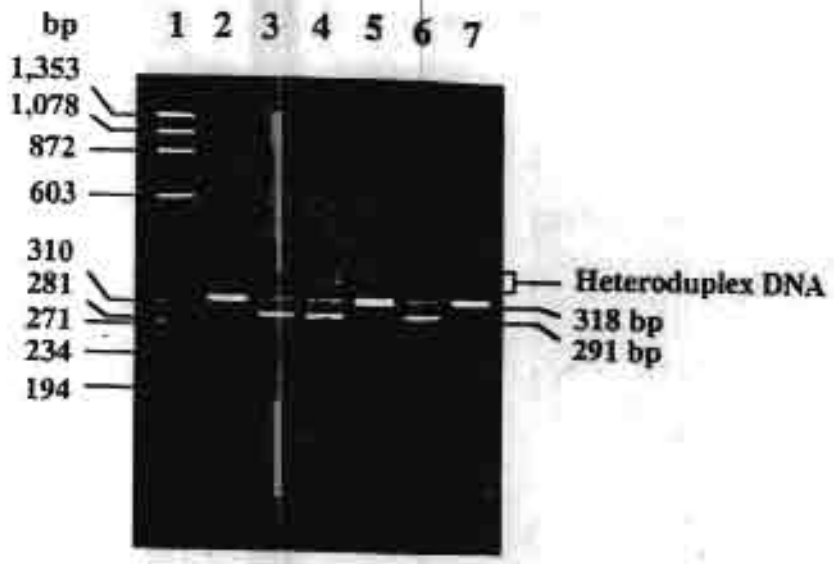

Fig 2. Agarose gel electrophoresis of polymerase chain reaction (PCR) products after amplifications of exon 11 of AE1 gene by PCR using exon 11 specific primers (AE1E×11L/AE1E×11R). Lane 1 is PhiX 174 DNA/HaeIII markers. Lanes 2 through 7 are PCR products resulted from amplifications of DNA samples of a healthy person, an individual with only SAO, patient's father, patient's mother, patient with dRTA and SAO, and patient's younger sister. The normal DNA sample gave PCR product with the size of 318 bp (lane 2), whereas that from the individual with SAO showed PCR products with the sizes of 318 and 291 bp, as well as heteroduplex DNA (lane 3). The DNA samples from the patient's father (lane 4) and the patient (lane 6) produced the PCR products the same as those of the individual with SAO, whereas those from the patient's mother (lane 5) and the patient's younger sister (lane 7) gave the PCR products the same as that of the healthy individual.

the urine P_{CO_2}.[17,24] A similar association has been reported in primary dRTA in an infant not previously exposed to amphotericin B[26] and in a patient with an early stage of primary Sjögren's syndrome[27] who also had the inability to decrease urinary pH in response to furosemide and markedly increased urinary excretion of NH_4^+. For this mechanism to operate, the urine pH must be much greater than the mid-6 range because the highest rates of NH_4^+ excretion occur when the urine pH is in the low-6 range in subjects with chronic metabolic acidosis (NH_4Cl loading,[28] chronic fasting).[29-31] There is a problem relating the urine pH to that in the lumen of the distal nephron when bicarbonate is the principal urine buffer because of the absence of luminal carbonic anhydrase in this nephron segment (for review, see[17,32,33]). As emphasized by Knepper

Table 5. ^{35}S-Sulfate Influx Studies for RBC Anion Transport

	Phenotype	SO_4^{2-} Uptake (10^{-7} mol/L/min/cell)*		
		No DIDS	+1.5 μmol/L DIDS†	%‡
Father	SAO	4.8 ± 0.02§	0.1 ± 0.00	1.1
Mother	Normal	8.1 ± 0.1	3.7 ± 0.5	45.3
Patient	SAO	5.1 ± 0.1	0.1 ± 0.02	1.8
Sister	Normal	7.7 ± 0.3	3.4 ± 0.3	44.8
Mean of 2 SAOs		4.9 ± 0.2	0.1 ± 0.01	1.5 ± 1
Mean of 5 controls		6.3 ± 0.5	4.9 ± 1.5	58.6 ± 12

*Initial rate of sulfate (SO_4^{2-}) uptake of the erythrocyte when incubated at 37°C with 3 mmol/L of [^{35}S] sodium sulfate, 70 mmol/L of sodium citrate, 10 mmol/L of Tris, pH 7.4 buffer.

†The erythrocytes were incubated at 37°C with 1.5 μmol/L of DIDS for 15 minutes before SO_4^{2-} uptake.

‡Percent of rate of SO_4^{2-} uptake, comparing with and without DIDS.

§Mean ± SD in duplicated experiment.

and Good,[34,35] one should expect high local carbonic acid concentrations in luminal fluid, and thus the $[H^+]$ in vivo will be much greater here than in the urine. Therefore, a greater luminal $[H^+]$ in the distal nephron would likely be present with bicarbonaturia and make the gradient limit for H^+ secretion a less likely explanation for the high urine P_{CO_2} in our patient. Third, the normal ability to increase urine P_{CO_2} during a bicarbonate diuresis could be the result of secretion of HCO_3^- by type A intercalated cells in these patients with AE1 abnormality (Fig 1). To explain why HCO_3^- might be secreted by type A intercalated cells, we suggest, as did Bruce et al,[15] that mistargeting of an active AE1 to the apical membrane of the type A intercalated cells might explain a decrease in net H^- (really HCO_3^-) secretion in patients with familial dRTA.[36] We hypothesize that the mutant AE1 protein in our patients was mistargeted to the apical membrane of the type A intercalated cells. The secretion of HCO_3^- would not only cause a high urine P_{CO_2}, but it should also cause an alkaline disequilibrium pH, making it even more difficult to trap ammonia in the luminal compartment. Secretion of HCO_3^- by type B intercalated cells is also a possible mechanism for the normal increased urine P_{CO_2}. Nevertheless, because AE in these cells is a different gene product and is not involved in the SAO abnormality, these cells probably do not have abnormal function in this patient. Moreover, if HCO_3^- were secreted by type B intercalated cells during a sodium bicarbonate load, the urine P_{CO_2} would be increased in most patients with a defect in distal H^+ secretion, but this is not consistent with the published data.[17]

The incidence of metabolic acidosis in SAO patients is low. However, the degree to which the maximum rate of excretion of NH_4^+ is decreased in SAO has never been studied. An incomplete form of dRTA might not produce clinical evidence of acidemia if there is enough capacity to excrete NH_4^+ relative to the acid load of the diet, especially if the subject is not on a high-protein diet. Future studies, including U–B P_{CO_2} measurements, are planned in affected persons with SAO.

The presenting feature in this patient was related to hypokalemia (weakness). Although her daily intake of potassium was not high (42 mmol/L/d), the major reason for her hypokalemia was excessive excretion of potassium (>10 to 15 mmol/L/d, reviewed in [18]). Because her osmole excretion rate was not high, the flow rate in her cortical collecting duct was not excessively high.[37] Hence, a high $[K^+]$ in the lumen of the cortical collecting duct was the principal reason for her high rate of excretion of potassium (TTKG, 7.7 [Table 2], rather than <2[18]). Because her urine consistently contained HCO_3^- (Table 2), perhaps the high TTKG reflected the kaliuretic actions of aldosterone when HCO_3^- remained in the lumen of the CCD because of low distal H^+ secretion, and possibly the secretion of HCO_3^-, as previously suggested.[23,38]

In summary, we report a case in which dRTA occurred in conjunction with SAO. The most likely explanation for the low rate of excretion of NH_4^+ was a low rate of H^+ secretion in the distal nephron, the result of an alkalinized type A intercalated cell consequent to impaired exit of HCO_3^-. There was an unanticipated high value for U–B P_{CO_2}, perhaps the result of secretion of HCO_3^-, which itself could also reduce the net rate of secretion of H^- in the distal nephron. The explanation might be from a mistargeting of the Cl^-/HCO_3^- exchanger to the luminal membrane of the type A intercalated cells.

ACKNOWLEDGMENT

The authors thank Nunghathai Sawasdee for her laboratory assistance.

REFERENCES

1. Mohandas N, Winardi R, Knowles D, Leung A, Parra M, George E, Conboy J, Chasis J: Molecular basis for membrane rigidity of hereditary ovalocytosis. A novel mechanism involving the cytoplasmic domain of band 3. J Clin Invest 89:686-692, 1992

2. Tanner MJA, Bruce L, Martin PG, Reardon DM, Jones DI: Melanesian hereditary ovalocytosis has a deletion in red cell band 3. Blood 78:2785-2787, 1991

3. Schofield AE, Reardon DM, Tanner MJA: Defective anion transport activity of the abnormal band 3 in hereditary ovalocytic red blood cells. Nature 355:836-838, 1992

4. Mohandas N, Lie-injo LE, Friedman M: Rigid membranes of Malayan ovalocytosis. Blood 63:1385-1392, 1984

5. Tanner MJA: Molecular and cellular biology of the erythrocyte anion exchanger (AE1). Semin Hematol 30:34-57, 1993

6. Peters LL, Shivdasani RA, Liu SC, Hanspal M, John KM, Gonzalez JM, Brugnara C, Gwynn B, Mohandas N, Alper SL, Orkin SH, Lux SE: Anion exchanger 1 (band 3) is required to prevent erythrocyte membrane surface loss but not to form the membrane skeleton. Cell 86:917-927, 1996

7. Showe LC, Ballantine M, Huebner K: Localization of the gene for the erythroid anion exchange protein, band 3 (EMPB3), to human chromosome 17. Genomics 1:71-76, 1987

8. Sabolic I, Brown D, Gluck SL, Alper SL: Regulation of AE1 anion exchanger and H+-ATPase in rat cortex by acute metabolic acidosis and alkalosis. Kidney Int 51:125-137, 1997

9. Alper SL, Natale J, Gluck S, Lodish HF, Brown D: Subtypes of intercalated cells in rat kidney collecting duct defined by antibodies against erythroid band 3 and renal vacuolar H+-ATPase. Proc Natl Acad Sci U S A 86:5429-5433, 1989

10. Wingo CS, Cain BD: The renal H,K-ATPase: Physiological significance and role in potassium homeostasis. Annu Rev Physiol 55:323-347, 1993

11. Bachner RL, Gilchrist GS, Anderson EJ: Hereditary elliptocytosis and primary renal tubular acidosis in a single family. Am J Dis Child 115:414-419, 1968

12. Rysava R, Tesar IV, Brabec IV, Jirsa IM, Merta IM, Jarolim P: Renal tubular acidosis associated with mutation in the AE1 gene, in Ritz E (ed): EDTA. Amsterdam, The Netherlands, p 17, 1996

13. Rysava R, Tesar V, Jirsa M, Brabec V, Jarolim P: Incomplete distal renal tubular acidosis coinherited with a mutation in the band 3 (AE1) gene. Nephrol Dial Transplant 12:1869-1873, 1997

14. Cope DL, Bruce LJ, Schofield AE, Unwin RJ, Wrong OM: Altered red cell anion exchanger (band 3, AE1) associated with familial distal renal tubular acidosis, in Grantham J (ed): Twenty-Ninth Annual ASN Meeting. Baltimore, MD, Williams & Wilkins, 1852:3028A, 1996 (abstr)

15. Bruce LJ, Cope DL, Jones JK, Schofield AE, Burley M, Povey S, Unwin RJ, Wrong O, Tanner MJA: Familial distal renal tubular acidosis is associated with mutations in the red cell anion exchanger (band 3, AE1) gene. J Clin Invest 100:1693-1707, 1997

16. Jarolim P, Shayakul C, Prabakaran D, Jiang L, Stuart-Tilley A, Rubin H, Simova S, Zavadil J, Herrin JT, Brouillette J, Somers MJG, Seemanova E, Brugnara C, Guay-Woodford LM, Alper SL: Autosomal dominant distal renal tubular acidosis is associated in three families with heterozygosity for the R589H mutation in the AE1(band 3) Cl^-/HCO_3^- exchanger. J Biol Chem 273:6380-6388, 1998

17. Halperin ML, Goldstein MB, Haig A, Johnson MD, Stinebaugh BJ: Studies on the pathogenesis of type I (distal) renal tubular acidosis as revealed by urine pCO_2 tensions. J Clin Invest 53:669-677, 1974

18. Ethier J, Kamel K, Magner P, LemannJJ, Halperin ML: The transtubular potassium concentration in patients with hypokalemia and hyperkalemia. Am J Kidney Dis 15:309-315, 1990

19. Jarolim P, Palek J, Amato D, Hassan K, Sapak P, Nurse GT, Rubin HL, Zhai S, Sahr KE, Liu SC: Deletion in erythrocyte band 3 gene in malaria-resistant southeast Asian ovalocytosis. Proc Natl Acad Sci U S A 88:11022-11026, 1991

20. Kamel KS, Briceno LF, Sanchez ML, Brenes L, Yorgin P, Kooh SW, Balfe W, Halperin ML: A new classification for renal defects in net acid excretion. Am J Kidney Dis 29:136-146, 1997

21. Vasuvattakul S, Gougoux A, Halperin ML: A method to evaluate renal ammoniagenesis in vivo. Clin Invest Med 16:265-273, 1993

22. Rastogi S, Crawford C, Wheeler R, Flanigan W, Arruda JAL: Effect of furosemide on urinary acidification in distal renal tubular acidosis. J Lab Clin Med 104:271-282, 1984

23. Carlisle EJF, Donnelly SM, Halperin ML: Renal tubular acidosis (RTA): Recognize the ammoniuum defect and pH or get the urine pH. Pediatr Nephrol 5:242-248, 1991

24. Dubose TJ, Caflisch C: Validation of the difference in urine and blood carbon dioxide tension during bicarbonate loading as an index of distal nephron acidification in experimental models of distal renal tubular acidosis. J Clin Invest 75:1116-1123, 1985

25. Steinmetz PR, Anderson OS: Electrogenic proton transport in epithelial membranes. J Membrane Biol 65:155-174, 1982

26. Bonilla-Felix M: Primary distal renal tubular acidosis as a result of a gradient defect. Am J Kidney Dis 27:428-430, 1996

27. Zawadzki J: Permeability defect with bicarbonate leak as a mechanism of immune-related distal renal tubular acidosis. Am J Kidney Dis 31:527-532, 1998

28. Madison LL, Seldin DW: Ammonia excretion and renal enzymatic adaptation in human subjects, as disclosed by administration of precursor amino acids. J Clin Invest 37:1615-1627, 1958

29. Schloeder FX, Stinebaugh BJ: Urinary ammonia content as a determinant of urinary pH during chronic metabolic acidosis. Metabolism 26:1321-1331, 1977

30. Rapoport A, From GLA, Husdan H: Metabolic studies in prolonged fasting. I. Inorganic metabolism and kidney function. Metabolism 14:31-46, 1965

31. Kamel KS, Lin S-H, Cheema-Dhadli S, Marliss EB, Halperin ML: Prolonged total fasting: A feast for the integrative physiologist. Kidney Int 53:531-539, 1998

32. Berliner RW, Dubose TDJ: Carbon dioxide tension of alkaline urine, in Seldin DW, Giebisch G (eds). The Kidney, Physiology and Pathophysiology. New York, NY, Raven, 1992, pp 2681-2694

33. Maren T: Carbon dioxide equilibria in the kidney: The problems of elevated carbon dioxide tension, delayed dehydration, and disequilibrium pH. Kidney Int 14:395-405, 1978

34. Knepper MA, Good DW, Burg MB: Mechanisms of ammonia secretion by cortical collecting ducts of rabbits. Am J Physiol 247:F729-F738, 1984

35. Knepper MA, Good DW, Burg MB: Ammonia and bicarbonate transport by rat cortical collecting ducts perfused in vitro. Am J Physiol 249:F870-F877, 1985

36. Schwartz GJ, Barasch J, Awqati AL: Plasticity of functional epithelial polarity. Nature 318:368-371, 1985

37. Steele A, deVeber H, Quaggin SE, Scheich A, Ethier J, Halperin ML: What is responsible for the diurnal variation in potassium excretion? Am J Physiol 36:R554-R560, 1994

38. Lin SH, Cheema-Dhadli S, Gowrishankar M, Marliss EB, Kamel KS, Halperin ML: Control of the excretion of potassium: Lessons from studies during prolonged fasting in human subjects. Am J Physiol 273:F796-F800, 1997

Long RT-PCR Amplification of the Entire Coding Sequence of the Polycystic Kidney Disease 1 (*PKD1*) Gene

BioTechniques 26:126-132 (January 1999)

Wanna Thongnoppakhun[1,2], Prapon Wilairat[2], Kriengsak Vareesangthip[1] and Pa-thai Yenchitsomanus[1]

[1]Faculty of Medicine-Siriraj Hospital, [2]Faculty of Science, Mahidol University, Bangkok, Thailand

ABSTRACT

Characterization of mutations of the PKD1 *gene has been limited by the fact that three-fourths of this gene at its 5′ end is homologous to sequences of at least three other genes on the same chromosome. We have therefore developed a method of long reverse transcription PCR for selective amplification of the entire coding sequence of the* PKD1 *gene from its mRNA. A PCR primer specific to the sequence in the 3′ unique region of the* PKD1 *gene was synthesized for use coupled with a primer binding to sequence in the homologous region at a distance of about 13.6 kb apart. The commercial availability of RNase H-free reverse transcriptase for long cDNA synthesis and of an enzyme mixture containing* Taq *and* Pfu *DNA polymerases for long-range PCR have made this development possible. The long PCR product was proven to be derived from* PKD1*-mRNA. The results clearly indicated that the long PCR product contained the coding sequence derived from* PKD1*-mRNA. To our knowledge, this is the first report of a procedure that can reproducibly isolate full-length* PKD1 *coding sequence from its mRNA transcript, which will prove useful for screening and characterization of mutations in the* PKD1 *gene.*

INTRODUCTION

Characterization of mutations of a gene responsible for a human genetic disease requires the availability of its entire coding and genomic sequences. The polycystic kidney disease 1 (*PKD1*) gene, which has the size of approximately 52 kb containing 46 exons and encoding a 14-kb transcript (5,11,32) and whose defects account for about 85% of autosomal dominant polycystic kidney disease (ADPKD) cases (23), is one of the genes that are most difficult to isolate and identify (5,11,31,32). This is because of the presence of at least three highly homologous sequences of genes mapped more proximally on the same chromosome at the 16p13.1 region (31). Three-fourths of the *PKD1* gene, located in the 5′ part extending to a length of approximately 40 kb of DNA, is duplicated. The three homologous genes (*HG*) encoding transcripts with sizes of 21 (*HG-A*), 17 (*HG-B*) and 8.5 kb (*HG-C*) share about 97% identity with the reiterated part of the *PKD1* gene. The only region of the *PKD1* gene that is different from its homologs is a 10-kb sequence at its 3′ end, encoding a part of the transcript (3.5 kb) covering exons 33–46; whereas, all of the homologs have similar 3′ regions (31). This has made *PKD1* gene isolation, identification and mutation analysis very difficult. Most of the mutations observed so far in the *PKD1* gene are clustered around the unique 3′ region of the gene, which is the only easily accessible region (3,17,19,21,22,27,31,33–35). Therefore, the detection rate of mutation is only 10%–15% of the cases analyzed, and all of them are different, indicating that there is no mutational "hot-spot" area. It is believed that most of *PKD1* gene mutations occur in the duplicated region (22).

The mRNA transcripts of several genes are present from their illegitimate or ectopic transcriptions in human peripheral blood lymphocytes (6), and these mRNAs are correctly processed; although, their levels are extremely low (28). The *PKD1*-mRNA has also been found to be present in human lymphocytes (17,25–27,33,34). Many research groups have attempted to isolate the coding sequence of the *PKD1* gene from its mRNA transcript by reverse transcription polymerase chain reaction (RT-PCR) (17,19–22,25–27,31,33,34), but only partial coding sequences were obtained with a maximum size of 2440 bp. Until now, to our knowledge, there is no report on a method for isolation of the entire coding sequence of the *PKD1* gene from its mRNA transcript. Limitations of the previous RT-PCR techniques have resulted from both the inability of reverse transcriptase to synthesize full-length cDNAs and from the failure of *Taq* DNA polymerase to efficiently amplify more than 4 kb of DNA fragment. Recently, the commercial availability of genetically engineered reverse transcriptases that lack RNase H activity allows the synthesis of full-length cDNA from a long mRNA (16). Furthermore, modified PCR conditions using the combination of *Taq* and *Pfu* DNA polymerases that contain proofreading activity have made it possible to amplify long DNA targets (1,7).

Table 1. Nucleotide Sequences of PCR Primers for the Long RT-PCR and Nested PCR of *PKD1* Gene

Primer	Primer Sequences (5'→3') (nucleotide position[a])	PCR Product Size (bp)	Annealing Temperature (°C)
TH1F	CTG GGG ACG GCG GGG CCA TGC G (nt 175–196)	13634	68
TH1B	GGC CTG GGG CAA GGG AGG ATG ACA A (nt 13808–13784)		
SI2F	AGG AGC CTA GAC GTG TGG ATC G (nt 1595–1616)	1678	65
SI2B	CCT GCA TCC TGT TCA TCC GCT C (nt 3272–3251)		
SI4F	ATC TCT GCT GCC AAT GAC TCA G (nt 4562–4583)	1473	60
SI4B	GGG GAA GCT GTG GGA GAA AC (nt 6034–6015)		
SI9F	CTT CAG CAC CAG CGA TTA CGA CGT T (nt 11533–11557)	1650	65
SI9B	AGA AAG TAA TAC TGA GCG GTG TCC ACT C (nt 13182–13155)		

[a]The nucleotide positions are according to HUMPKD1A, GenBank Accession No. L33243 by Hughes et al. (11).

In this paper, we report a long RT-PCR method for amplification and isolation of the entire coding sequence of the *PKD1* gene from its mRNA transcript. Advantage was taken of the unique sequence at the 3′ region of the *PKD1* gene (and hence in its mRNA transcript) to design a PCR primer for selective amplification by PCR. This long PCR product with the length of 13634 bp was analyzed and shown to contain the full-length coding sequence of the *PKD1* gene, which could be used for screening, characterization of mutations and other types of studies.

MATERIALS AND METHODS

Peripheral Blood Samples and Lymphocyte Preparation

Blood samples were taken from 21 normal individuals and 15 ADPKD patients with prior informed consent. Approximately 15 mL of peripheral blood were collected into a tube containing EDTA-disodium salt as anticoagulant. Lymphocytes were prepared from peripheral blood samples by Ficoll Hypaque® gradient centrifugation using Lymphoprep™ (Nycomed Pharma AS, Oslo, Norway).

RNA Isolation

Total RNA was isolated from peripheral blood lymphocytes by using TRIzol® reagent (Life Technologies, Gaithersburg, MD, USA), following the manufacturer's instruction, with careful and gentle handling to preserve the integrity of long mRNA required. RNA pellet obtained in the final step was dissolved in 50 µL of sterile diethyl pyrocarbonate (DEPC)-treated water. RNA solution was diluted, and its concentration was determined from optical density $(OD)_{260}$ readings that were measured by a UV spectrophotometer. RNA was kept in DEPC-treated water at -70°C. For long-term storage, RNA was precipitated and kept in 75% ethanol at -70°C.

PCR Primers

Sequence of *PKD1*-mRNA (HUMPKD1A, Accession No. L33243) was retrieved from the Entrez database (GenBank®). PCR primers were designed by using the MacVector™ 4.5.1 Program (Scientific Imaging Systems [Eastman Kodak], New Haven, CT, USA) and OLIGO® Version 4.03 Primer Analysis Software (National Biosciences, Plymouth, MN, USA). The primers used for long RT-PCR (TH1F/TH1B), flanking the open reading frame (ORF) of *PKD1* (12906 bp), were designed and selected with the additional criterion that their melting temperatures (T_ms) were high enough to be able to perform PCR with two-step cycling conditions that combine annealing and extension steps at 68°C. The backward (TH1B) primer is specific to the 3′ unique sequence in the *PKD1* transcript; whereas, the forward (TH1F) primer is specific to the sequence in the reiterated region (Figure 1). Three pairs of primers for nested PCRs (SI2F/SI2B, SI4F/SI4B and SI9F/SI9B) were designed to amplify two regions in the homologous and one region in the unique sequences (Figure 1). These primers were custom-synthesized by BioService Unit, National Center for Biotechnology and Genetic Engineering (BIOTEC), National Science and Technology Development Agency (NSTDA), Bangkok, Thailand. Table 1 shows the sequences of PCR primers.

Synthesis of Full-Length cDNA

Full-length cDNA was synthesized by the reaction of RNase H-free reverse transcriptase and by using oligo$(dT)_{12-18}$ primer. An aliquot of total RNA (1–5 µg) was used for cDNA synthesis. The reaction mixture in a total volume of 21 µL contained 20 mM Tris-HCl (pH 8.4), 50 mM KCl, 2.5 mM $MgCl_2$, 500 µM dNTP mixture, 10 mM dithiothreitol (DTT), 0.5 µg of oligo$(dT)_{12-18}$ and 200 U of RNase H-free SUPERSCRIPT™ II RT (Life Technologies). RNasin® Ribonuclease Inhibitor (Promega, Madison, WI, USA) (30 U) was also added to protect mRNA template. The cDNA synthesis was performed at 42°C for 75 min and terminated by incubation at 70°C for 15 min.

Then, 2 U of RNase H (Life Technologies) were added, and the reaction mixture was incubated at 37°C for 20 min.

Long PCR

The full-length *PKD1*-cDNA sequence was amplified by long PCR using a pair of primers flanking the *PKD1*-ORF (TH1F/TH1B). The cDNA was amplified by using ELONGASE™ Enzyme Mix (Life Technologies) following the manufacturer's instructions. The enzyme mixture included thermostable *Taq* and *Pfu* DNA polymerases; the latter has proofreading activity, which reduces error rate of DNA synthesis. The reaction mixture (50 µL) contained 2 µL of cDNA, 1 U of ELONGASE Enzyme Mix, 60 mM Tris-SO_4 (pH 9.1), 18 mM $(NH_4)_2SO_4$, 1.2 mM $MgSO_4$, 200 µM dNTP mixture, 10% dimethyl sulfoxide (DMSO) and 200 nM of each primer.

A hot start at 95°C for 1 min and 30 s was performed before adding the enzyme mixture. PCR was carried out for 30 cycles in a GeneAmp® PCR System 2400 (PE Applied Biosystems, Foster City, CA, USA). Each cycle consisted of denaturation at 94°C for 15 s and a combined step of annealing and extension at 68°C for 15 min. A final extension step was carried out at 70°C for 10 min. The long RT-PCR product was analyzed by electrophoresis on 0.8% agarose gel in 0.5× TBE buffer (0.045 M Tris-borate, 0.001 M EDTA, pH 8.3) and visualized after staining by ethidium bromide.

Restriction Endonuclease Analysis of Long PCR Product

Restriction endonuclease sites in the *PKD1*-mRNA sequence were first analyzed by the MacVector™ 4.5.1 computer program. The restriction endonuclease digestions were performed by taking 20-µL aliquots of the long RT-PCR product and adding the following: *(i)* 20 U of either *Bam*HI, *Kpn*I or *Xho*I enzymes (Promega), *(ii)* a suitable buffer as supplied by the manufacturer and *(iii)* 0.1 µg/mL of bovine serum albumin (BSA) in a final volume of 30 µL. The reaction mixtures were incubated at 37°C for 2 h. The restriction fragments were then resolved by electrophoresis on 1% agarose gel followed by ethidium bromide staining.

Nested PCR

To reduce nonspecific amplifications caused by excessive templates, the long PCR product was diluted 100–1000-fold before amplification with each pair of primers in nested PCR. The nested PCR mixture (25 µL) contained 10 mM Tris-HCl (pH 8.3), 50 mM KCl, 1.5 mM $MgCl_2$, 200 µM dNTPs, 10% DMSO, 400 nM of each primer and 0.625 U of AmpliTaq Gold™ (PE Applied Biosystems). After an initial denaturation at 95°C for 10 min, 25 PCR cycles were performed as follows: *(i)* denaturation at 95°C for 20 s, *(ii)* annealing at 60°C for 20 s and *(iii)* extension at 72°C for 1 min and 30 s, followed by another 10 min of extension at 72°C in the final step. The sizes of nested PCR products were analyzed by electrophoresis on a 1.2% agarose gel in TBE buffer with ethidium bromide staining.

Direct Sequencing of Nested PCR Products

The nested PCR products were purified from gel by using the QIAquick™ Gel Extraction Kit (Qiagen GmbH, Hilden, Germany), following the manufacturer's instructions. Their sequences were determined by the manual direct-sequencing method using the AmpliCycle™ Sequencing Kit (PE Applied Biosystems).

RESULTS

We have developed a long RT-PCR method to isolate the entire coding region of the *PKD1* gene from its mRNA

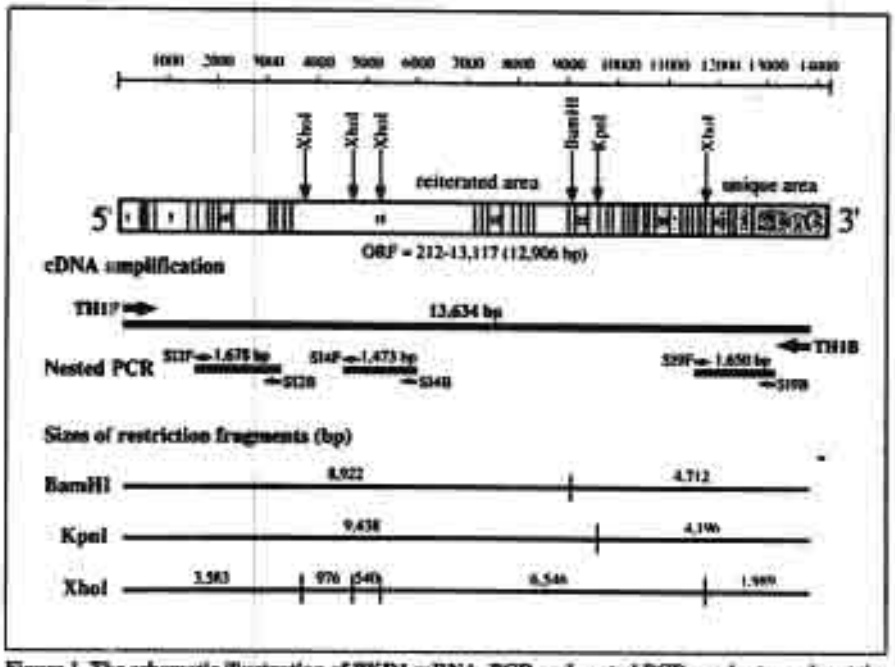

Figure 1. The schematic illustration of PKD1 mRNA, PCR and nested PCR products, and restriction fragments. The entire mRNA containing sequences of exons 1–46 is represented by horizontal bar. The boundaries of exons in the mRNA are indicated by vertical lines, and exon numbers are given for some exons. The ORF consisting of 12906 bp is located between the nt positions 212 and 13117 (HUMPKD1A; GenBank Accession No. L33243; Reference 11). The light shade area (between exons 1 and 32) represents the reiterated region, which is highly homologous to sequences in at least three other genes on the same chromosome. The darker shade area (between exons 33 and 46) represents the 3' unique region. Sites of restriction endonucleases *Bam*HI, *Kpn*I and *Xho*I, used to digest *PKD1* cDNA, are indicated by vertical arrows above the bar of mRNA, and the lower part of the figure shows sizes of fragments after digestions with the restriction enzymes. The extents of long PCR products are represented by solid lines under the bar of mRNA and of nested PCR products by solid lines under the long PCR product. Locations and directions of oligonucleotide primers for long PCR and nested PCR are indicated as solid horizontal arrows.

transcript that was prepared from peripheral blood lymphocytes. The first-strand cDNA synthesis was primed by oligo(dT)$_{12-18}$. The cDNA was subjected to amplification by using the forward (TH1F) primer specific to the reiterated region and the backward (TH1B) primer specific to the unique sequence in the coding region of *PKD1* transcript. The expected PCR product amplified by this pair of primers would be 13 634 bp in length (Figure 1). The conditions for long RT-PCR were optimized by varying amounts of RNA, concentrations of $MgSO_4$ and numbers of PCR cycles. The technique described herein can efficiently amplify the long PCR product by using 1–5 μg of good-quality total RNA. Amounts of RNA greater than 9 μg were found to be less efficient in generating the long PCR product. The optimal conditions for long cDNA synthesis and PCR are described in Materials and Methods.

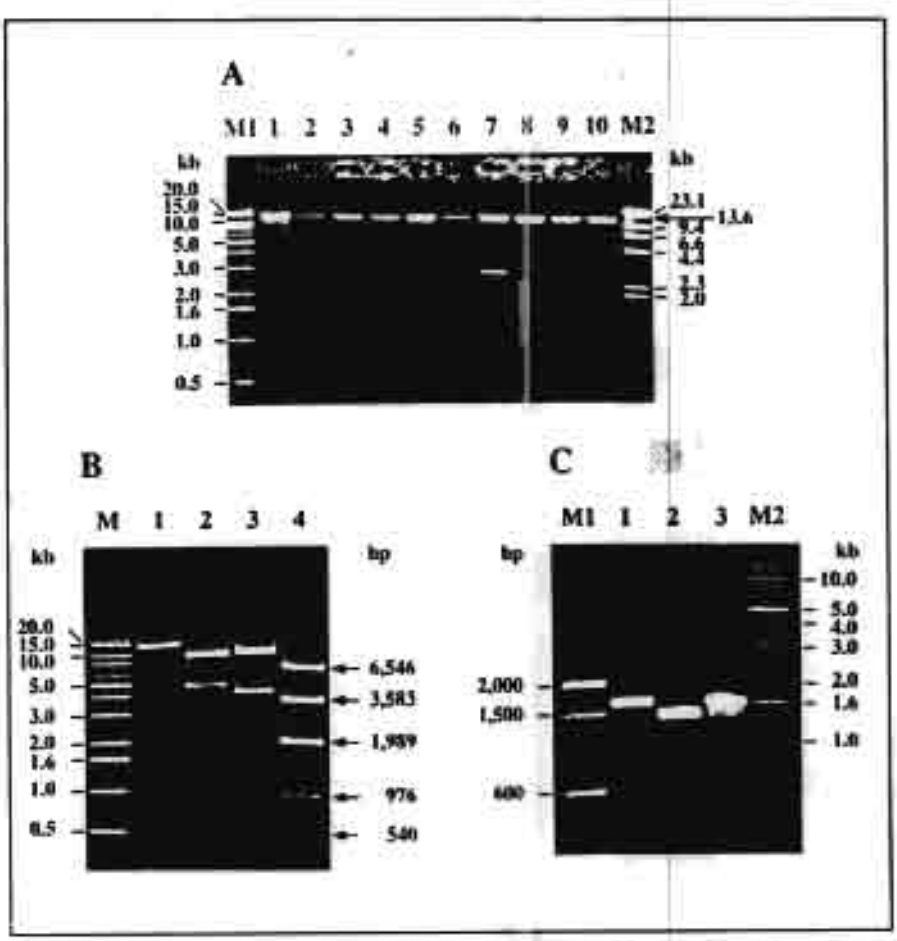

Figure 2. (A) Agarose gel-electrophoresis of PCR products from amplification of the entire coding sequence of the *PKD1* gene from its mRNA by the long RT-PCR method. Lanes M1 and M2 are 1-kb DNA Extension Ladder and λDNA/*Hin*dIII markers (Life Technologies), respectively. Lanes 1 and 2 are PCR products from samples of normal individuals. Lanes 3–10 are PCR products from samples of patients with ADPKD. The PCR product with the size of about 13.6 kb was detected in all samples. A smaller product with the size of <3 kb, present in lane 7, was also irregularly observed in other samples from both normal individuals and patients; it is possibly a nonspecific PCR product. (B) Gel electrophoresis of restriction fragments of the long PCR product. Lane M is 1-kb DNA Extension Ladder. Lane 1 is undigested PCR product. Lanes 2–4 are products after digestions with *Bam*HI, *Kpn*I and *Xho*I, respectively. Digestions of the long PCR product with *Bam*HI (lane 2) and *Kpn*I (lane 3) resulted in two restriction fragments with the lengths of 8922 and 4712 bp, and of 9438 and 4196 bp, respectively, and with *Xho*I (lane 4), five restriction fragments with the lengths of 6546, 3583, 1989, 976 and 540 bp. (C) Agarose gel-electrophoresis of nested PCR products from amplifications of the long PCR product by using three sets of *PKD1*-specific primers. Lanes M1 and M2 are 100-bp DNA Ladder and 1-kb DNA Extension Ladder, respectively. Lanes 1–3 are the nested PCR products from amplifications of the long PCR product with three sets of primers, SI2F/SI2B, SI4F/SI4B and SI9F/SI9B, resulting in DNA fragments sizes of 1678, 1473 and 1650 bp, respectively.

We have successfully tested this procedure with RNA samples that were prepared from peripheral blood lymphocytes of 21 normal individuals and 15 patients with ADPKD. Figure 2A shows part of the data.

To prove that the long PCR product contained *PKD1* coding sequence, we initially analyzed restriction endonuclease sites known to be present in the sequence of *PKD1* mRNA in the long PCR product. The three restriction enzymes selected for this analysis were *Bam*HI, *Kpn*I and *Xho*I, which have 1, 1 and 4 sites, respectively, in the *PKD1* coding sequence (Figure 1). The predicted sizes of fragments after digestions of the *PKD1* coding sequence with the restriction enzymes were 8922 and 4712 bp for *Bam*HI, 9438 and 4196 bp for *Kpn*I and 3583, 976, 540, 6546 and 1989 bp for *Xho*I (see Figure 1). When the long PCR product that was prepared from a normal RNA sample was digested with the three selected enzymes, it was found that the digested DNA fragments had predicted lengths (Figure 2B).

To further prove the authenticity of the long-PCR product, DNA fragments were amplified by nested PCR using 3 pairs of primers (SI2F/SI2B, SI4F/SI4B and SI9F/SI9B) that were specific to sequences in the reiterated and unique regions of the *PKD1*-mRNA transcript (Figure 1) to observe whether the PCR products with expected sizes would be produced or not. The expected lengths of the nested PCR products amplified by these three pairs of primers were 1678, 1473 and 1650 bp, respectively (Figure 1). In this experiment, when the long PCR product was amplified without dilution, both larger PCR products on a smear of background and also product with the expected length were obtained. The larger PCR products and smear seemed to result from excessive DNA templates. Amplifications of the homologous sequences would produce single-stranded products and their amounts should be minute since the backward primer in the primary PCR (TH1B) was specific only to the 3′ unique sequence of the *PKD1* gene. Serial dilution of the long PCR product from 10–10000-fold was performed to reduce the template before using it in the nested PCRs. We found that 100–1000-fold dilutions of the primary PCR product generated the best results. Less dilution still produced nonspecific products, and more dilution resulted in less or no specific products. The results showed that the three nested PCR products had the lengths as expected (Figure 2C).

Finally, to verify that the long PCR product was derived from *PKD1* mRNA, we performed direct sequencing of the three nested PCR products amplified by the three pairs of primers (SI2F/SI2B, SI4F/SI4B and SI9F/SI9B). The nucleotide sequences thus determined were identical to the corresponding regions in the *PKD1* transcript. The nucleotide sequences obtained were located between the positions 1633–1841 (209 nucleotides [nt]), 4610–4709 (100 nt) and 11575–11699 (125 nt) in the *PKD1* mRNA (with reference to the sequence of HUMPKD1A; GenBank Accession No. L33243; Reference 11) (data not shown).

DISCUSSION

The main problem that has delayed progress in studies of the *PKD1* gene is the presence of homologous sequences in at least three potentially active genes on the same chromosome, which interfere with isolation of both the gene and its transcript. We first attempted to isolate *PKD1*-mRNA, which was ectopically transcribed in peripheral blood lymphocytes, by capture with a biotinylated specific-oligonucleotide probe and streptavidin-coated magnetic beads. However, this was unsuccessful, probably because of a minute amount of the *PKD1* transcript present in the peripheral blood lymphocytes. We have therefore developed a long RT-PCR method to selectively amplify the entire coding sequence of the *PKD1* gene from its transcript, by using one PCR primer specific to the sequence in the 3′ unique region of the *PKD1* gene together with the primer specific to the sequence located within the reiterated area at a distance of 13634 bp. The long RT-PCR method could successfully amplify the entire coding sequence of *PKD1* gene from its mRNA. The long RT-PCR product was proven to be derived from *PKD1*-mRNA by demonstrating the presence of *(i)* identical restriction endonuclease maps, *(ii)* correct sizes of the nested PCR products and *(iii)* identical nucleotide sequences in three separated regions.

Although nucleotide sequences of the three homologous genes (*HG-A*, *HG-B* and *HG-C*) have not been available for comparison with the sequences obtained from sequencing experiments, the presence of 100% identity between sequences analyzed in the three regions (altogether 434 nt) with those of the corresponding regions in the reference *PKD1* mRNA confirms that the sequence of amplified product is the bona fide *PKD1* sequence. The most compelling evidence is the absolute identity of the 125-nt sequence of the nested PCR product from the unique region, amplified by SI9F/SI9B primers, to the corresponding region in the reference *PKD1* mRNA.

Many research groups have previously attempted to isolate the coding sequence of the *PKD1* gene from its mRNA for characterization of mutations. However, this was mainly successful in isolation of its unique sequence in the 3′ region (17,19,21,22, 27,31,33–35). Three groups could carry out amplifications of the unique sequence in the 3′ region (between exons 33–46) and part of the reiterated region (located before exons 32) of the *PKD1* gene. Roelfsema et al. (26) isolated the *PKD1* coding sequence from its mRNA prepared from peripheral blood lymphocytes by cDNA synthesis and amplifications of eleven overlapping fragments (each fragment of less than 1 kb) covering 6336 bp (between exons 16 and 46), and seven out of eight novel mutations were identified in the repeated part of the *PKD1* gene. Peral et al. (20) developed an anchored RT-PCR to amplify the *PKD1* coding sequence from its mRNA isolated from lymphoblastoid cell lines, using one primer situated within the single-copy region and one within the reiterated area to identify mutations in the duplicated region. The size of longest PCR product that could be isolated was 2440 bp, extending from exons 22–34 in the *PKD1* transcript, and six out of eleven mutations were identified within the duplicated region. A long-range PCR using a primer specific to the unique region was developed by Watnick et al. (36) to

amplify the *PKD1* gene spanning 10 kb (between exons 23–34) from genomic DNA. Although the methods of these workers could amplify parts of the sequence in the duplicated region, the entire coding sequence of the *PKD1* gene was not obtained.

To our knowledge, the long RT-PCR method developed in this report is the only one that could successfully and reproducibly generate the entire coding sequence of the *PKD1* gene as a single PCR product from the mRNA that was prepared from peripheral blood lymphocytes. This method is rapid—the whole process can be finished within 15 h.

The full-length *PKD1* coding sequence generated by long RT-PCR can be used for cloning or mutation analysis. Some mis-incorporations or errors might be introduced during generation of the full-length *PKD1* cDNA by the long RT-PCR method. However, the use of a mixture of *Taq* and *Pfu* DNA polymerases would alleviate this problem since *Pfu* polymerase contains proofreading activity (1). The clone containing full-length *PKD1* cDNA generated by the long RT-PCR method should be thoroughly evaluated by complete sequence analysis before using it in other work or further study. In cloning complete cDNAs generated from genomes of three RNA viruses including tick-borne encephalitis (10), hepatitis A (30) and hepatitis C (24) by the long RT-PCR method similar to the one described in this work, it was found that the cDNA clones had characteristics of the original genomes, confirming the high fidelity of cDNA generation by the long RT-PCR method.

The long RT-PCR method for analyzing *PKD1* mutations can be of limited usefulness in some cases in which mutations diminish the quantity of *PKD1* mRNA (14); although, the normal and stable expression of mutant alleles at the mRNA level has been observed in peripheral blood lymphocytes (17,25,27,33), cell lines and tissues (22,31). Analysis of mRNA for *PKD1* mutations can have an advantage over analysis from the *PKD1* gene, because mutations that cause abnormal RNA processing (such as exon skipping, RNA deletion or insertion) could also be detected (20,31). However, one should be aware of aberrantly spliced transcripts that can be unrelated to hereditary defects and can complicate detection and analysis of truly abnormal transcripts (2,13). Therefore, the mutations causing abnormal RNA processing must be demonstrated.

The entire coding sequence of the *PKD1* gene that was amplified and isolated by the long RT-PCR method can be used for screening mutations by the following methods: *(i)* single-strand conformation polymorphisms (SSCP) (18), *(ii)* heteroduplex analysis (HA) (12), *(iii)* denaturing gradient gel electrophoresis (DGGE) (9), *(iv)* ribonuclease (RNase) cleavage (15), *(v)* chemical cleavage of mismatch (CCM) (8), *(vi)* dideoxy fingerprinting (ddF) (29) and *(vii)* cleavage fragment-length polymorphism (CFLP) (4). The study of mutations of the *PKD1* gene will provide insight into the functions of polycystin and its peptide domains, the molecular pathogenesis of ADPKD and the effect(s) of the mutations on clinical phenotypes of the patients.

ACKNOWLEDGMENTS

We are grateful to Dr. Chintana Sirinavin, the Head of both the Division of Medical Genetics, Department of Medicine and of the Molecular Genetics Unit, Office for Research and Development, Faculty of Medicine-Siriraj Hospital, Mahidol University for initiating research on ADPKD and for support to this activity. We also thank Dr. Prida Malasit, the Head of the Medical Molecular Biology Unit, Office for Research and Development for allowing us to use laboratory facilities, the staff of the Renal Unit, Department of Medicine, Faculty of Medicine-Siriraj Hospital for taking blood samples from the ADPKD patients and all the patients and laboratory personnel who donated the blood samples. This work was partly supported by a grant from Siriraj-China Medical Board.

REFERENCES

1. **Barnes, W.M.** 1994. PCR amplification of up to 35-kb DNA with high fidelity and high yield from lambda bacteriophage templates. Proc. Natl. Acad. Sci. USA *91*:2216-2220.
2. **Berg, L.P., J.M. Soria, C.J. Formstone, M.**

Morell, V.V. Kukkar, X. Estivill, N. Sala and D.N. Cooper. 1996. Aberrant RNA splicing of the protein C and protein S genes in healthy individuals. Blood Coagul. Fibrinolysis 7:625-631.

3. Brook-Carter, P.T., B. Peral, C.J. Ward, P. Thompson, J. Hughes, M.M. Maheshwar, M. Nellist, V. Gamble, P.C. Harris and J.R. Sampson. 1994. Deletion of the TSC2 and PKD1 genes associated with severe infantile polycystic kidney disease—a contiguous gene syndrome. Nature Genet. 8:328-332.

4. Brow, M.A., M.C. Oldenburg, V. Lyamichev, L.M. Heisler, N. Lyamicheva, J.G. Hall, N.J. Eagan, D.M. Olive, L.M. Smith, L. Fors and J.E. Dahlberg. 1996. Differentiation of bacterial 16S rRNA genes and intergenic regions and *Mycobacterium tuberculosis katG* genes by structure-specific endonuclease cleavage. J. Clin. Microbiol. 34:3129-3137.

5. Burn, T.C., T.D. Connors, W.R. Dackowski, L.R. Petry, T.J. Van Raay, J.M. Millholland, M. Venet, G. Millier, R.M. Hakim, G.M. Landes et al. 1995. Analysis of the genomic sequence for the autosomal dominant polycystic kidney disease (PKD1) gene predicts the presence of a leucine-rich repeat. The American PKD1 Consortium (APKD1 Consortium). Hum. Mol. Genet. 4:575-582.

6. Chelly, J., J.P. Concordet, J.C. Kaplan and A. Kahn. 1989. Illegitimate transcription: transcription of any gene in any cell type. Proc. Natl. Acad. Sci. USA 86:2617-2621.

7. Cheng, S., C. Fockler, W.M. Barnes and R. Higuchi. 1994. Effective amplification of long targets from cloned inserts and human genomic DNA. Proc. Natl. Acad. Sci. USA 91:5695-5699.

8. Cotton, R.G., N.R. Rodrigues and R.D. Campbell. 1988. Reactivity of cytosine and thymine in single-base-pair mismatches with hydroxylamine and osmium tetroxide and its application to the study of mutations. Proc. Natl. Acad. Sci. USA 85:4397-4401.

9. Fischer, S.G. and L.S. Lerman. 1983. DNA fragments differing by single base-pair substitutions are separated in denaturing gradient gels: correspondence with melting theory. Proc. Natl. Acad. Sci. USA 80:1579-1583.

10. Gritsun, T.S. and E.A. Gould. 1995. Infectious transcripts of tick-borne Encephalitis virus, generated in days by RT-PCR. Virology 214:611-618.

11. Hughes, J., C.J. Ward, B. Peral, R. Aspinwall, K. Clark, J.L. Sanmillan, V. Gamble and P.C. Harris. 1995. The polycystic kidney disease 1 (PKD1) gene encodes a novel protein with multiple cell recognition domains. Nature Genet. 10:151-160.

12. Keen, J., D. Lester, C. Inglehearn, A. Curtis and S. Bhattacharya. 1991. Rapid detection of single base mismatches as heteroduplexes on Hydrolink gels. Trends Genet. 7:5.

13. Kohonen-Corish, M., V.L. Ross, W.F. Doe, D.A. Kool, E. Edkins, L. Faragher, J. Wijnen, P.M. Khan, F. Macrae and D.J. St. John. 1996. RNA-based mutation screening in hereditary nonpolyposis colorectal cancer. Am. J. Hum. Genet. 59:818-824.

14. McIntosh, I., A. Hamosh and H.C. Dietz. 1993. Nonsense mutations and diminished mRNA levels. Nature Genet. 4:219.

15. Myers, R.M., Z. Larin and T. Maniatis. 1985. Detection of single base substitutions by ribonuclease cleavage at mismatches in RNA:DNA duplexes. Science 230:1242-1246.

16. Nathan, M., L.M. Mertz and D.K. Fox. 1995. Optimizing long RT-PCR. Focus 17:78-80.

17. Neophytou, P., R. Constantinides, A. Lazarou, A. Pierides and C.C. Deltas. 1996. Detection of a novel nonsense mutation and an intragenic polymorphism in the PKD1 gene of a cypriot family with autosomal dominant polycystic kidney disease. Hum. Genet. 98:437-442.

18. Orita, M., H. Iwahana, H. Kanazawa, K. Hayashi and T. Sekiya. 1989. Detection of polymorphisms of human DNA by gel electrophoresis as single-strand conformation polymorphisms. Proc. Natl. Acad. Sci. USA 86:2766-2770.

19. Peral, B., V. Gamble, J.L.S. Millan, C. Strong, J. Sloanestanley, F. Moreno and P.C. Harris. 1995. Splicing mutations of the polycystic kidney disease 1 (PKD1) gene induced by intronic deletion. Hum. Mol. Genet. 4:569-574.

20. Peral, B., V. Gamble, C. Strong, A.C.M. Ong, J. Sloanestanley, K. Zerres, C.G. Winearls and P.C. Harris. 1997. Identification of mutations in the duplicated region of the polycystic kidney disease 1 gene (PKD1) by a novel approach. Am. J. Hum. Genet. 60:1399-1410.

21. Peral, B., A.C.M. Ong, J.L. Sanmillan, V. Gamble, L. Rees and P.C. Harris. 1996. A stable, nonsense mutation associated with a case of infantile onset polycystic kidney disease 1 (PKD1). Hum. Mol. Genet. 5:539-542.

22. Peral, B., J.L. Sanmillan, A.C.M. Ong, V. Gamble, C.J. Ward, C. Strong and P.C. Harris. 1996. Screening the 3' region of the polycystic kidney disease 1 (PKD1) gene reveals six novel mutations. Am. J. Hum. Genet. 58:86-96.

23. Peters, D.J.M. and L.A. Sandkuijl. 1992. Genetic heterogeneity of polycystic kidney disease in Europe, p. 128-139. *In* M.H. Breuning, M. Devoto and G. Romeo (Eds.), Contributions to Nephrology: Polycystic Kidney Disease, Vol. 97. S. Karger AG, Basel.

24. Rispeter, K., M. Lu, S. Lechner, A. Zibert and M. Roggendorf. 1997. Cloning and characterization of a complete open reading frame of the hepatitis C virus genome in only two cDNA fragments. J. Gen. Virol. 78:2751-2759.

25. Roelfsema, J.H., D.J.M. Peters and M.H. Breuning. 1996. Detection of translation terminating mutations in the PKD1 gene. Nephrol. Dial. Transplant. 11:5-9.

26. Roelfsema, J.H., L. Spruit, J.J. Saris, P. Cheng, Y. Pirson, G.J.B. Vanommen, D.J.M. Peters and M.H. Breuning. 1997. Mutation detection in the repeated part of the PKD1 gene. Am. J. Hum. Genet. 61:1044-1052.

27. Rossetti, S., E. Bresin, G. Restagno, A. Carbonara, S. Corra, O. Deprisco, P.F. Pignatti and A.E. Turco. 1996. Autosomal dominant polycystic kidney disease (ADPKD) in an italian family carrying a novel nonsense mutation and two missense changes in exons 44 and 45 of the PKD1 gene. Am. J. Med. Genet. 65:155-159.

28. Sarkar, G. and S.S. Sommer. 1989. Access to a messenger RNA sequence or its protein product is not limited by tissue or species specificity [see comments]. Science 244:331-334.

29. Sarkar, G., H.S. Yoon and S.S. Sommer. 1992. Dideoxy fingerprinting (ddF): a rapid and efficient screen for the presence of mutations. Genomics 13:441-443.

30. Tellier, R., J. Bukh, S.U. Emerson and R.H. Purcell. 1996. Amplification of the full-length hepatitis A virus genome by long reverse transcription-PCR and transcription of infectious RNA directly from the amplicon. Proc. Natl. Acad. Sci. USA 93:4370-4373.

31. The European Polycystic Kidney Disease Consortium. 1994. The polycystic kidney disease 1 gene encodes a 14 kb transcript and lies within a duplicated region on chromosome 16. Cell 78:725.

32. The International Polycystic Kidney Disease Consortium. 1995. Polycystic kidney disease: the complete structure of the PKD1 gene and its protein. Cell 81:289-298.

33. Turco, A.E., S. Rossetti, E. Bresin, S. Corra, L. Gammaro, G. Maschio and P.F. Pignatti. 1995. A novel nonsense mutation in the PKD1 gene (c3817t) is associated with autosomal dominant polycystic kidney disease (ADPKD) in a large three-generation Italian family. Hum. Mol. Genet. 4:1331-1335.

34. Turco, A.E., S. Rossetti, E. Bresin, S. Corra, G. Restagno, A. Carbonara, O. Deprisco, L. Gammaro, G. Maschio and P.F. Pignatti. 1996. Detection of two different nonsense mutations in exon 44 of the PKD1 gene in two unrelated Italian families with severe autosomal dominant polycystic kidney disease. Nephrol. Dial. Transplant. 11:10-12.

35. Turco, A.E., S. Rossetti, E. Bresin, S. Englisch, S. Corra and P.F. Pignatti. 1997. Three novel mutations of the PKD1 gene in Italian families with autosomal dominant polycystic kidney disease. Hum. Mutat. 10:164-167.

36. Watnick, T.J., K.B. Piontek, T.M. Cordal, H. Weber, M.A. Gandolph, F. Qian, X.M. Lens, H.P.H. Neumann and G.G. Germino. 1997. An unusual pattern of mutation in the duplicated portion of PKD1 is revealed by use of a novel strategy for mutation detection. Hum. Mol. Genet. 6:1473-1481.

Received 23 June 1998; accepted 8 September 1998.

Address correspondence to:

Dr. Pa-thai Yenchitsomanus
Molecular Genetics and Medical Molecular Biology Units
Office for Research and Development
Faculty of Medicine-Siriraj Hospital
Mahidol University
2 Prannok Road, Bangkok-noi
Bangkok 10700, Thailand
Internet: grpye@mahidol.ac.th

Kidney International, Vol. 56 (1999), pp. 1674–1682

Autosomal recessive distal renal tubular acidosis associated with Southeast Asian ovalocytosis

SOMKIAT VASUVATTAKUL, PA-THAI YENCHITSOMANUS, PRAYONG VACHUANICHSANONG, PETI THUWAJIT, CHAROEN KAITWATCHARACHAI, VICHAI LAOSOMBAT, PRIDA MALASIT, PRAPON WILAIRAT, and SUMALEE NIMMANNIT

Renal Division and Medical Molecular Biology Unit, Siriraj Hospital, Mahidol University; Songklanakarin Hospital, Prince of Songkla University, Songkla; and Department of Biochemistry, Faculty of Science, Mahidol University, Bangkok, Thailand

Autosomal recessive distal renal tubular acidosis associated with Southeast Asian ovalocytosis.

Background. A defect in the anion exchanger 1 (AE1) of the basolateral membrane of type A intercalated cells in the renal collecting duct may result in a failure to maintain a cell-to-lumen H^+ gradient, leading to distal renal tubular acidosis (dRTA). Thus, dRTA may occur in Southeast Asian ovalocytosis (SAO), a common *AE1* gene abnormality observed in Southeast Asia and Melanesia. Our study investigated whether or not this renal acidification defect exists in individuals with SAO.

Methods. Short and three-day NH_4Cl loading tests were performed in 20 individuals with SAO and in two subjects, including their families, with both SAO and dRTA. Mutations of *AE1* gene in individuals with SAO and members of the two families were also studied.

Results. Renal acidification in the 20 individuals with SAO and in the parents of the two families was normal. However, the two clinically affected individuals with SAO and dRTA had compound heterozygosity of 27 bp deletion in exon 11 and missense mutation G701D resulting from a CGG→CAG substitution in exon 17 of the *AE1* gene. Red cells of the two subjects with dRTA and SAO and the family members with SAO showed an approximate 40% reduction in sulfate influx with normal 4,4'-di-isothiocyanato-stilbene-2,2'-disulfonic acid sensitivity and pH dependence.

Conclusion. These findings suggest that compound heterozygosity of abnormal *AE1* genes causes autosomal recessive dRTA in SAO.

Southeast Asian ovalocytosis (SAO) is a hereditary condition that is widespread in parts of Southeast Asia and Melanesia. It has been shown that SAO results from a mutation in the red cell membrane band 3 or the anionic (HCO_3^-/Cl^-) exchanger 1 (AE1) [1, 2]. The N-terminal fragment of the abnormal band 3 migrates slower than normal in sodium dodecyl sulfate-polyacrylamide gel electrophoresis (SDS-PAGE) [3]. Sequencing of the abnormal erythrocyte *AE1* gene in SAO showed that it contained two linked mutations: a deletion of codons 400 to 408 in the boundary of cytoplasmic and membrane domains and a point mutation in the first base of codon 56 (K56E), the Memphis I polymorphism [4].

Anion exchanger 1 is also found in the basolateral membrane of the type A intercalated cells of renal collecting ducts, which are involved in H^+ secretion [5, 6]. Studies of human kidneys have indicated that, although the protein in the basolateral membrane of type A intercalated cells is reactive toward monoclonal antibodies to the membrane transport domain of AE1 [6, 7], several antibodies to the cytoplasmic domain of AE1 are unreactive [6], which is consistent with renal AE1 being truncated at the NH_2 terminus [8]. A promoter that gives rise to these kidney transcripts is present in erythroid intron 3 of the human *AE1* gene [8, 9].

A defect in AE1 of the basolateral membrane of type A intercalated cells of the collecting duct may result in a failure to establish or maintain a cell-to-lumen H^+ gradient, and leads to distal renal tubular acidosis (dRTA) [5, 10]. Three studies and a review have shown that mutations of the *AE1* gene affect renal acidification [11–14]. There are at least two reports indicating an association between dRTA and hereditary elliptocytosis [15, 16], which is uncommon among Caucasians, but a related condition, SAO, is widespread in parts of Southeast Asia, with a prevalence reaching 30% in certain ethnic groups [17].

To examine the possibility that a defect in renal acidification may be associated with subjects with SAO, the renal acidification function and a detailed characterization of the *AE1* gene were studied in SAO individuals and members of two unrelated families with dRTA and

Key words: band 3 protein, anion exchanger 1, *AE1* gene, DNA sequencing, renal acidification.

Received for publication November 17, 1998
and in revised form June 15, 1999
Accepted for publication June 16, 1999

SAO. In this report, we describe a novel compound heterozygosity of mutated *AE1* genes in the subjects with SAO and dRTA, and an autosomal recessive mode of inheritance of the abnormal genes associated with the two combined defects.

METHODS

Subjects

The study population consisted of 20 individuals with SAO, two unrelated subjects with SAO and dRTA (as defined by a low rate of NH_4^+ excretion and an inability to lower the urine pH below 5.5 in the presence of systemic acidosis, $HCO_3^- < 20$ mEq/liter) and their family members and 11 individuals with normal red blood cell morphology living in the same region as the control subjects. All subjects were placed on a normal diet, and medications were terminated one week prior to the study. This investigation was approved by the Human Ethics Committee of the Prince of Songkla University, Thailand.

Clinical studies

Renal acidification was studied using a short acid loading by administration of 0.1 g/kg NH_4Cl, as previously described by Wrong and Davies [18], in 10 individuals with SAO, the two family members and seven normal control subjects; simultaneously, a chronic acid loading was achieved by administration of 0.1 g/kg/day NH_4Cl for three days with diuresis on the fourth day induced by furosemide (20 mg p.o.) [19] in another 10 individuals with SAO and four normal control subjects. To achieve urinary osmolality >800 mOsm/kg H_2O, intranasal 1-deamino-D-arginine vasopressin (DDAVP) was given after 16 hours of water deprivation [20].

Venous blood pH was measured using blood gas analyzer (model 178, Corning). The concentration of bicarbonate in plasma was calculated using the pK value of 6.10 and a solubility factor of 0.0301 [21, 22]. Analytical methods for determination of NH_4^+, sodium, potassium, chloride, creatinine, and osmolality were as previously described [23].

The clearance of creatinine provided an approximation of the glomerular filtration rate [24]. The transtubular K concentration gradient (TTKG) was calculated to reflect the driving force for K secretion [25].

Values were reported as mean ± SEM, and comparisons between groups were made by analysis of variance (ANOVA).

DNA analysis

Polymerase chain reaction primers. The sequence of *AE1* gene was retrieved from Entrez database (GenBank, NCBI). Nineteen pairs of polymerase chain reaction (PCR) primers were designed for amplifications of two overlapping regions in intron 3 (one for the potential kidney promoter and another for the possible 5' sequence of transcript expressed in kidney) and 17 regions in exons 4 to 20 of the *AE1* gene (Table 1). The primers for each exon would anneal to sequences in introns, flanking both sides of the exon. The sizes of PCR products obtained from amplifications using these primers were usually less than 400 bp, except those for the two regions in intron 3. These primers were synthesized by BioService Unit of the National Center for Genetic Engineering and Biotechnology (Biotec, Bangkok, Thailand).

DNA samples. Leukocyte genomic DNAs were prepared from 10 ml ethylenediaminetetraacetic acid (EDTA) blood samples by standard DNA extraction method, which consisted of steps of proteinase K digestion, phenol-chloroform extractions, and ethanol precipitation [26]. DNA samples were finally dissolved in sterile distilled water, and their amounts were estimated from absorbances measured by ultraviolet-visible spectrophotometer at wavelength 260. A small part of stock DNA sample was diluted to 50 ng/μl for using in PCR.

Polymerase chain reaction. Polymerase chain reaction was performed by mixing 125 ng DNA sample, 2.5 μl of 10 × buffer (Perkin-Elmer Cetus, Norwalk, CT, USA), 1.5 μl of 25 mM $MgCl_2$, 2.5 μl of 2 mM dNTP mix, 12.5 pmol each of forward (L) and reverse (R) primers, and 0.25 units of *Taq* polymerase (Perkin-Elmer Cetus) in a total volume of 25 μl. The reaction mixture was overlaid with one drop of mineral oil, and amplification was performed for 35 cycles in Thermal Cycler 480 (Perkin-Elmer Cetus). Each cycle was comprised of denaturation at 94°C for one minute (5 min for the first cycle), annealing at 58 to 70°C (depending on pair of primers; Table 1) for one minute, and extension at 72°C for one minute (5 min for the final cycle). After amplifications, PCR products were examined by running on 2% agarose gel electrophoresis and ethidium bromide staining.

Single strand conformational polymorphism (SSCP). Two microliters of the PCR product were mixed with 8 μl of sample running buffer (containing 95% formamide, 0.05% bromophenol blue, 0.05% xylene cyanol, 20 mM EDTA, and 10 mM NaOH). The mixture was heated at 95°C for 10 minutes to denature DNA into single strands and was then cooled on ice for five minutes before loading onto nondenaturing polyacrylamide gel. The polyacrylamide gel with the size of 90 × 80 mm and thickness of 1 mm contained 10% acrylamide:bis-acrylamide (49:1). Electrophoresis was run in 1 × TBE buffer at 20 mA for two to six hours at room temperature. Double-stranded DNA might also be run by mixing 2 μl of the PCR product with 8 μl sample running buffer (without 10 mM NaOH) and loading onto the same gel without heating.

After electrophoresis, the gel was fixed with 40% methanol for 10 minutes, soaked in 160 mM HNO_3 for

Table 1. Oligonucleotide primers for amplifications of the *AE1* gene

Exon	PCR primer sequence	Position	Annealing temp °C	Product size bp
Intron 3.1	5'-CAGTTTGGGACAAGGGCCTG-3'	6995–7014	67	491
	5'-TGATGAAGTGAAGGGACCTCTCC-3'	7463–7485		
Intron 3.2	5'-TGGGAGGAGAGAAGGGAGTCTG-3'	7364–7383	67	402
	5'-CGGTGTCGTGAGCTGAAAACC-3'	7745–7765		
Exon 4	5'-GTCTCTGAGGCTCACAGTGGATG-3'	7673–7695	63	226
	5'-ATCCCCTTGCTCCTCTCTTCC-3'	7878–7898		
Exon 5	5'-TGAGCACCCACTATGCCCTG-3'	8522–8541	63	299
	5'-CAGCACCCCACAACAATCCTC-3'	8800–8820		
Exon 6	5'-AGATGAGGATTGTTGTGCGGTG-3'	8796–8817	63	262
	5'-CAAGTGGGCTGGGGAAGTG-3'	9039–9057		
Exon 7	5'-CACCACTGATAGCTCAGCCTGAAC-3'	9407–9430	60	343
	5'-TGAGAAAGCTCTCTCCTTGCCC-3'	9628–9649		
Exon 8	5'-GAGAATGGGAAGGGGAGGATG-3'	9739–9760	60	244
	5'-GGTCCAGGCTGAGGGAAAGAC-3'	9963–9983		
Exon 9	5'-TCTTCAGCACACCCACCCTG-3'	9998–10017	60	299
	5'-TCAGCCACCATGCAGGTCC-3'	10278–10296		
Exon 10	5'-TCCTTTCCCTCCGCAGGTC-3'	10726–10744	58	332
	5'-ACAGAGGCTACGCTGAGGTGTC-3'	11036–11057		
Exon 11	5'-CCTCACCTCCTCCAGCTACTCC-3'	11163–11184	62	318
	5'-CAGAAGTTGGGGCTGAGACAGAG-3'	11458–11480		
Exon 12	5'-GCTCTATGGGCTCCTGGAAATG-3'	11529–11550	58	293
	5'-AAAGGGTCTTGGGGCAAGG-3'	11803–11821		
Exon 13	5'-CTGTCATGTCCCCCGCAC-3'	11765–11782	58	339
	5'-TGTCTCAGTCTTATACACAACCTCC-3'	12079–12103		
Exon 14	5'-TGGTGGTATTTTCCAGCCCAAG-3'	13484–13505	60	320
	5'-GCACTGAGGAATTTGGAGCGG-3'	13783–13803		
Exon 15	5'-AAGGCAGGAGGTGGGGAGTGACTG	14045–14078	70	201
	5'-GGAAATGAGGACCTGGGGGGTATC	14222–14245		
Exon 16	5'-TCCTGCTCCCACCCTTCCCC-3'	14673–14692	68	276
	5'-TCTGCCTCCCACCCTCCCAG-3'	14929–14948		
Exon 17	5'-TGGAGGAGGCAGGGGAGAAC-3'	15980–15999	70	347
	5'-GGGGCAGGAGGATGGTGAAG-3'	16307–16326		
Exon 18	5'-ATATGGTGCCTGTGTTTTATTCCC-3'	17705–17728	65	332
	5'-TGCCTATCACACCCCAGCAC-3'	18017–18036		
Exon 19	5'-GGTACAGGACCCTTTTCTGG-3'	17973–17992	60	334
	5'-GCCTGCCCTAGTTCTGAGAC-3'	18287–18306		
Exon 20	5'-TCTCACCCTGTCTCTCTCCTG-3'	18819–18839	65	198
	5'-GAGGTGCCCATGAACTTCTG-3'	18997–19016		

six minutes, washed with deionized water, and soaked in deionized water for five minutes. It was then stained in 0.2% $AgNO_3$ solution for 20 minutes with gentle shaking, washed with deionized water, and soaked in deionized water for five minutes. The $AgNO_3$ solution and washing water were pooled and added with a few drops of HCl to convert $AgNO_3$ to AgCl before discarding. The gel was soaked in developer containing 3% Na_2CO_3 and 0.0185% formamide in deionized water for 4 to 10 minutes. When DNA bands were clearly observed, a solution of 10% citric acid in deionized water was immediately added into the developer to stop the staining reaction. The SSCP pattern on the gel was recorded into a computer by scanning with a scanner. The gel was also dried on a piece of filter paper for long-term storage.

Mobility shift of single strand DNA from the normal pattern indicated the presence of a possible mutation. The PCR product of the exon that showed mobility shift was analyzed by direct DNA sequencing.

Direct DNA sequencing. To identify mutation in the exons of *AE1* gene observed in the PCR-SSCP analysis, the PCR product was purified from a preparative agarose gel and sequenced by manual direct DNA sequencing using Thermo Sequenase Cycle Sequencing Kit (Amersham Life Science Inc., Arlington Heights, IL, USA) or by an automated sequencing machine (ABI-PRISM™ 310 Genetic Analyzer; ABI, USA) using an ABI PRISM™ Dye Terminator Cycle Sequencing Ready Reaction Kit.

Red cell anion transport studies

^{35}S-SO_4 influx into red blood cells was measured in the two patients with SAO and dRTA and their family members, and normal controls in the presence and absence of the inhibitor, 4,4'-di-isothiocyanato-stilbene-2,2'-disulfonic acid (DIDS). The studies were performed at 37°C in buffer of 70 mM sodium citrate, 3 mM sodium sulfate, and 10 mM Tris, pH 7.4 [13].

Table 2. Renal acidification function after three days of NH_4Cl loading in individuals with Southeast Asian ovalocytosis (SAO) compared with controls

	SAO (N = 10)	Controls (N = 4)
Serum		
Creatinine *mg/dL*	0.9 ± 0.1	1.1 ± 0.1
K^+ *mM*	3.8 ± 0.1	3.7 ± 0.1
HCO_3^- *mM*		
Pre-acid loading	26 ± 0.8	27 ± 0.1
Post-acid loading	20 ± 0.7	20 ± 1.6
Venous pH		
Pre-acid loading	7.35 ± 0.02	7.37 ± 0.03
Post-acid loading	7.32 ± 0.01	7.29 ± 0.02
Urine		
C_{Cr} *ml/min*	93 ± 6	87 ± 9
pH		
Pre-acid loading	6.0 ± 0.1	6.0 ± 0.3
Post-acid loading	5.0 ± 0.1	4.9 ± 0.1
After furosemide	4.5 ± 0.1	4.4 ± 0.1
NH_4^+ *μmol/min*		
Pre-acid loading	22 ± 0.3	23 ± 4
Post-acid loading	65 ± 6	65 ± 4
After furosemide	75 ± 6	63 ± 7

Table 3. Renal acidification after short acid loading in individuals with Southeast Asian ovalocytosis (SAO) compared with controls

	SAO (N = 10)	Controls (N = 7)
Serum		
Creatinine *mg/dL*	1.1 ± 0.1	1.0 ± 0.2
K^+ *mM*	3.8 ± 0.04	3.9 ± 0.1
HCO_3^- *mM*		
Pre-acid loading	25 ± 0.7	25 ± 0.9
Post-acid loading	20 ± 0.6	22 ± 0.8
Venous pH		
Pre-acid loading	7.37 ± 0.02	7.35 ± 0.01
Post-acid loading	7.31 ± 0.05	7.30 ± 0.02
Urine		
C_{Cr} *ml/min*	83 ± 6	90 ± 14
pH		
Pre-acid loading	5.9 ± 0.1	5.6 ± 0.1
Post-acid loading	5.0 ± 0.1	4.9 ± 0.1
NH_4^+ *μmol/min*		
Pre-acid loading	28.6 ± 3	21.5 ± 6
Post-acid loading	39.4 ± 6	36.7 ± 4

RESULTS

Clinical studies

Renal acidification was performed in 20 individuals with SAO and the 11 controls. The NH_4^+ excretion rate and urine pH after a three-day NH_4Cl load are shown in Table 2. Neither subject groups (10 individuals vs. 4 controls) had a statistical significant difference in the NH_4^+ excretion rate (65 ± 6 vs. 65 ± 4 μmol/min) or urinary pH (5.0 ± 0.1 vs. 4.9 ± 0.1) following the acid load. After diuresis with oral furosemide on the fourth day of the acid load, the urinary pH decreased significantly in both groups, but there was no significant difference between the two groups (4.5 ± 0.1 vs. 4.4 ± 0.1). The increment of NH_4^+ excretion during the peak diuresis was not significantly different between the two groups (75 ± 6 vs. 63 ± 7 μmol/min). The maximum urine osmolality after 16 hours of water deprivation and intranasal DDAVP administration was also not significantly different between the two groups (940 ± 41 vs. 850 ± 46 mOsm/kg/H_2O).

Table 3 provides a summary of the results of urinary acidification studies after the short acid load. Blood pH values after the acid loading of 10 SAO and 7 control subjects were less than 7.35. Urine pH and NH_4^+ excretion rate after the acid load between both groups were not significantly different (5.0 ± 0.1 vs. 4.9 ± 0.1 and 39 ± 6 vs. 37 ± 4 μmol/min, respectively)

Pedigrees (KSN and YAT) of two subjects with SAO and dRTA are shown in Figure 1. Propositi (II-1 in both families) presented with history of growth retardation, SAO, and hypokalemia (Table 4). Complete dRTA was diagnosed by low NH_4^+ excretion rate in both propositi (3.3 and 4.3 μmol/min, respectively) as well as by the inability to lower the urine pH below 5.5 (7.3 and 6.7, respectively) in the presence of metabolic acidosis (venous pH 7.26 and 7.27 and serum HCO_3^- 9 and 14 mEq/liter, respectively). No abnormal renal acidification was detected in both sets of parents (I-1 and I-2).

Screening and characterization of AE1 gene mutations

Polymerase chain reaction-SSCP analysis was used to screen for mutations in exons 4 to 20 of the *AE1* gene and in intron 3, the promoter region of the kidney isoform. DNA samples from the propositi, siblings, as well as the parents of the two families were also analyzed. Figure 1 shows the results of PCR-SSCP analysis for exons 11 and 17 of one normal individual (N) and members of the two families. In the YAT family, the father (I-1) showed a mobility shift in exon 17, and the mother (I-2) showed a mobility shift in exon 11. In the KSN family, the father (I-1) demonstrated a mobility shift in exon 11, whereas the mother (I-2) showed a shift in exon 17. The DNA samples of both KSN and YAT families revealed mobility shifts in both exons 11 and 17. Except for a mobility shift of exon 4 (caused by the MspI polymorphism, confirmed by sequencing; Fig. 5), the PCR-SSCP patterns of all other exons, including intron 3, were normal (data not shown).

Because the mobility shifts of exons 11 and 17 of *AE1* gene detected by PCR-SSCP in the two patients were the same, amplified DNA of these two exons from the propositus of KSN family were sequenced. Exon 11 had a deletion of 27 bp corresponding to codons 400 to 408 (Fig. 2), whereas exon 17 contained a nucleotide substitution of G to A in codon 701 (CGG→CAG), resulting in an amino acid change from glycine to aspartic acid (G701D) (Fig. 3). Thus, the *AE1* gene of the propositi of

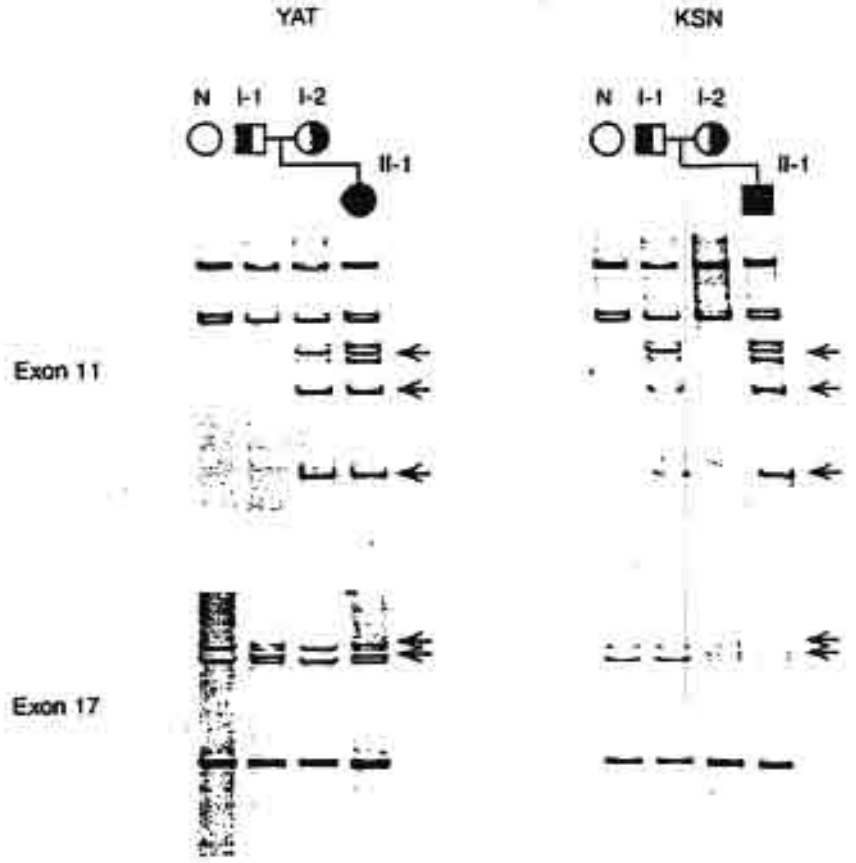

Fig. 1. Screening of mutations in exons 11 and 17 of the *AE1* gene in the two patients with Southeast Asian ovalocytosis (SAO) and distal renal tubular acidosis (dRTA) and their parents by the PCR-SSCP technique. The two patients (II-1 in both families) had mobility shifts of single-stranded DNAs in both exons 11 and 17 (arrows), whereas their parents had the mobility shifts in either exon 11 (I-2 in family of YAT and I-1 in family of KSN) or exon 17 (I-1 in family of YAT and I-2 in family of KSN). "N" is normal individual.

Table 4. Values in blood and urine collections from the two patients with SAO and dRTA

	KSN: II-1	YAT: II-1
Serum		
Creatinine *mg/dL*	0.5	0.6
BUN *mg/dL*	13	13
Na^+ *mM*	137	141
K^+ *mM*	3.3	3.4
Cl^- *mM*	116	111
HCO_3^- *mM*	8.7	14
Venous pH	7.26	7.27
Urine		
TTKG	10.4	10.3
Flow rate *ml/min*	0.4	0.8
pH	7.3	6.7
NH_4^+ *μmol/min*	3.3	4.3

Abbreviations are: SAO, Southeast Asian ovalocytosis; dRTA, distal renal tubular acidosis; BUN, blood urea nitrogen; TTKG, transtubular K^+ concentration gradient.

both families was a compound heterozygosity of 27 bp deletion in exon 11 and missense mutation (CGC→CAG) in exon 17. The sequencing results also showed the presence of homozygous band 3 Memphis I (Fig. 5) in the two patients. The presence of exon 11 deletion and exon 17 missense mutation in both patients was also confirmed by the detection of a shorter PCR product and elimination of *HpaII* restriction site on the amplified DNA, respectively, by gel electrophoresis (Fig. 4). Mutations of *AE1* gene were also analyzed by PCR-SSCP method in 20 individuals with SAO and in normal subjects. SAO individuals had mobility shifts in exons 4 and 11.

Anion transport property of the red cells of the two families

An influx of [^{35}S] sulfate into the red cells of members of the two families was compared with that of red cells from 10 normal controls taken at the same time. Red cell samples from the propositi of the KSN and YAT families and family members with SAO showed a consistently lower anion transport activity than the normal samples in both the presence and absence of DIDS (Table 5). Family members with only the exon 17 mutation had normal anion transport and DIDS activity.

DISCUSSION

Mutation of the *AE1* gene in SAO has been the subject of a number of studies [1, 4, 27]. The underlying molecular defect is a 27 bp deletion in exon 11 of the *AE1* gene, resulting in the loss of 9 amino acids (codons 400 to 408) in the band 3 protein, which is also associated with the

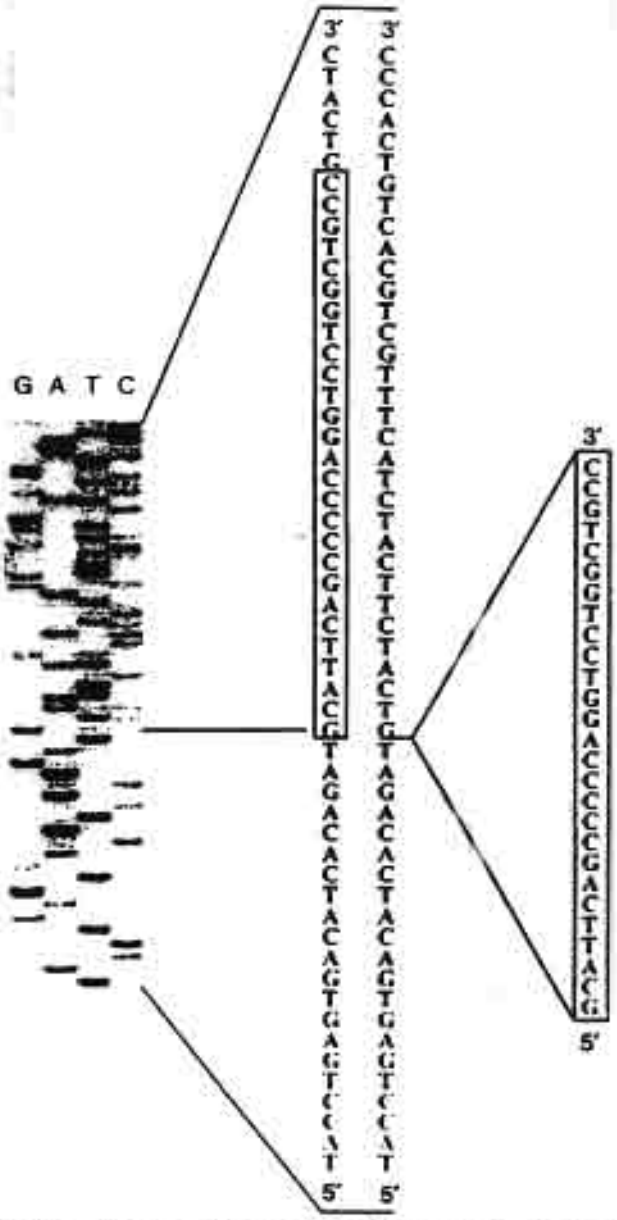

Fig. 2. Sequencing analysis of exon 11 of the *AE1* gene in the patient with dRTA and SAO (II-1, family of KSN), showing nucleotide sequence of exon 11 with 27 nucleotide deletion superimposing the normal sequence. Identical 27 nucleotides in the normal and deleted alleles (the latter is separated from the nucleotide stretch) are blocked. The deletion of 27 nucleotides in one allele resulted in shifting of the remaining nucleotide sequence superimposing the normal sequence in the autoradiogram.

Memphis I (K56E) polymorphism. Although SAO occurs with high frequency in parts of Southeast Asia and Melanesia, no homozygous individual for the *AE1* mutation has been identified, suggesting that homozygosity for this mutation may be lethal [1].

Anion exchanger 1 in red cells is important for the transport of carbon dioxide from the tissue to the lung and for acid secretion in type A intercalated cells of the kidney [28]. Total deficiency of red cell band 3 caused by a nonsense mutation has been reported in cattle [29]. Animals showed a moderate uncompensated anemia with hereditary spherocytosis and retarded growth, which was attributed to mild acidosis. The band 3-deficient animals had defective renal acid secretion and could not acidify urine pH below 7.5 despite metabolic acidosis. In dRTA, acid secretion in the distal nephron is impaired, leading to the development of metabolic acidosis [10, 30]. Recently, several studies have demonstrated associations of the *AE1* mutations and dRTA: Rysava et al reported that 2 out of 10 patients with hereditary spherocytosis and band 3 PRIBRAM (G—A in the first nucleotide of intron 12) had an incomplete form of dRTA [14]; Bruce et al reported an association between familial dRTA and point mutations of the *AE1* gene, namely, R589H, R589C, and S613F [12]. The *AE1* mutation, R589H, has also been reported in two other studies [13, 31]. An intragenic 13 bp duplication resulting in deletion of the last 11 amino acids of *AE1* gene in one dRTA subject has also been demonstrated [31]. Mutations in the *AE1* gene appear to cause autosomal dominant dRTA [12, 13, 31], but the molecular mechanism is unknown.

There have been two previous studies showing the association between dRTA and elliptocytosis or SAO [15, 16]. The presence of the two conditions in the same individuals suggests that there may be a common underlying molecular defect. However, mutation of the *AE1* gene in individuals with both of these conditions was not demonstrated. In this study, 20 individuals with SAO, confirmed by the presence of 27 bp deletion in exon 11 of the *AE1* gene, showed no abnormal renal acidification following the three-day NH_4Cl loading ($N = 10$; Table 2) or by short acid loading ($N = 10$; Table 3). The rate of excretion of NH_4^+ increased by almost threefold, and the urine pH decreased below 5.0 after three-day acid loading and during the furosemide-induced diuresis to typical values of normal subjects [19]. This suggests that the rate of production of NH_4^+ in the proximal tubular cells was not appreciably depressed. Thus, SAO mutation of the *AE1* gene in the heterozygous condition is not sufficient to cause dRTA.

The two clinically affected unrelated patients in the KSN and YAT families with dRTA and SAO showed a low rate of NH_4^+ excretion and an inability to lower the urine pH below 5.5 in the presence of systemic acidosis (Table 4). There was also a high transtubular $[K^+]$ gradient (TTKG) [25] given the degree of hypokalemia. No abnormal renal acidification was detected in either set of parents. Analysis of *AE1* gene mutation by PCR-SSCP method showed that the two patients (II-1 in both families) had the same mobility shifts in exons 11 and 17, whereas the parents had mobility shift in either exon

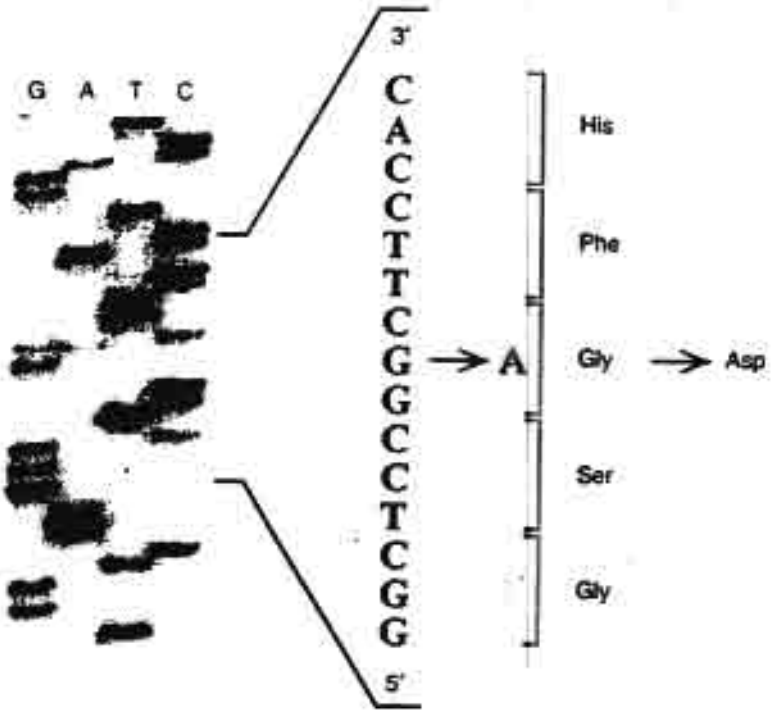

Fig. 3. Sequencing analysis of exon 17 of *AE1* gene in the patient with SAO and dRTA (II-1, family of KSN). A substitution from G to A in the second nucleotide of codon 701 was observed. This substitution results in missense mutation changing the amino acid at the position 701 from glycine to aspartic acid (G701D).

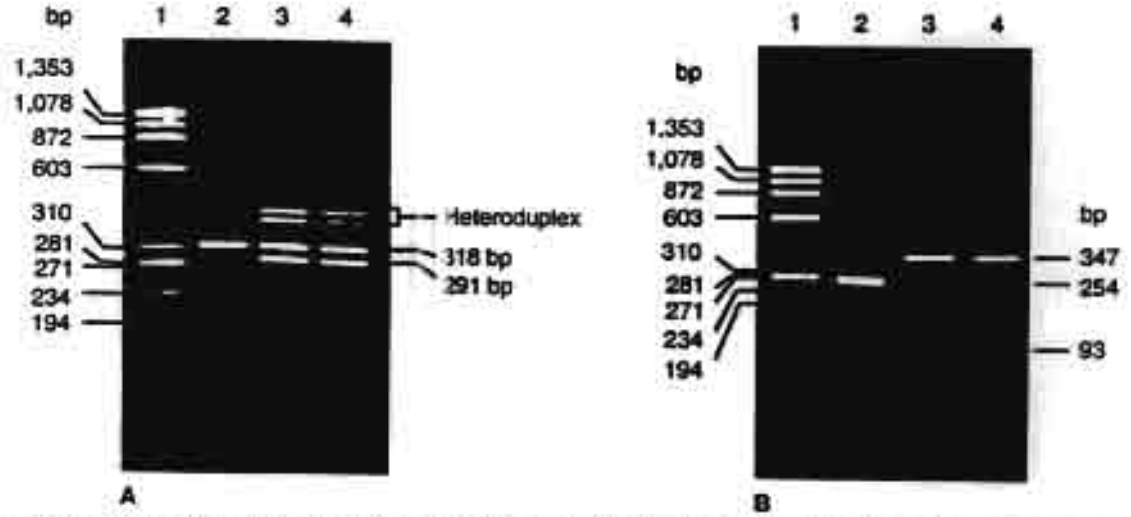

Fig. 4. Detection of exon 11 deletion and exon 17 (CGG→CAG) missense mutation in the patients (II-1) of KSN and YAT families by agarose gel electrophoresis. (*A*) PCR products from amplifications of exon 11 of *AE1* gene with AE1Ex11L/AE1Ex11R primers. Normal control sample (lane 2) showed only a PCR product with the size of 318 bp. DNA samples from the patients of the KSN (lane 3) and YAT (lane 4) families who had 27 bp deletion in exon 11 in one allele of the *AE1* gene resulted in PCR products with the sizes of 318 and 291 bp, and also their heteroduplexes. (*B*) PCR products from amplifications of exon 17 with AE1Ex17L/AE1Ex17R primers and digestions with *Hpa*II restriction endonuclease, which could digest the normal (CCGG) but not the mutant (CCAG) sequences. A normal control sample (lane 2) showed digested fragments with the sizes of 254 and 93 bp. DNA samples from the patients of the KSN (lane 3) and YAT (lane 4) families who had exon 17 missense mutation in one allele of the *AE1* gene revealed both digested (254 and 93 bp) and undigested (347 bp) PCR products. Lane 1 in both sets is Phix174 DNA/*Hae*III markers.

11 (I-2 in family YAT and I-1 in family KSN) or exon 17 (I-1 in family YAT and I-2 in family KSN; Fig. 1). DNA sequencing (Figs. 2 and 3) and gel electrophoresis (Fig. 4) revealed that exon 11 contained a 27 bp deletion typical of SAO [4] and exon 17 had a single nucleotide substitution of G to A in the second nucleotide of codon 701 (CGG→CAG), resulting in a G701D missense mutation. This is the first report of a compound heterozygosity

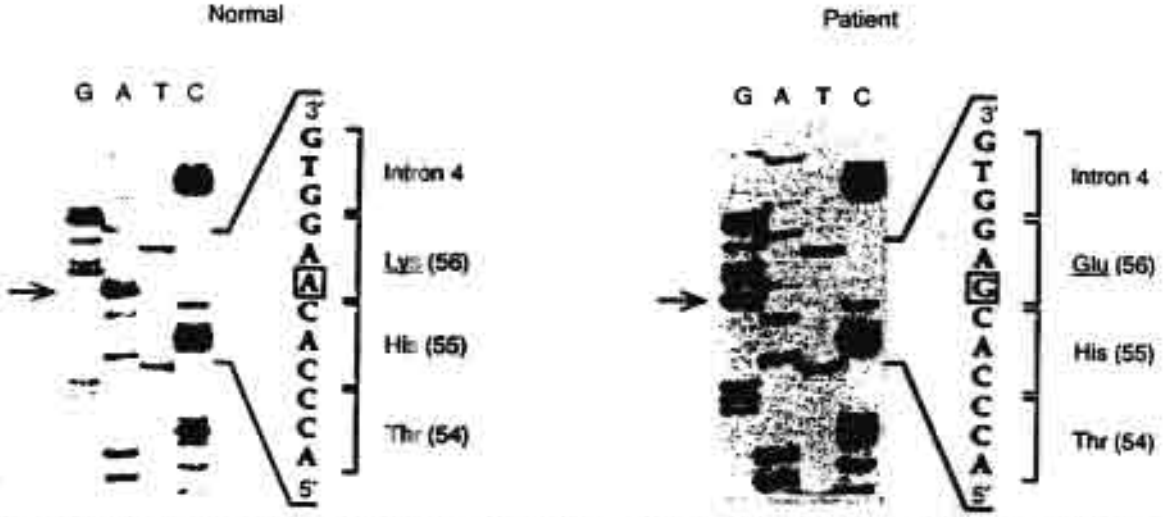

Fig. 5. Sequencing analysis of exon 4 of the *AE1* gene in a normal individual and the patient with SAO and dRTA (II-1, the family of KSN). The normal individual had AAG (code for lysine), but the patient had GAG (code for glutamic acid) at codon 56. The band 3 variant that had glutamic acid at the position 56 was previously described as band 3 Memphis I. The patient who had the 27 bp deletion in exon 11 and the G→A substitution in codon 701 in exon 17 was homozygous for band 3 Memphis I. Therefore, these two mutations were linked to band 3 Memphis I polymorphism.

Table 5. Characterization of [^{35}S]SO_4 influx into red cells from members of families of YAT and KSN, compared with healthy control cells

	Genotype	Phenotype	SO_4 uptake *10–17 mol/min/cell*		
			No DIDS	1.5 μM DIDS	%
YAT family					
I–1	G701D		6.45	2.12	32.9
I–2	Ex 11Δ27	SAO	4.78	0.08	1.7
II–1	Ex11Δ27/G701D	SAO + RTA	4.77	0.13	2.7
KSN family					
I–1	Ex 11Δ27	SAO	3.57	1.48	24.1
I–2	G701D		6.56	2.35	35.8
II–1	Ex11Δ27/G701D	SAO + RTA	4.03	0.15	3.7
Controls			6.0 ± 0.8		

for *AE1* mutations associated with SAO and dRTA, to our knowledge. The sequencing results also showed the presence of homozygous band 3 Memphis I (Fig. 5) in the two patients, indicating that the two mutations linked with band 3 Memphis I polymorphism. Studies of the influx of [^{35}S] sulfate into red cells of the two patients and their family members with SAO indicated a consistently lower anion transport activity than the normal red cells (Table 5). Individuals with exon 17 mutation had normal red cell anion transport activity.

Glycine 701 is located at the beginning of membrane span 9 of band 3, which is in a highly conserved region in the AE protein family across several species [28], which indicates its structural or functional importance. Although the presence of both SAO and G701D mutations had no additional affect on the influx of [^{35}S] sulfate into red cells than the presence of the SAO mutation alone, the HCO_3^-/Cl^- anion exchanger activity in the type A intercalated cells of the renal collecting duct in individuals with the combined mutations may be abnormal. Two siblings with dRTA and hemolytic anemia have recently been found to carry a homozygous G701D missense mutation of the *AE1* gene, which causes recessively transmitted dRTA in this kindred with apparently normal erythroid anion transport in the parents and affected children [32].

An expression study of the G701D mutation in *Xenopus* oocytes has shown that the mutant protein was not transported to the surface of the cell membrane [32]. However, when it was co-expressed with glycophorin A, the erythroid band 3 chaperonin, both AE1 surface expression and AE1-mediated Cl^- transport were rescued. This suggests that the G701D mutation may lead to decreased or absent AE1 accumulation at the basolateral membrane of the type A intercalated cells in the collecting duct. Therefore, the presence of both SAO and G701D mutations would have a greater effect to the type A intercalated cells than the presence of either mutation alone.

and this would explain the abnormal urinary acidification in the patients with the compound heterozygosity.

Although mutations of the *AE1* gene have been reported to be associated with autosomal dominant dRTA [12, 13, 31], the presence of the compound heterozygosity of *AE1* mutations associated with SAO and dRTA shown in our study, and of homozygosity of AE1 mutation associated with dRTA and hemolytic anemia in that of Tanphaichitr et al [32] indicate an autosomal recessive mode of inheritance.

ACKNOWLEDGMENTS

This study has been supported by grants from Research Development and Medical Education Fund of the Faculty of Medicine, Siriraj Hospital. P. Malasit and P. Wilairat are recipients of the Senior Research Grant of The Thailand Research Fund (TRF). The Medical Molecular Biology Laboratory also operates as a Medical Biotechnology Unit of the National Center for Genetic Engineering (BIOTEC) of the National Science and Technology Development Agency (NSTDA), Thailand. We thank Miss Duangporn Chuawatana, Sumitra Mingkum, and Nunghathai Sawasdee for their technical assistance.

Reprint requests to Somkiat Vasuvattakul, M.D., Renal Unit, Department of Medicine, Siriraj Hospital, Mahidol University, Bangkok 10700, Thailand.
E-mail: sisva@mucc.mahidol.ac.th

REFERENCES

1. Liu S, Zhai S, Palek J, Golan DE, Amato D, Hassan K, Nurse GT, Babona D, Coetzer T, Jarolim P, Zaik M, Borwein S: Molecular defect of the band 3 protein in Southeast Asian ovalocytosis. *N Engl J Med* 323:1530–1538, 1990
2. Jones GL, Edmundson HM, Wesche D, Saul A: Human erythrocyte band 3 has an altered N-terminus in malaria resistant Melanesian ovalocytosis. *Biochim Biophys Acta* 1096:33–40, 1991
3. Schofield AE, Reardon DM, Tanner MJA: Defective anion transport activity of the abnormal band 3 in hereditary ovalocytic red blood cells. *Nature* 355:836–838, 1992
4. Jarolim P, Palek J, Amato D, Hassan K, Sapak P, Nurse GT, Rubin HL, Zhai S, Sahr KE, Liu SC: Deletion in erythrocyte band 3 gene in malaria-resistant Southeast Asian ovalocytosis. *Proc Natl Acad Sci USA* 88:11022–11026, 1991
5. Alper SL, Natale J, Gluck S, Lodish HF, Brown D: Subtypes of intercalated cells in rat kidney collecting duct defined by antibodies against erythroid band 3 and renal vacuolar H+ ATPase. *Proc Natl Acad Sci USA* 86:5429–5433, 1989
6. Wagner S, Vogel R, Lietzke R, Koob R, Drenckhahn D: Immunochemical characterization of a band 3-like anion exchanger in collecting duct of human kidney. *Am J Physiol* 253:213–221, 1987
7. Wainwright SD, Tanner MJA, Martin GEM, Yendle JE, Holmes C: Monoclonal antibodies to the membrane domain of the human erythrocyte anion transport protein. *Biochem J* 258:211–220, 1989
8. Kollerton-Jons A, Wagner S, Hubner S, Appelhans H, Drenckhahn D: Anion exchanger 1 in human kidney and oncocytoma differs from erythroid AE1 in its NH2 terminus. *Am J Physiol* 265:F813–F821, 1993
9. Schofield AE, Martin PG, Spillett D, Tanner MJA: The structure of the human red blood cell anion exchanger (EPB3, AE1, band 3) gene. *Blood* 84:2000–2012, 1994
10. Wrong O, Unwin R, Cohen E, Tanner M, Thakker R: Unraveling the molecular mechanisms of kidney stones. *Lancet* 348:1561–1565, 1996
11. Batlle D, Flores G: Underlying defects in distal renal tubular acidosis: New understandings. *Am J Kidney Dis* 27:896–915, 1996
12. Bruce LJ, Cope DL, Jones JK, Schofield AE, Burley M, Povey S, Unwin RJ, Wrong O, Tanner MJA: Familial distal renal tubular acidosis is associated with mutations in the red cell anion exchanger (band 3, AE1) gene. *J Clin Invest* 100:1693–1707, 1997
13. Jarolim P, Shayakul C, Prabakaran D, Jiang L, Stuart-Tilley A, Rubin H, Simova S, Zavadil J, Herrin JT, Brouillette J, Somers MJG, Seemanova E, Brugnara C, Guay-Woodford LM, Alper SL: Autosomal dominant distal renal tubular acidosis is associated in three families with heterozygosity for the R589H mutation in the AE1 (band 3) Cl^-/HCO_3^- exchanger. *J Biol Chem* 273:6380–6388, 1998
14. Rysava R, Tesar V, Jirsa M, Brabec V, Jarolim P: Incomplete distal renal tubular acidosis coinherited with a mutation in the band 3 (AE1) gene. *Nephrol Dial Transplant* 12:1869–1873, 1997
15. Thong MK, Tan AAL, Lim HP: Distal renal tubular acidosis and hereditary elliptocytosis in a single family. *Singapore Med J* 38:388–390, 1997
16. Bathner RL, Gilchrist GS, Anderson EJ: Hereditary elliptocytosis and primary renal tubular acidosis in a single family. *Am J Dis Child* 115:414–419, 1968
17. Lie-Injo LE, Fix A, Bolton JM, Gilman RH: Haemoglobin E-hereditary elliptocytosis in Malayan aborigines. *Acta Haematol* 47: 210–216, 1972
18. Wrong O, Davies H: The excretion of acid in renal disease. *Q J Med* 28:259–313, 1959
19. Vasuvattakul S, Gougoux A, Halperin ML: A method to evaluate renal ammoniagenesis in vivo. *Clin Invest Med* 16:265–273, 1993
20. Vasuvattakul S, Nimmannit S, Chaovakul VWS, Shayakul C, Malasit P: The spectrum of endemic renal tubular acidosis in the northeast of Thailand. *Nephron* 74:541–547, 1996
21. Van Slyke DD, Linder GS, Hiller A, Letter L, McIntosh JF: The excretion of ammonia and titrable acid in nephritis. *J Clin Invest* 2:255–288, 1926
22. Hastings AB, Sendroy J: The effect of variation in ionic strength on the apparent first and second dissociation constants of carbonic acid. *J Biol Chem* 65:445–455, 1925
23. Halperin ML, Vinay P, Gougoux A, Pichette C, Jungas RL: Regulation of the maximum rate of renal ammoniagenesis in the acidotic dog. *Am J Physiol* 248:F607–F615, 1985
24. Camara AA, Abn KD, Reimer A, Newburgh LH: The twenty-four hourly endogenous creatinine clearance as a clinical measure of the functional state of the kidneys. *J Lab Clin Med* 37:743–763, 1951
25. Ethier J, Kamel K, Magner P, Lemann JJ, Halperin ML: The transtubular potassium concentration in patients with hypokalemia and hyperkalemia. *Am J Kidney Dis* 15:309–315, 1990
26. Gruneraun L, Cazenave J-P, Canerino G, Kloepfer C, Mandel J-L, Tolstoshev P, Jaye M, De la Salle H, Lecocq J-P: Carrier detection of hemophilia B by using a restriction site polymorphism associated with the coagulation factor IX gene. *J Clin Invest* 73:1491–1495, 1984
27. Tanner MJA: Molecular and cellular biology of the erythrocyte anion exchanger (AE1). *Semin Hematol* 30:34–57, 1993
28. Tanner MJA: The structure and function of band 3 (AE1): Recent developments. (review) *Mol Membr Biol* 14:155–165, 1997
29. Inaba M, Yawata A, Koshino I, Sato K, Takeuchi M, Takakuwa Y, Manno S, Yawata Y, Kanzaki A, Ji S, Ban A, Ki O, Maede Y: Defective anion transport and marked spherocytosis with membrane instability caused by hereditary total deficiency of red cell band 3 in cattle due to a nonsense mutation. *J Clin Invest* 97:1804–1817, 1996
30. Morris RC, Ives HE: Inherited disorders of the renal tubule, in *The Kidney*, edited by Brenner BM, Philadelphia, W. B. Saunders, 1996, pp 1764–1827
31. Karet FE, Gainza FJ, Gyory AZ, Unwin RJ, Wrong O, Tanner MJA, Nayir A, Alpay H, Santos F, Hulton SA, Bakkaloglu A, Ozen S, Cunningham MJ, Di Pietro A, Walker WG, Lifton RP: Mutations in the chloride-bicarbonate exchanger gene AE1 cause autosomal dominant but not autosomal recessive distal renal tubular acidosis. *Proc Natl Acad Sci USA* 95:6337–6342, 1998
32. Tanphaichitr VS, Sumboonnanonda A, Ideguchi H, Shayakul C, Brugnara C, Takao M, Veerakul G, Alper SL: Novel AE1 mutations in distal renal tubular acidosis: Loss-of-function rescued by glycophorin A. *J Clin Invest* 102:2173–2179, 1998

Biochemical and Biophysical Research Communications 269, 406–409 (2000)
doi:10.1006/bbrc.2000.2305, available online at http://www.idealibrary.com on IDEAL®

Cleavage of DNA Induced by 9-Anilinoacridine Inhibitors of Topoisomerase II in the Malaria Parasite *Plasmodium falciparum*

Saranya Auparakkitanon and Prapon Wilairat[1]
Department of Biochemistry, Faculty of Science, Mahidol University, Bangkok, 10400, Thailand

Received February 4, 2000

Due to resistance by *Plasmodium falciparum*, the most virulent strain of the four species of human malaria parasites, to most currently used antimalarial drugs, development of new effective antimalarials is urgently needed. Derivatives of 9-anilinoacridine, an antitumor drug, have been shown to inhibit *P. falciparum* growth in culture and to inhibit parasite DNA topoisomerase II activity *in vitro*. Using KCl–SDS precipitation assay to detect the presence of protein–DNA complexes within parasite cells, an indicator of DNA topoisomerase II inactivation, derivatives containing 3,6-diNH, substitutions with 1′-electron donating (NMe_2, CH_2NMe_2, $NHSO_2Me$, OH, OMe), and 1′-electron withdrawing (SO_2NH_2) groups produced protein–DNA complexes. However, the antimalarial pyronaridine, 9-anilinoazaacridine, did not generate protein–DNA complexes, although it was capable of inhibiting *P. falciparum* DNA topoisomerase II activity *in vitro*. These results should prove useful in future designs of novel antimalarial compounds directed against parasite DNA topoisomerase II. © 2000 Academic Press

Malaria is one of the most prevalent of human parasitic diseases caused by unicellular organisms. Approximately 300 million people worldwide are affected by malaria and between 1 and 1.5 million people, mostly children in sub-Sahara Africa, die every year from the disease (1). The most virulent malaria parasite, *Plasmodium falciparum*, has become widely resistant to nearly all currently employed antimalarials and new drugs are urgently needed (2). As the malaria parasite divides rapidly within the host red cell, DNA replicating enzymes offer suitable key targets for new antimalarial drugs.

Antimicrobial and anticancer therapeutic agents have recently been synthesized and employed against DNA topoisomerases (3–5). Topoisomerases are essential for the modification of topology of nucleic acids. One important function that the enzymes perform is to transiently cleave a phosphodiester bond in DNA, and then transfer a segment of another DNA strand through the break before resealing. DNA topoisomerases are divided into two types: type I enzyme breaks one DNA strand for the passage of a second strand, and the type II enzyme breaks both strands of one DNA duplex for the passage of a second DNA double strand (4, 6–10). DNA cleavage is a transesterification reaction, and a covalent protein–DNA intermediate is formed during the transient DNA cleavage stage. This covalent topoisomerase II–DNA complex can be trapped *in vitro* by the addition of a protein denaturant such as sodium dodecyl sulfate (SDS) and is termed a cleavable complex (11, 12).

Topoisomerase inhibitors act by stabilizing the covalent topoisomerase–DNA complexes with an enzyme-linked DNA break on a single strand or both strands (13). The trapping of such cleavable complexes prevents enzyme turnover and hinders the reclosure of DNA breaks. This enhances DNA cleavage levels in living cells (13, 14). Drug-promoted DNA–protein adducts have proven extremely valuable because they provide a simple method to detect the existence of inhibitor-sensitive topoisomerase activity within cells and a means for assaying inhibitor potency *in vivo* (15, 16).

9-Anilinoacridine derivatives have well described biological actions and many have been used successfully to treat different forms of leukemia (17). The mammalian topoisomerase II is the intracellular target of these drugs, which stabilize the cleavable complexes (18, 19). Cell death is dependent on the formation of these cleavage complexes, resulting in DNA damage, rather than from loss of topoisomerase II activity per se (15). Available evidences support a model whereby the acridine moiety intercalates into DNA and the 9-anilino side group projects into the DNA minor groove where it

[1] To whom correspondence should be addressed. Fax: 66 2 248-0375. E-mail: scpwl@mahidol.ac.th.

0006-291X/00 $35.00

interacts with the enzyme (20). The antitumor activity of 9-anilinoacridines is significantly affected by alterations to the chemical groups on the 9-anilino moiety, presumably due to changes to their contact with the enzyme. Thus moving the 3'-OMe group of the clinical antileukemic drug, amsacrine, to the 2'-position abolishes activity (21).

These observations led us to seek 9-anilinoacridine compounds with specificity for topoisomerase II in other organisms, by modifying the substituents on the anilino moiety. Consistent with this notion, a series of 9-anilinoacridines were synthesized with varied anilino substituents which showed differences in structure-activity relationship against *P. falciparum* and human Jurkat leukemia cells (22). Previous studies have identified 3,6-diamino substitution on the acridine ring as greatly increasing drug potency against malaria parasite *in vitro* (23, 24). However these results do not prove that these compounds actually inhibit the target, DNA topoisomerase II, within the malaria parasite. We have, therefore, taken advantage of the ability of topoisomerase II inhibitors to generate *in situ* enzyme–DNA adducts (the so-called cleavable complexes) to examine the ability of a series of antimalarial 9-anilinoacridines, including pyronaridine (an azaacridine), to reach their putative parasite target.

MATERIALS AND METHODS

Parasite culture. *Plasmodium falciparum* K1 (chloroquine- and pyrimethamine-resistant) was isolated in 1979 from an infected individual in Kanchanaburi province, Thailand (25) and was maintained under continuous culture *in vitro* using the candle jar method of Trager and Jensen (26).

In vitro assessment of antimalarial activity. *In vitro* antimalarial testing of drugs against *Plasmodium falciparum*-infected erythrocytes was a modification of the [^{3}H]-hypoxanthine incorporation method of Desjardins *et al.* (27). In brief, unsynchronized parasite culture with mostly ring stages was used. Drugs were initially dissolved in dimethyl sulfoxide (DMSO) and diluted with RPMI 1640 culture medium supplemented with 25 mM Hepes buffer, 32 mM $NaHCO_3$, and 10% human serum to the required concentrations, with a final concentration of DMSO not exceeding 0.01% (v/v). A 200-μl aliquot of 1.5% cell suspension with 1.0% parasitemia was preexposed to 25 μl of the medium containing drug for 24 h in 96-well tissue culture plate and incubated at 37°C prior to the addition of 0.5 μCi [^{3}H]hypoxanthine (specific activity = 28.0 Ci/mmol, Amersham) in 25 μl of medium. After further incubation for 18–24 h, parasite DNA was harvested from each microtiter well onto filter paper (Whatman grade 934 AH) using an automated sample harvester. [^{3}H]-hypoxanthine incorporation in each well was determined in a Beckman liquid scintillation counter model LS-1801. The IC_{50} values (concentrations of drug to inhibit parasite growth by 50%) were obtained from the dose–response curves. Each drug concentration was investigated in triplicate.

KCl–SDS precipitation assay of protein–DNA complex. Parasite culture was synchronized to yield ring stage (5.0% parasitemia and 1.5% cell suspension) (28). A 0.3 ml aliquot of this mixture (50% cell suspension, 5.0% parasitemia) was added to 9.7 ml of complete medium. This cell suspension was then dispensed into 60 × 15 mm plastic culture petri dish. One μCi of [^{3}H]hypoxanthine (specific activity = 28.0 Ci/mmol, Amersham) was added to each culture dish which was incubated in a candle jar at 37°C for 18 h. Formation of topoisomerase II–DNA covalent complexes was quantitated using the KCl–SDS precipitation assay (12). Infected erythrocytes were treated for 4 h with drugs (IC_{50} concentration); negative control was a parasite suspension without drug. Erythrocytes were sedimented and washed once with phosphate-buffered saline (PBS: 137 mM NaCl, 2.7 mM KCl, 10 mM Na_2HPO_4, 1.8 mM KH_2PO_4, pH 7.4). Parasites were liberated by adding 0.15% (v/v) saponin in PBS at room temperature for 15 min, and then were sedimented by centrifuging for 10 min at 2000 *g* and washed with PBS. The parasite pellet was lysed by adding 500 μl of prewarmed lysis solution (1.25% SDS, 5 mM EDTA, 0.5 mg/ml salmon sperm DNA, pH 8.0, 65°C). The suspension was vortexed vigorously and heated to 65°C for 10 min with occasional mixing. One sample was resuspended in 3 ml of cold 325 mM KCl, and a duplicate in 10% TCA. Precipitates were collected by a minicell harvester onto Whatman grade 934 AH paper filter discs and washed with either 325 mM KCl or 10% TCA solution. The filter discs were dried and radioactivity incorporated counted as described above. The amount of protein–DNA complex formed was reported as percent radioactivity in KCl-precipitated pellet compared to TCA-precipitated sample.

RESULTS AND DISCUSSION

We have previously shown that analogs of 9-anilinoacridines inhibited the growth of *P. falciparum* K1 strain in culture (22–24). Studies using partially purified *P. falciparum* DNA topoisomerase II indicated that these compounds could also inhibit parasite enzyme activity as determined by a decatenation assay. Whether topoisomerase II was primarily the target of 9-anilinoacridines within the parasite was unclear. To obtain evidence for inhibition by 9-anilinoacridines of parasite topoisomerase II *in situ* the formation of topoisomerase II–DNA cleavable complexes (protein-linked DNA breaks) was evaluated by using a KCl–SDS assay (12).

The 9-anilinoacridine derivatives employed were selected from our previous study (22), choosing both those that are highly effective and others less effective in inhibiting malaria parasite growth in culture. These compounds can also be divided into two groups on the basis of their minimum inhibitory concentration (MIC) against *P. falciparum* topoisomerase II. One group consists of compounds (7c, 7e, 7i, 7j, and 7n) that have low MIC values (6–12.5 μM) and contain C-3,6-acridine ring substitution with amine moiety (see Table 1). The other group, which have compounds with higher MIC values (50–100 μM), contains one compound (7d) with a C-3,6-diamino-acridine ring substitution and two compounds containing other substituents (3,6-dichloro (22n) and 3,6-diazido (17r)) at these positions. In addition, two anticancer drugs that act by stabilizing covalent enzyme-cleaved DNA complexes (amsacrine and etoposide) and the two other currently used antimalarial agents (chloroquine and pyronaridine) were included in the study.

Because the compounds tested do not affect the parasites equally, quantitation of cleavable complex formation was conducted at the IC_{50} value of each drug.

TABLE 1

Effects of 9-Anilinoacridines and Other Drugs on *Plasmodium falciparum* Growth *in Vitro* and Formation of Cleavable Complex *in Situ*

Compound	Acridine substituent	Anilino substituent	IC_{50} (μM)[a]	Percent precipitated DN.
7c	3,6-diNH$_2$	1′-NMe$_2$	0.034	18.0 ± 1.4[b]
7d	3,6-diNH$_2$	1′-CH$_2$NMe$_2$	0.04	11.2 ± 1.6[b]
7e	3,6-diNH$_2$	1′-NHSO$_2$Me	0.03	22.7 ± 3.0[b]
7i	3,6-diNH$_2$	1′-OH	0.05	18.0 ± 1.7[b]
7j	3,6-diNH$_2$	1′-OMe	0.15	13.8 ± 1.8[b]
7n	3,6-diNH$_2$	1′-SO$_2$NH$_2$	0.02	12.1 ± 2.9[b]
17r	3,6-diN$_3$	1′-CONH$_2$	0.06	5.2 ± 1.2
22n	3,6-diCl	1′-SO$_2$NH$_2$	6.2	8.9 ± 1.7
Amsacrine	H	1′-NHSO$_2$Me 3′-OMe	3.2	14.7 ± 0.5[b,c]
Etoposide			31	17.3 ± 2.1[b,c]
Chloroquine			0.59	2.1 ± 0.2
Pyronaridine			0.003	6.4 ± 1.2
None				4.1 ± 1.2

[a] Concentration of drug to reduce incorporation of [^{3}H]hypoxanthine by *P. falciparum* K1 by 50%.
[b] Statistically significantly different from nodrug control, $P < 0.01$, $n = 3$.
[c] Measured at IC_{90}.

Table 1 clearly demonstrates that 9-anilinoacridine derivatives with 3,6-diamino substituents were inhibiting *P. falciparum* growth by targeting parasite topoisomerase II *in situ*. The nature of the 1′-anilino substituents (electron donating: 7c, 7e, 7i, 7j; and electron withdrawing: 7n) had little effect on the amount of DNA precipitation (cleavable complex) although compound 7d, without such a group, produced the least product. Compound 7d was the least effective drug among the group in inhibiting *P. falciparum* topoisomerase II *in vitro* (MIC = 50 μM) (22). Comparable yields of cleavable complexes for the six derivatives of 3,6-diamino-9-anilinoacridine indicated that the drugs acted by binding to DNA, and that differences in their IC_{50} values against *P. falciparum* growth reflected variation in uptake efficiency and cytotoxicity. Alterations of the acridine moiety have been reported to affect mammalian cell cytotoxicity and DNA binding affinity similarly, but modifications of the anilino group alter cytotoxicity without affecting DNA binding (20).

On the other hand, derivatives with 3,6-diN$_3$ (17r) and 3,6-diCl (22n) substitutions could not stimulate DNA-protein covalent adduct formation, even when the drug concentrations were raised to IC_{90} values (data not shown), consistent with their insensitivity to inhibition of parasite DNA topoisomerase II *in vitro*. These anilinoacridine analogs may be acting at other targets within the malaria parasite. It has been suggested that the azido derivative could be a prodrug, in which case its metabolite need not affect DNA topoisomerase II (22).

The antitumor drugs, amsacrine and etoposide, have been shown to stimulate the formation of cleavable complex formation in mammalian cells (11, 29). However, these drugs are not effective against *P. falciparum* topoisomerase II (MIC = 1000 μM) and treatment with IC_{90} levels was required to produce significant amounts of cleavable complex formation within the parasites.

As expected the antimalarial drug chloroquine failed to stabilize topoisomerase II–DNA complex. Chloroquine is known to inhibit malaria parasite heme polymerization activity (30).

Pyronaridine, which has 1′-OH and two pyrrolidine residues on an anilino ring attached to a benzonaphthyridine nucleus, is effective for treatment of chloroquine-resistant *P. falciparum* (31). Its IC_{50} value against *P. falciparum in vitro* is 0.003 μM with MIC against topoisomerase II of 11 μM (23). Surprisingly it failed to show inhibitory activity against *P. falciparum* topoisomerase II *in situ*. Studies of pyronaridine on *P. falciparum* ultrastructure revealed that the earliest and most distinct changes induced by the drug occurred in the parasite food vacuole (32). Recently it has been demonstrated that pyronaridine exhibits *in vitro* heme polymerization inhibitory property (33).

The 9-anilinoacridine analogs with C-3,6-diamino ring substitution have proven to be superior to the 3,6-diCl and 3,6-diN$_3$ derivatives both in terms of biological activity and toxicity toward parasite topoisomerase II. However, as this study has shown, it is not possible to predict *a priori* that inhibition of *Plasmodium falciparum* topoisomerase II *in vitro* necessarily indicates that this is indeed the target *in situ*. Inhibitors that act against malaria parasite topoisomerase II both *in vitro* and *in vivo* can be identified based upon the additional demonstration of their ability to generate *in situ* cleavable complexes. Such knowledge will be of assistance in the design of future antimalarial drugs based on the 9-anilinoacridine structure.

ACKNOWLEDGMENTS

The anilinoacridine compounds used in the study were kindly provided by Professors W. A. Denny and R. K. Ralph, University of Auckland, New Zealand. P.W. is a Senior Research Scholar of the Thailand Research Fund.

REFERENCES

1. WHO (1998) WHO Fact sheet No 94, Geneva.
2. Olliaro, P., Cattani, J., and Wirth, D. (1996) *JAMA* 275, 230–233.
3. Liu, L. F. (1989) *Annu. Rev. Biochem.* 58, 351–375.
4. Wang, J. C. (1996) *Annu. Rev. Biochem.* 65, 635–692.
5. Caron, P. R., and Wang, J. C. (1993) *in* Molecular Biology of DNA Topoisomerases and Its Application to Chemotherapy (Andoh, T., Ikeda, H., and Oguro, M., Eds.), pp. 1–20, CRC Press, Boca Raton, FL.
6. Watt, P. M., and Hickson, I. D. (1994) *Biochem. J.* 303, 681–695.
7. Pommier, Y., and Bertrand, R. (1993) *in* The Causes and Consequences of Chromosomal Aberrations (Kirsch, I. R. Ed.) pp.277–309, CRC Press, Boca Raton, FL.
8. Kornberg, A., and Baker, T. A. (1992) *in* DNA Replication (Kornberg, A., and Baker, T. A., Eds.), 2nd ed., pp. 379–401, Freeman, New York.
9. Roca, J. (1995) *Trends Biochem. Sci.* 20, 156–160.
10. Wang, J. C. (1997) *Nature* 386, 329–331.
11. Chen, G. L., Yang, L., Rowe, T. C., Halligan, B. D., Tewey, K. M., and Lui, L. F. (1984) *J. Biol. Chem.* 259, 13560–13566.
12. Rowe, T. C., Chen, G. L., Hsiang, Y. H., and Lui, L. F. (1986) *Cancer Res.* 46, 2021–2026.
13. Sinha, B. K. (1995) *Drugs* 49, 11–19.
14. Capranico, G., Binaschi, M., Borgnetto, M. E., Zunico, F., and Palumbo, M. (1997) *Trends Pharmacol. Sci.* 18, 323–329.
15. D'Arpa, P. (1994) *in* Advances in Pharmacology. DNA Topoisomerases: Topoisomerase-Targeting Drugs (Liu, L. F., Ed.), Vol. 29B, pp. 127–143, Academic Press, San Diego, CA.
16. Wang, J. C. (1994) *in* Advances in Pharmacology. DNA Topoisomerases: Biochemistry and Molecular Biology (Liu, L. F., Ed.), Vol. 29A, pp. 1–19, Academic Press, San Diego, CA.
17. Miller, L. P., Pyesmany, A. F., Wolff, L. J., Rogers, P. C., Siegel, S. E., Wells, R. J., Buckley, J. D., and Hammond, G. D. (1991) *Cancer* 67, 2235–2240.
18. Nelson, E. M., Tewey, K. M., and Liu, L. F. (1984) *Proc. Natl. Acad. Sci. USA* 81, 1361–1365.
19. Robinson, M. J., and Osheroff, N. (1990) *Biochemistry* 29, 2511–2515.
20. Zwelling, L. A., Mitchell, M. J., Satitpunwaycha, P., Mays, J., Altschuler, E., Hinds, M., and Baguley, B. C. (1992) *Cancer Res.* 52, 209–217.
21. Cain, B. F., Atwell, G. J., and Denny, W. A. (1975) *J. Med. Chem.* 18, 1110–1117.
22. Gamage, S. A., Tepsiri, N., Wilairat, P., Wojcik, J., Figgitt, D. P., Ralph, R. K., and Denny, W. A. (1994) *J. Med. Chem.* 37, 1486–1494.
23. Chavalitshewinkoon, P., Wilairat, P., Gamage, S. A., Denny, W. A., Figgitt, D. P., and Ralph, R. K. (1993) *Antimicrob. Agents Chemother.* 37, 403–406.
24. Figgitt, D. P., Denny, W. A., Chavalitshewinkoon, P., Wilairat, P., and Ralph, R. K. (1992) *Antimicrob. Agents Chemother.* 36, 1644–1647.
25. Thaithong, S., Beale, G. H., and Chutmongkonkul, M. (1983) *Trans. R. Soc. Trop. Med. Hyg.* 77, 228–231.
26. Trager, W., and Jensen, J. B. (1976) *Science* 193, 673–675.
27. Desjardins, R. E., Canfield, C. J., Haynes, J. D., and Chulay, J. C. (1979) *Antimicrob. Agents Chemother.* 16, 710–718.
28. Lambros, C., and Vanderberg, J. P. (1979) *J. Parasitol.* 65, 418–420.
29. Zwelling, L. A., Estey, E., Silberman, L., Doyle, S., and Hittelman, W. (1987) *Cancer Res.* 47, 251–7.
30. Slater, A. F. G., and Cerami, A. (1992) *Nature* 355, 167–169.
31. Chen, C., and Zheng, X. (1992) *Biomed. Environ. Sci.* 5, 149–160.
32. Kawai, S., Kano, S., Chang, C., and Suzuki, M. (1996) *Am. J. Trop. Med. Hyg.* 55, 223–229.
33. Dorn, A., Vippagunta, S. R., Matile, H., Jaquet, C., Vennerstrom, J. L., and Ridley, R. G. (1998) *Biochem. Pharmacol.* 55, 727–736.

Biochemical Pharmacology, Vol. 59, pp. 1337–1344, 2000.

ISSN 0006-2952/00/$–see front matter
PII S0006-2952(00)00271-9

Inactivation of Artemisinin by Thalassemic Erythrocytes

Juree Charoenteeraboon, Sumalee Kamchonwongpaisan,† Prapon Wilairat,* Phantip Vattanaviboon‡ and Yongyuth Yuthavong†§*

*Department of Biochemistry, Faculty of Science, Mahidol University, Bangkok 10400; †National Science and Technology Development Agency, Bangkok 10400; and ‡Department of Clinical Microscopy, Faculty of Medical Technology, Mahidol University, Bangkok 10600, Thailand

ABSTRACT. *Plasmodium falciparum* infecting α-thalassemic erythrocytes (Hb H or Hb H/Hb Constant Spring) is resistant to artemisinin derivatives. Similar resistance, albeit at a much lower level, is shown by the parasite infecting β-thalassemia/Hb E erythrocytes. The resistance is due to host-specific factors, one of which is the higher uptake of the drugs by thalassemic erythrocytes than normal erythrocytes, due to binding with Hb H. In addition to higher drug binding, incubation of artemisinin with α-thalassemic erythrocytes resulted in preferential inactivation of the drug. Both thalassemic and normal erythrocytes have the capability to inactivate the drug. Addition of serum can protect against inactivation by normal erythrocytes, but not by thalassemic erythrocytes. Incubation with either the hemolysate or the membrane fraction from these erythrocytes also resulted in preferential inactivation of the drug. The drug was also inactivated by purified Hb H. It is concluded that the ineffectiveness of artemisinin derivatives against *P. falciparum* infecting thalassemic erythrocytes is due partly to competition of the host cell components for binding with the drugs, and partly to inactivation of the drugs by the cell components. BIOCHEM PHARMACOL 59;11:1337–1344, 2000. © 2000 Elsevier Science Inc.

KEY WORDS. *Plasmodium falciparum*; malaria; thalassemia; artemisinin; erythrocytes; artemisinin inactivation

Falciparum malaria continues to afflict increasing millions across the tropical latitudes of the world. It remains one of the most lethal and widespread diseases due to the emergence of parasites resistant to most available antimalarial drugs [1]. Artemisinins, highly effective antimalarial drugs derived from *Artemisia annua* Linn., have played an important role for many years in the treatment of these resistant parasites, with no significant occurrence of resistance as yet [2]. *In vitro* evidence for artemisinin resistance was found when α-thalassemic erythrocytes, both Hb H[1] and Hb H/Hb CS, with genotypes of α-thal1/α-thal2 (--/-α) and α-thal1/Hb CS (--/α^{cs}α), respectively, were used as parasite hosts [3–5]. Similar reduction in artemisinin sensitivity of the parasite was also found in the old cell fractions of α-thal trait (αα/-α) and β-thal trait erythrocytes, compared with the same cell fraction of normal erythrocytes [6]. This host-dependent artemisinin resistance may be of epidemiological significance, since α-thalassemic genes are found in malaria endemic areas, and, thus, are potential sources of drug resistance [7]. Therefore, it is important to understand the factors responsible for this host-dependent artemisinin resistance.

We have shown previously that the apparent artemisinin resistance of *Plasmodium falciparum* infecting α-thalassemic erythrocytes is due mainly to the higher capacity of uninfected α-thalassemic erythrocytes for drug accumulation as compared with that of genetically normal erythrocytes [4]. This phenomenon results in depletion of the drug from the parasite environment. Subsequently, we showed that Hb H accounts for the increased binding capacity of Hb H erythrocytes, and that the binding capacity of Hb H is 5–7 times that of Hb A [5]. There is also an increase in these cells of other intraerythrocytic components, such as heme and non-heme irons [8, 9]. These react with artemisinins [2] and may also interfere with drug effectiveness. In this report, we present evidence for preferential artemisinin inactivation by α-thalassemic erythrocytes as an additional mechanism for this host-dependent artemisinin resistance.

MATERIALS AND METHODS

Materials

Artemisinin was purchased from the National Center of Natural Science and Technology, Hanoi, Vietnam. Artemisinin was recrystallized from a methylene chloride/hex-

§ Corresponding author: Professor Yongyuth Yuthavong, National Science and Technology Development Agency, 73/1 Rama VI Rd., Rajdhevee, Bangkok 10400, Thailand. Tel. (66) 2-6448002; FAX (66) 2-6448027; E-mail: yongyuth@nstda.or.th

[1] Abbreviations: Hb, hemoglobin; Hb CS, hemoglobin Constant Spring; α-thal, α-thalassemia; β-thal, β-thalassemia; and K_d, dissociation constant.

Received 11 August 1999; accepted 5 November 1999.

ane mixture to give white needles (m.p. 154–156°). Dihydroartemisinin was prepared from artemisinin by reduction with sodium borohydride [10] and recrystallized from a methylene chloride/hexane mixture to give white needles (m.p. 151–153°). Radioactive 15-[^{14}C]artemisinin was a gift from the Research Triangle Institute. The specific activity of [^{14}C]artemisinin was 26.1 Ci/mol. 2,8-[^{3}H]Hypoxanthine was purchased from Moravek Biochemicals. The specific activity of [^{3}H]hypoxanthine was 20–30 Ci/mmol.

Subjects

Thalassemic blood samples were obtained from the Division of Hematology, Department of Medicine, Faculty of Medicine, Siriraj Hospital, Mahidol University, where hemoglobin types were identified. Subjects had the following genotypes: Hb H (α-thal1/α-thal2), Hb H/Hb CS (α-thal1/Hb CS), and β-thalassemia with Hb E (β-thal/Hb E). All were non-splenectomized and had received no blood transfusions for at least 3 months before the collection of blood. Citrate–phosphate–dextrose solution was used as an anticoagulant.

In Vitro Culture of P. falciparum

A chloroquine-resistant strain of *P. falciparum* (K1) was obtained from an infected individual in the Kanchanaburi province of Thailand [11]. Parasites were maintained continuously in human erythrocytes using RPMI 1640 medium supplemented with 25 mM HEPES, pH 7.4, 0.2% $NaHCO_3$, 40 μg/mL of gentamicin, and 10% human serum [12]. Parasite growth was synchronized at the ring stage by 5% sorbitol treatment [13], and the schizont stage was collected by Percoll centrifugation [14]. Washed thalassemic blood cells were co-cultivated with schizont-infected erythrocytes for at least 96 hr before determining antimalarial sensitivity of the infecting parasites.

Antimalarial Activity Assay

In vitro antimalarial activity was determined by using the [^{3}H]hypoxanthine incorporation method [15]. Briefly, 25-μL aliquots of drug solutions of different concentrations were placed in a 96-well plate together with 200 μL of a 1.5% cell suspension of parasitized erythrocytes containing 1–2% parasitemia at the early ring stage. The mixtures were incubated in a candle jar at 37°. After 24 hr of incubation, 25 μL (0.25 μCi) of [^{3}H]hypoxanthine was added to each well. The mixtures were incubated further under the same conditions for 18–24 hr. DNA of parasites was harvested onto glass filter paper (Unifilter®, Packard). The filters were dried, and liquid scintillation fluid was added for radioactivity measurement in a 6-probe liquid scintillation counter (Packard). An IC_{50} value was determined from the sigmoid curve of percent [^{3}H]hypoxanthine incorporation against drug concentration.

In some experiments, to explore the effect of Hb H on the antimalarial activity of dihydroartemisinin, isolated Hb A and Hb H prepared from lysate of Hb H erythrocytes [5] were added to the parasites together with dihydroartemisinin. Final concentrations of Hb H and Hb A in the tests ranged from 7.5 to 60 μM.

Effect of Intact Erythrocytes on Artemisinin Inactivation

An aliquot (70 μL) of washed erythrocytes was incubated at 37° with 630 μL of [^{14}C]artemisinin in culture medium without serum (incomplete medium) for 2 hr. The final concentration of the radiolabelled drug was 1 μM. At the end of the incubation, the cell mixture was centrifuged at 10,053 *g* (Hettich, Mikro 24–48R centrifuge) for 30 sec at 4° to separate free drug from intact cells. The supernatant was used for determining artemisinin effectiveness, and the cell pellet was used for measuring artemisinin accumulation.

In some experiments, to determine the protective effect of serum on artemisinin inactivation by erythrocytes, medium containing from 10 to 100% serum was used in place of incomplete medium. In these experiments, cells were incubated with the radiolabelled drug, and then the drug effectiveness was determined from the supernatants of the cell mixtures at various time points for up to 4 hr.

Determination of Artemisinin Effectiveness

Supernatant was diluted to appropriate concentrations with culture medium. Antimalarial activity of diluted samples was determined in triplicate as described above. An aliquot (100 μL) of the undiluted supernatant was mixed with 900 μL of water and 4 mL of Triton X-100-based liquid scintillation fluid for determination of radioactivity. Then the concentration of [^{14}C]artemisinin was calculated from its specific activity. The drug effectiveness index was defined as IC_{50} of control/IC_{50} of sample.

Determination of [^{14}C]Artemisinin Accumulation in Intact Erythrocytes

After the incubation, cells were washed three times with cold 10 mM PBS solution to remove excess drug. Cells were lysed with 10 vol. of hypotonic solution (10 mM phosphate, pH 7.4). An aliquot of the lysate (500 μL) was incubated with an equal volume of 2% SDS solution at 60° for 1 hr. Then the mixture was bleached with 2 mL of 15% hydrogen peroxide at 60° for 12 hr. Next, 4 mL of Triton X-100-based liquid scintillation fluid was added for measurement of radioactivity in a liquid scintillation counter (Beckman). The results were expressed as amount of the drug (picomoles) per 10^{7} cells.

TABLE 1. Amount of artemisinin accumulation in intact cells, cytosol (D_c), and membrane (D_m) compartments of uninfected normal and thalassemic erythrocytes

Erythrocyte Compartment	[^{14}C]Artemisinin (pmol/10^9 cells)			
	Normal	Hb H	Hb H/Hb CS	β-thal/Hb E
Intact cells	57.0 ± 10.0	337.1 ± 129.9*	657.0 ± 122.5*	223.8 ± 45.3*
Cytosol (D_c)	63.8 ± 11.3	304.1 ± 103.9*	509.2 ± 124.8*	207.9 ± 44.7*
$\%D_c$†	88.6 ± 1.6	85.2 ± 5.0‡	83.3 ± 8.1‡	88.9 ± 3.4‡
Membrane (D_m)	8.3 ± 2.0	58.3 ± 35.2*	95.2 ± 22.9*	26.2 ± 10.1*
$\%D_m$§	12.1 ± 2.5	14.8 ± 5.0‡	16.7 ± 8.1‡	11.1 ± 3.4‡
D_c/D_m Ratio	7.5 ± 1.7	6.4 ± 2.8‡	5.8 ± 2.7‡	8.6 ± 2.7‡

Intact erythrocytes, membrane, and cytosol were incubated at 37° for 2 hr, with 1 μM of [^{14}C]artemisinin in culture medium without serum as a 10% cell suspension or equivalent. After incubation, free drug was separated from the intact cells, membrane, and cytosol by centrifugation for intact cells and membrane, and by ultracentrifugation through 10-kDa cut-off membranes for cytosol. After washing, the pellets and the cytosol-retentate were treated as described in the text for measurement of radioactivity. The results (means ± SEM), expressed as amounts of the drug per 10^9 cells, are from three duplicate experiments. Statistical analyses were performed by using a non-parametric Mann-Whitney U test.

*$P = 0.05$, $N = 3$.

† $\%D_c = D_c \times 100/(D_c + D_m)$.

‡ Not significantly different, $N = 3$.

§ $\%D_m = D_m \times 100/(D_c + D_m)$.

Effect of Cytosol and Membrane on Artemisinin Inactivation

One milliliter of 50% (v/v) erythrocyte suspension was lysed with 3.5 mL of hypotonic solution with freeze-thawing to obtain complete lysis. An aliquot (630 μL) of the lysate was centrifuged at 22,620 *g* for 10 min at 4°. The pellet was washed with 10 mM phosphate buffer, pH 7.4, five times, to remove bound hemoglobin. Supernatant and pellet were used as cytosol and membrane samples, respectively.

Cytosol and membrane preparations equivalent to 10% (v/v) of red blood cells were incubated with 1 μM [^{14}C]artemisinin at 37° for 2 hr. The cytosol sample was centrifuged in a Centricon 10® tube to separate free drug from hemolysate. The filtrate was used for determining the drug effectiveness index. The retentate was adjusted to its original volume with hypotonic solution and treated with SDS and hydrogen peroxide to determine artemisinin accumulation as described. Free drug was separated from membrane by centrifugation at 22,620 *g*. Drug effectiveness index and accumulation then were determined as described.

Statistical Analysis

The Mann–Whitney U test was used for comparing the data from normal and variant erythrocytes based on independent random samples.

RESULTS AND DISCUSSION

Artemisinin Resistance of P. falciparum *Infecting Variant Erythrocytes*

Resistance to artesunate of normally susceptible *P. falciparum* when infecting thalassemic erythrocytes was first reported in 1989 [3]. Similar findings of resistance to artemisinin [4] and dihydroartemisinin [5] were reported subsequently. In this study, the resistance of *P. falciparum* to artemisinin was confirmed again in Hb H-containing erythrocytes *in vitro*. The IC_{50} values were 42.3 ± 29.5 nM for Hb H ($N = 9$) and 62.5 ± 43.3 nM for Hb H/Hb CS ($N = 6$), approximately 12 and 17 times higher than that of *P. falciparum* infected normal erythrocytes (3.6 ± 1.8 nM, $N = 5$). This host-specific resistance also was found with parasites infecting β-thal/Hb E erythrocytes, albeit with a lower IC_{50} value (9.0 ± 1.8 nM, $N = 4$). The IC_{50} values for artemisinin against the parasites in these variant erythrocytes were significantly higher than those in normal erythrocytes ($P < 0.01$) for the three variants. These findings are also in line with a recent report where artemisinin sensitivities of the parasites were found to be reduced in the old cell fractions of α- and β-thal trait erythrocytes as compared with the same fraction of normal controls [6].

Increased Artemisinin Accumulation in Thalassemic Erythrocytes

Preferential accumulation [4, 5] and increased binding of artemisinin in Hb H-containing erythrocytes due to the presence of Hb H [5] are the major factors that contribute to the apparent resistance of parasites to the drug. The increase in artemisinin accumulation was also confirmed in this study. As shown in Table 1, after incubation of [^{14}C]artemisinin with variant erythrocytes, the amounts of artemisinin accumulated in Hb H and Hb H/Hb CS erythrocytes were, respectively, 5.9 and 11.5 times that for normal erythrocytes. This phenomenon was also observed, but to a lesser extent, in β-thal/Hb E erythrocytes. The levels of [^{14}C]artemisinin accumulation of these variant erythrocytes were significantly higher than that of normal erythrocytes ($P < 0.05$).

Artemisinin Inactivation by Erythrocytes

The differences between the fold increase in IC_{50} values and in drug accumulation of artemisinin in α-thalassemic erythrocytes compared with normal erythrocytes indicated the presence of an additional mechanism for decreasing artemisinin effectiveness. We hypothesize that this mechanism involves preferential inactivation of the drug by the thalas-

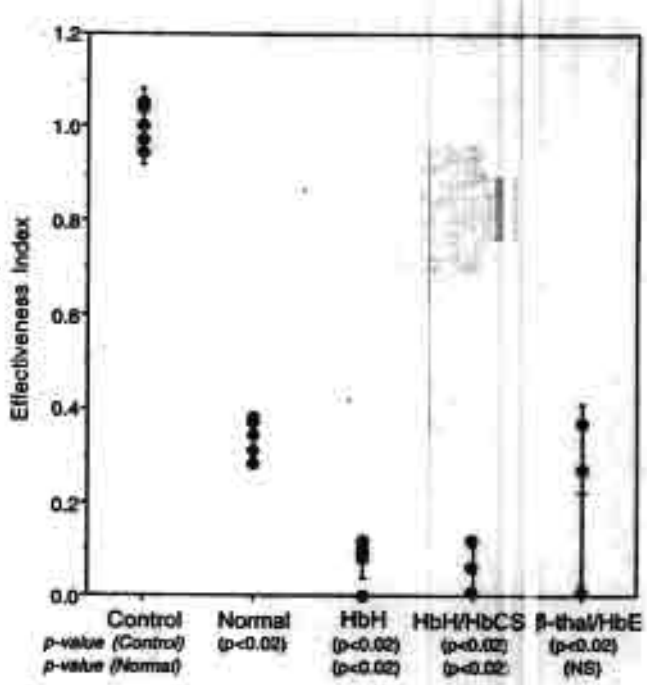

FIG. 1. Effectiveness index of [^{14}C]artemisinin following exposure to thalassemic and normal erythrocytes for 2 hr. Data points and means ± SEM are shown. Numbers of samples in the tests were 6 for control and normal, 5 for Hb H, 4 for Hb H/Hb Constant Spring (Hb CS), and 3 for β-thal/Hb E.

semic erythrocytes. To explore this artemisinin-inactivation hypothesis, the effectiveness of the drug, defined as IC_{50} for artemisinin in control incubated without erythrocytes/IC_{50} in the sample, was determined after incubation of [^{14}C]artemisinin with intact erythrocytes from normal and thalassemic individuals in incomplete medium for 2 hr. The results are shown in Fig. 1. The effectiveness index of [^{14}C]artemisinin following exposure to normal erythrocytes decreased significantly to 0.34 ± 0.04 (N = 6) as compared with control without erythrocytes (1.00 ± 0.08). This decrease in [^{14}C]artemisinin effectiveness was not due to instability of the drug, since the effectiveness index of [^{14}C]artemisinin incubated in the medium remained unchanged up to 12 hr of incubation (data not shown). The effectiveness indices of [^{14}C]artemisinin following exposure to both types of Hb H-containing erythrocytes significantly decreased to a greater extent than that of [^{14}C]artemisinin exposed to normal erythrocytes: 0.08 ± 0.04 for Hb H (N = 5) and 0.05 ± 0.05 for Hb H/Hb CS (N = 4). The effectiveness index of [^{14}C]artemisinin exposed to β-thal/Hb E erythrocytes (0.22 ± 0.19, N = 3) was not significantly different from that when exposed to normal erythrocytes. These results indicated that artemisinin was inactivated by all types of erythrocytes, but preferentially by Hb H-containing erythrocytes.

Protective Effect of Human Serum against Artemisinin Inactivation

Since artemisinin and its derivatives are effective against malarial parasites *in vitro* and *in vivo*, where serum is present, it is possible that serum exerts a protective effect against inactivation of artemisinin by the erythrocytes. To investigate the effect of serum on artemisinin activity upon exposure to erythrocytes, similar incubations were carried out in the presence of increasing amounts of serum. The data are shown in Fig. 2. Upon exposure to normal erythrocytes, [^{14}C]artemisinin effectiveness was retained in the presence of serum (Fig. 2A). The presence of 50% serum resulted in full retention of artemisinin effectiveness for up to 4 hr of incubation. However, for Hb H-containing erythrocytes, the presence of serum did not improve the effectiveness index of artemisinin, only delaying the inactivation process (Fig. 2, B and C). These data indicate that serum protects against artemisinin inactivation by decreasing artemisinin entry into the erythrocytes.

The role of human serum in protecting or stabilizing the drug against inactivation by normal erythrocytes could be due to the presence of proteins in serum. It has been reported that serum albumin, the major protein in serum, can bind non-covalently to many drugs and small molecules [16, 17] including artemisinin [18]. In addition, α_1-acid glycoprotein, an acute phase protein found at high levels during infection, has also been reported to bind artemisinin non-covalently with a greater binding affinity than albumin [19]. Binding of the drug to these serum proteins may account for the protection of the drug *in vitro* by decreasing the rate of drug transportation into uninfected normal erythrocytes or by competing for the drug with components in the cells.

In Hb H-containing erythrocytes, human serum was not able to protect artemisinin from inactivation. The results also showed a faster rate of artemisinin inactivation by both Hb H and Hb H/Hb CS erythrocytes than by normal erythrocytes. This indicates that there was competition for artemisinin by components within the cells (e.g. Hb H and Hb A) and those outside (e.g. serum components such as serum albumin and α_1-acid glycoprotein). The binding affinities of four major binding components can be listed as follows: α_1-acid glycoprotein with arteether (K_d = 4.4 ± 0.4 μM), human serum albumin with arteether (K_d = 84 ± 7 μM), Hb H with dihydroartemisinin (K_d = 66 ± 17 μM), and Hb A with dihydroartemisinin (K_d = 224 ± 15 μM) [5, 19]. There are two artemisinin binding sites in α_1-acid glycoprotein and Hb H, and one in human serum albumin and Hb A [5, 19]. Although α_1-acid glycoprotein may possess stronger drug binding affinity than Hb H, assuming that artemisinin derivatives have similar binding characteristics, the glycoprotein is present in much lower concentration in normal human serum, thus driving the binding towards Hb H. Binding of artemisinin to Hb H probably is also favored over binding to human serum albumin. These considerations argue for favored localization of artemisinin in Hb H-containing cells and its subsequent inactivation there. Even if artemisinin does not bind to Hb H with as high affinity as to the serum proteins, inactivation would still result if it could dissociate from the serum proteins and penetrate the erythrocytes.

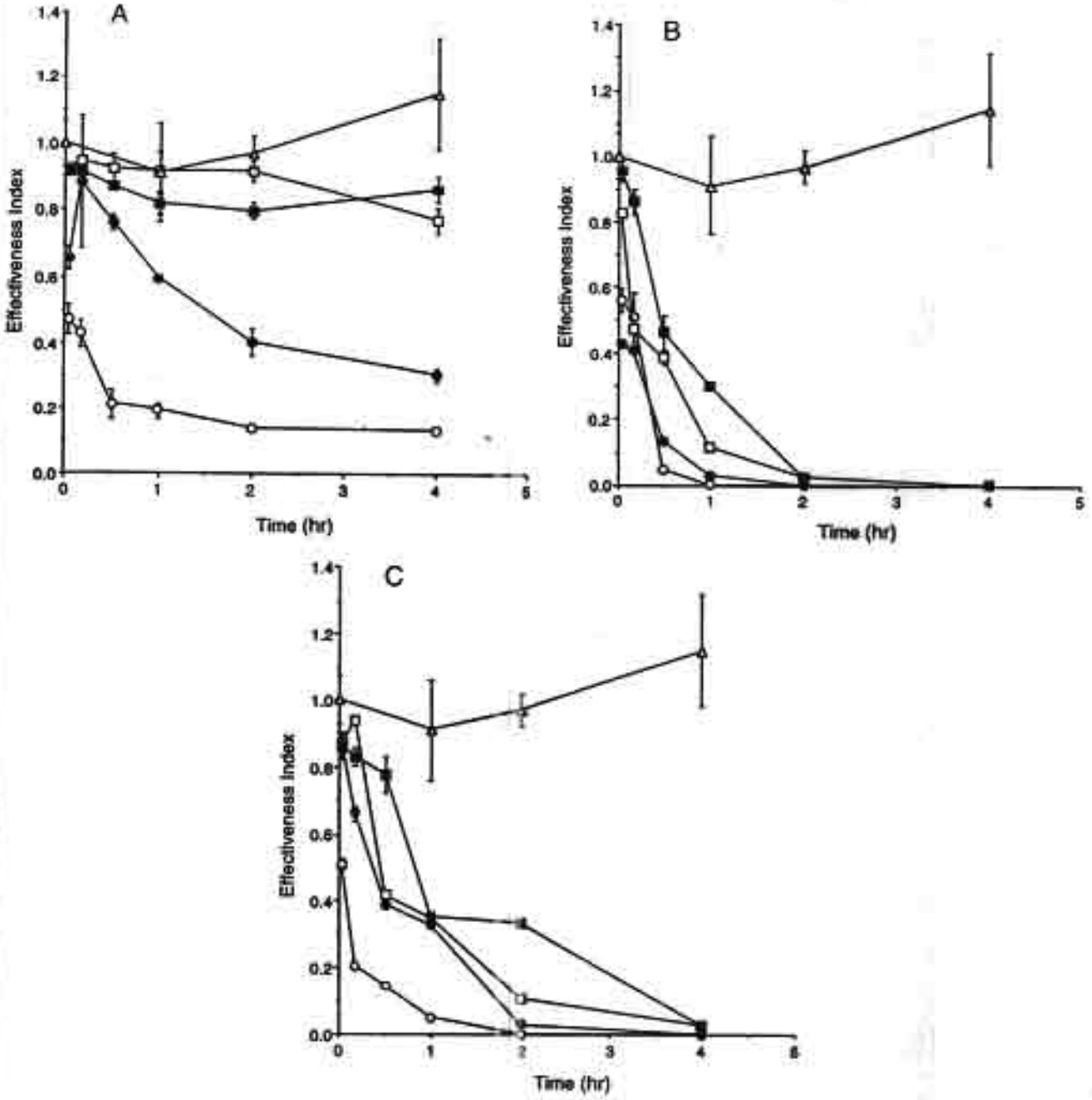

FIG. 2. Effectiveness index of [^{14}C]artemisinin following exposure to erythrocytes in the absence (○) and presence of 10% (●), 50% (□), and 100% (■) human serum, and (△) in the control medium without cells and serum. (A) Normal erythrocytes, (B) Hb H erythrocytes, and (C) Hb H/Hb CS erythrocytes. The experiments were performed twice using two different sets of samples. The data shown here are means ± SD from one of the two experiments where similar results were obtained.

Effect of Cytosolic and Membrane Compartments on Artemisinin Inactivation

Distributions of [^{14}C]artemisinin in erythrocyte membrane and cytosolic fractions were investigated. As shown in Table 1, the amount of drug was higher in the cytosol compartment than in the membrane fraction of both normal and variant erythrocytes. Cytosol and membrane from both types of Hb H-containing erythrocytes accumulated [^{14}C]artemisinin to a higher extent than those of normal and β-thal/Hb E erythrocytes. The ratios of the drug in the two compartments for these variant erythrocytes were not significantly different from normal. These values were also in line with the previous report using dihydroartemisinin [5].

To investigate further the role of the two compartments in inactivating artemisinin, radiolabelled drug was incubated with washed membrane and cytosol of normal and thalassemic erythrocytes, and free drug fractions were separated for determination of drug effectiveness. The results of the effects of cytosolic fractions and of membrane

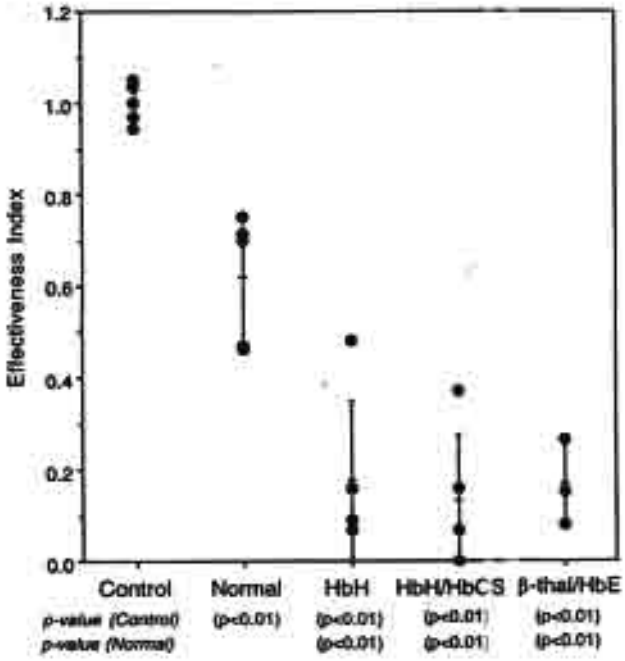

FIG. 3. Effectiveness index of free [^{14}C]artemisinin obtained from thalassemic and normal hemolysates after a 2-hr incubation. Data points and means ± SEM are shown. Numbers of samples in the tests were 5 for all.

fractions are shown in Figs. 3 and 4, respectively. The effectiveness index of free artemisinin extracted after 2 hr of incubation with the cytosolic fraction of Hb H, Hb H/Hb CS, β-thal/Hb E, and normal erythrocytes decreased markedly from 1.0 in control to 0.18 ± 0.17, 0.14 ± 0.14, 0.17 ± 0.08, and 0.62 ± 0.14, respectively. These effectiveness indices of the drugs from the cytosolic fractions of variant erythrocytes were also significantly less than the index from normal erythrocytes (Fig. 3). Upon incubation with membrane fraction, drug effectiveness was also decreased significantly in the presence of Hb H and Hb H/Hb CS membranes (the indices were 0.41 ± 0.17 for Hb H and 0.41 ± 0.09 for Hb H/Hb CS), and to a lesser extent in the presence of membrane from β-thal/Hb E (0.67 ± 0.26) and normal erythrocytes (0.81 ± 0.05). Both cytosolic and membrane components of normal and thalassemic erythrocytes inactivated artemisinin, and the inactivation was most pronounced in the cytosolic fraction of Hb H-containing erythrocytes.

Role of Hb H on Artemisinin Inactivation

The role of Hb H in Hb H-containing erythrocytes on artemisinin antimalarial activity has been suggested to be due to preferential binding of artemisinin and its derivatives to Hb H, thereby causing the drugs to accumulate at high concentrations in these variant erythrocytes [5]. To determine whether Hb H could also inactivate the drug, purified Hb H was added to the culture medium, and the antimalarial activity of dihydroartemisinin was tested. Addition of Hb H to the malaria culture caused a large increase in the dihydroartemisinin IC_{50} value, whereas addition of Hb A showed little effect (Fig. 5). When the concentrations of dihydroartemisinin were corrected for the portion of the drug bound to added Hb H (K_d = 66 μM) [5], IC_{50} values were still anomalously high, indicating a role of Hb H in dihydroartemisinin inactivation.

Since artemisinin inactivation occurred in normal as well as β-thal/Hb E erythrocytes, with the cytosolic fraction playing a major role in the inactivation process, factors other than Hb H alone must also be responsible for drug inactivation. It has been reported that antioxidant enzymes, e.g. catalase, glutathione peroxidase, glutathione reductase, and superoxide dismutase, are present in increased amounts in thalassemic erythrocytes [20, 21]. Iron is also found at high levels in both α- and β-thalassemic erythrocytes [8, 9]. Interaction of artemisinin with some of these cytosolic components may lead to its inactivation. In addition, in the presence of iron [2], artemisinin binding and/or alkylation of proteins in the cells can also lead to a decrease in drug availability. This hypothesis is supported by various reports on the interaction of artemisinin with iron, redox metal, heme, and proteins [2, 22–27].

In a study of the pharmacokinetics of artesunate in α-thalassemic subjects, it was found that plasma drug concentrations of biologically active drug metabolites in the plasma of the thalassemic subjects are higher than normal, and the volume of distribution is 15-fold lower [28]. Although this result is surprising, since higher uptake of the drug by thalassemic erythrocytes [4, 5] would be expected to lead to lower plasma concentrations and higher volume of distribution, possible explanations were given as slow re-

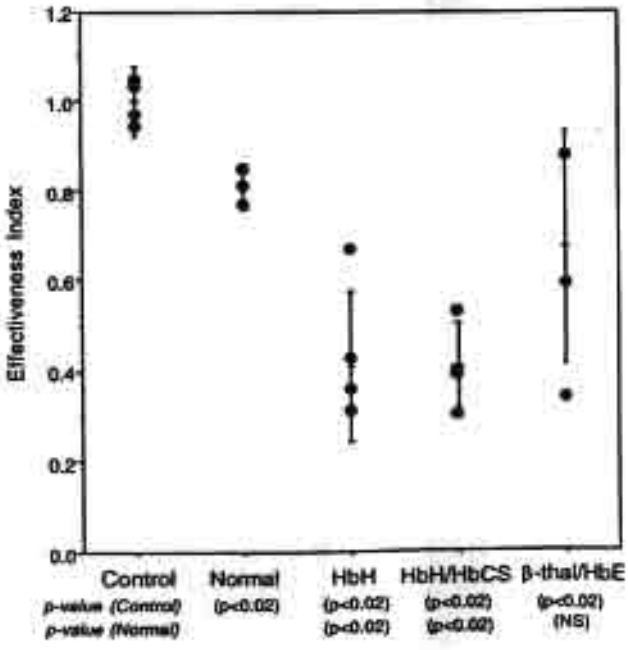

FIG. 4. Effectiveness index of free [^{14}C]artemisinin obtained from thalassemic and normal membranes after a 2-hr incubation. Data points and means ± SEM are shown. Numbers of samples in the tests were 4 for all.

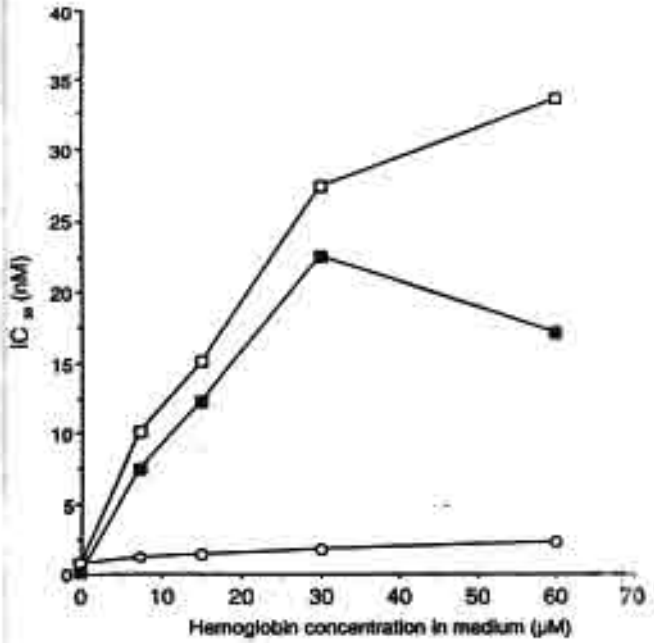

FIG. 5. Effect of Hb H on the IC_{50} values of artemisinin against *P. falciparum* in vitro. Key: (○) Hb A; (□) Hb H; and (■) corrected Hb H. The data were averaged from a triplicate measurement.

lease of the drug and metabolites into the plasma, and differences in drug metabolism. Our present report of artemisinin inactivation by thalassemic erythrocytes is not necessarily in conflict with the pharmacokinetic studies on artesunate [28], since different drugs were used, and plasma concentrations are determined by complex factors not limited to drug inactivation.

In conclusion, the results reported here show the presence of an additional mechanism responsible for resistance to artemisinin by *P. falciparum* infecting α-thalassemic red cells in vitro, namely, the inactivation of artemisinin. The host-specific resistance, resulting both from drug binding to Hb H and other erythrocyte components and from its inactivation, may be an important consideration in the clinical use of the drug for malaria treatment, especially in areas with a high frequency of thalassemic genes. Although no artemisinin-resistant malaria parasites have been detected to date, drug-resistant parasites and high recrudescence rates may result if artemisinin and its derivatives are used without awareness of the significance of this host-specific effect.

This work was supported by National Institutes of Health International Collaborations in Infectious Disease Research Grant U01-AI35827, a Senior Research Scholarship (P. W.) from The Thailand Research Fund, and Thailand's National Center for Genetic Engineering and Biotechnology (S. K.). The assistance of Professor Suthat Fucharoen in supplying blood samples is gratefully acknowledged.

References

1. Olliaro PL and Yuthavong Y, An overview of chemotherapeutic targets for antimalarial drug discovery. *Pharmacol Ther* 81: 91–110, 1999.
2. Meshnick SR, Taylor TE and Kamchonwongpaisan S, Artemisinin and the antimalarial endoperoxides: From herbal remedy to targeted chemotherapy. *Microbiol Rev* 60: 301–315, 1996.
3. Yuthavong Y, Butthep P, Bunyaratvej A and Fucharoen S, Decreased sensitivity to artesunate and chloroquine of *Plasmodium falciparum* infecting hemoglobin H and/or hemoglobin Constant Spring erythrocytes. *J Clin Invest* 83: 502–505, 1989.
4. Kamchonwongpaisan S, Chandra-ngam G, Avery MA and Yuthavong Y, Resistance to artemisinin of malaria parasites (*Plasmodium falciparum*) infecting α-thalassemic erythrocytes in vitro: Competition in drug accumulation with uninfected erythrocytes. *J Clin Invest* 93: 467–473, 1994.
5. Vattanaviboon P, Wilairat P and Yuthavong Y, Binding of dihydroartemisinin to hemoglobin H: Role in drug accumulation and host-induced antimalarial ineffectiveness of α-thalassemic erythrocytes. *Mol Pharmacol* 53: 492–496, 1998.
6. Senok AC, Li K, Nelson EAS and Chung KW, *In vitro* sensitivity of artemeter in *Plasmodium falciparum*-infected beta-thalassaemic trait erythrocytes. *Parasitology* 118: 145–149, 1999.
7. Yuthavong Y and Wilairat P, Protection against malaria by thalassemia and haemoglobin variants. *Parasitol Today* 9: 241–245, 1993.
8. Shalev O, Repka T, Goldfarb A, Grinberg L, Abrahamov A, Olivieri NF, Rachmilewitz EA and Hebbel RP, Deferiprone (L1) chelates pathologic iron deposits from membranes of intact thalassemic and sickle red blood cells both *in vitro* and *in vivo*. *Blood* 86: 2008–2013, 1995.
9. Schrier SL, Thalassemia, Pathophysiology of red cell changes. *Annu Rev Med* 45: 211–218, 1994.
10. Brossi A, Venugopalan B, Dominguez Gerpe L, Yeh HJC, Flippen-Anderson JL, Buchs P, Luo XD, Milhous W and Peters W, Arteether, a new antimalarial drug: Synthesis and antimalarial properties. *J Med Chem* 31: 645–650, 1988.
11. Thaithong S, Beale GH and Chutmongkonkul M, Susceptibility of *Plasmodium falciparum* to five drugs: An *in vitro* study of isolates mainly from Thailand. *Trans R Soc Trop Med Hyg* 77: 228–231, 1983.
12. Trager W and Jensen JB, Human malarial parasites in continuous culture. *Science* 193: 673–675, 1976.
13. Lambros C and Vanderberg JP, Synchronization of *Plasmodium falciparum* erythrocytic stages in culture. *J Parasitol* 65: 418–420, 1979.
14. Tosta CE, Sedegah M, Henderson DC and Wedderburn N, *Plasmodium yoelii* and *Plasmodium berghei*: Isolation of infected erythrocytes from blood by colloidal silica gradient centrifugation. *Exp Parasitol* 50: 7–15, 1980.
15. Desjardins RE, Canfield CJ, Haynes JD and Chulay JD, Quantitative assessment of antimalarial activity *in vitro* by a semiautomated microdilution technique. *Antimicrob Agents Chemother* 16: 710–718, 1979.
16. Peters T Jr, Serum albumin. *Adv Protein Chem* 37: 161–245, 1985.
17. Fehske KJ, Muller WE and Wollert U, The location of drug binding sites in human serum albumin. *Biochem Pharmacol* 30: 687–692, 1981.
18. Yang YZ, Little B and Meshnick SR, Alkylation of proteins by artemisinin: Effects of heme, pH, and drug structure. *Biochem Pharmacol* 48: 569–573, 1994.
19. Wanwimolruk S, Edwards G, Ward SA and Breckenridge AM, The binding of the antimalarial arteether to human plasma proteins *in vitro*. *J Pharm Pharmacol* 44: 940–942, 1992.

20. Prasertkaew S, Bunyaratvej A, Fucharoen S and Wasi P, Comparison of erythrocyte antioxidative enzyme activities between two types of haemoglobin H disease. *J Clin Pathol* 39: 1299–1303, 1986.
21. Gerli GC, Beretta L, Bianchi M, Pellegatta A and Agnoletti A, Erythrocyte superoxide dismutase, catalase and glutathione peroxidase activities in β-thalassemia (major and minor). *Scand J Haematol* 25: 87–92, 1980.
22. Kamchonwongpaisan S, Vanitcharoen N and Yuthavong Y, The mechanism of antimalarial action of artemisinin (qinghaosu). In: *Lipid-Soluble Antioxidants: Biochemistry and Clinical Applications* (Eds. Ong ASH and Packer L), pp. 363–372. Birkhauser, Basel, 1992.
23. Meshnick SR, Yang YZ, Lima V, Kuypers F, Kamchonwongpaisan S and Yuthavong Y, Iron-dependent free radical generation from the antimalarial agent artemisinin (qinghaosu). *Antimicrob Agents Chemother* 37: 1108–1114, 1993.
24. Zhang F, Gosser DK Jr and Meshnick SR, Hemin-catalyzed decomposition of artemisinin (qinghaosu). *Biochem Pharmacol* 43: 1805–1809, 1992.
25. Muhia DK, Thomas CG, Ward SA, Edwards G, Mberu EK and Watkins WM, Ferriprotoporphyrin catalysed decomposition of artemether: Analytical and pharmacological implications. *Biochem Pharmacol* 48: 889–895, 1994.
26. Hong YL, Yang Y-Z and Meshnick SR, The interaction of artemisinin with malarial hemozoin. *Mol Biochem Parasitol* 63: 121–128, 1994.
27. Pandey AV, Tekwani BL, Singh RL and Chauhan VS, Artemisinin, an endoperoxide antimalarial, disrupts the hemoglobin catabolism and heme detoxification systems in malarial parasite. *J Biol Chem* 274: 19383–19388, 1999.
28. Ittarat W, Looareesuwan S, Pootrakul P, Sumpunsirikul P, Vuttanavibool P and Meshnick SR, Effects of α-thalassemia on pharmacokinetics of the antimalarial agent artesunate. *Antimicrob Agents Chemother* 42: 2332–2335, 1998.

ELSEVIER

Parasitology International 48 (2000) 275–280

www.elsevier.com/locate/parint

Gametocytocidal activity of pyronaridine and DNA topoisomerase II inhibitors against multidrug-resistant *Plasmodium falciparum* in vitro

Porntip Chavalitshewinkoon-Petmitr[a,*], Ganokwan Pongvilairat[a], Saranya Auparakkitanon[b], Prapon Wilairat[b]

[a]*Department of Protozoology, Faculty of Tropical Medicine, Mahidol University, Bangkok 10400, Thailand*
[b]*Department of Biochemistry, Faculty of Science, Mahidol University, Bangkok 10400, Thailand*

Received 12 November 1998; accepted 6 October 1999

Abstract

Gametocytocidal activities of pyronaridine and DNA topoisomerase II inhibitors against two isolates of multidrug-resistant *Plasmodium falciparum*, KT1 and KT3 were determined. After sorbitol treatment, pure gametocyte cultures of *Plasmodium falciparum* containing mostly young gametocytes (stage II and III) obtained on day 11 were exposed to the drugs for 48 h. The effect of the drugs on gametocyte development was assessed by counting gametocytes on day 15 of culture. Pyronaridine was the most effective gametocytocidal drug against *P. falciparum* isolates KT1 and KT3 with 50% inhibitory concentration of 6 and 20 nM, respectively. Moreover, the 50% inhibitory concentration of pyronaridine was lower than that of primaquine which is the only drug used to treat malaria patients harboring gametocytes. Prokaryotic (norfloxacin) and eukaryotic (amsacrine and etoposide) DNA topoisomerase II inhibitors were only effective against asexual but not sexual stages of the malaria parasites. Pyronaridine has both schizontocidal and gametocytocidal activities against the human malaria parasite, *P. falciparum*.

Keywords: Gametocytocidal activity; Pyronaridine; DNA topoisomerase II inhibitors; *Plasmodium falciparum*

*Corresponding author. Tel.: +66-2-246-9000; fax: +66-2-248-3189.
E-mail address: tmppm@mahidol.ac.th (P. Chavalitshewinkoon-Petmitr)

1383-5769/00/$ - see front matter
PII: S1383-5769(99)00028-8

1. Introduction

Malaria still remains one of the major health problems in tropical countries, and among the four species of malaria parasites infecting humans, *Plasmodium falciparum* is the most virulent. Chemotherapy has played a major role in alleviating suffering and in reducing mortality caused by *P. falciparum* infection. Unfortunately, resistance to most currently used antimalarials has appeared in *P. falciparum* and continues to increase in many parts of the world [1]. Most of the currently used antimalarial drugs affect only the asexual stage of the parasite, except primaquine which can also act as a gametocytocidal drug.

Pyronaridine, a 9-anilino-aza-acridine synthesized in the 1970s, has been developed primarily from Chinese research efforts and has been used in China for more than 15 years [2,3]. It is highly effective against chloroquine-sensitive and -resistant strains of *P. falciparum* [4,5] and good antimalarial activity has also been reported in Thailand [6]. Pyronaridine is a highly active blood schizontocide and has already undergone extensive trials in human against both *P. falciparum* and *P. vivax* [7,8]. Although an effect of pyronaridine on the ultrastructure of malaria parasite has been reported [9,10] and our previous study showed that decatenation activity of *P. falciparum* DNA topoisomerase II was inhibited by pyronaridine [11], the mechanism of action of pyronaridine is still not known.

Since inhibition of *P. falciparum* sexual stage should not be overlooked, and only one drug, primaquine, is currently used to combat *P. falciparum* gametocytes, a search for new gametocytocidal drugs is urgently needed. Therefore, in this study, in vitro gametocytocidal activities of pyronaridine and a number of DNA topoisomerase II inhibitors were determined against two isolates of gametocyte-producing *P. falciparum* from Thailand.

2. Materials and methods

2.1. Parasites

Gametocyte-producing isolates, KT1 and KT3, of *Plasmodium falciparum* were collected from two infected patients at Thong Pha Phum District, Kanchanaburi Province, Thailand. Multidrug resistant K1 strain originally taken from this province [12] was used as a control parasite for determination of drug resistance. KT1 and KT3 isolates were successfully cultured in our laboratory for at least 3 years and continuously produced gametocytes under our culture conditions [13,14]. Morphological and functional maturation of KT3 isolate have already been reported [13] and KT1 isolate behaved similarly.

2.2. Cultivation of Plasmodium falciparum

P. falciparum KT1 and KT3 isolates were cultured continuously in RPMI medium supplement with 15% human plasma using human erythrocytes (O,Rh+) previously treated with PIGPA (Pyruvate, Inosine, Glucose, Phosphate, Adenine) solution [13]. In gametocyte cultivation, 50 mg/l (final concentration) of hypoxanthine were also added. Culture dishes were placed in candle jars and incubated at 37°C. The culture medium was changed every 3 days.

2.3. Test of in vitro drug sensitivity against asexual stage of P. falciparum KT1 and KT3 isolates

Mefloquine, amsacrine, etoposide and primaquine were dissolved in dimethylsulfoxide (DMSO). The final concentration of DMSO did not exceed 0.1% (v/v). Chloroquine, cycloguanil and pyronaridine were dissolved in sterile distilled water. Pyrimethamine was dissolved in 0.5% lactic acid and the final concentration of lactic acid in culture was not allowed to exceed 0.0005%. Norfloxacin was diluted with 0.1 M HCl and the final concentration of HCl was less than 1 μM. The stock drug solutions were diluted to the desired concentrations with culture medium.

The activities of drugs against *P. falciparum* KT1 and KT3 were measured as 50% inhibitory concentration (IC_{50}) by incubating 1.5% erythrocyte suspension containing 0.5% initial parasitemia with drugs for 24 h at 37°C. [^{3}H]hypoxanthine (0.25 μCi, 6.2 Ci/mmol, Amersham, UK) was then added to each sample and parasite cultures were incubated for an additional 24 h. IC_{50}

values were recorded as the concentration of drug required to inhibit (by 50%) the incorporation of [^{3}H]hypoxanthine into parasite DNA, compared with untreated control.

2.4. Test of in vitro gametocytocidal effect

After synchronization of *P. falciparum* growth with sorbitol treatment [15], gametocyte culture was started with 1% initial parasitemia containing mostly ring forms in 2% erythrocyte suspension. The medium was changed on day 4, 6 and 8 of the culture. Pure gametocytes of *P. falciparum* KT1 and KT3 isolates were obtained by adding 2.5 volumes of 5% (w/v) sorbitol to packed erythrocytes for 5 min once a day, starting from day 9 until day 11 of culture. Approximately 450 μl aliquots of this suspension were transferred to a 24-well plate which contained 50 μl of drug in each well. After 24 h incubation, drug was again replaced and cultures were incubated for an additional 24 h. All wells then received complete medium without drug and cultivations were continued for 2 more days. Thin blood films were prepared on day 15 of cultivation and gametocytes were counted per 10000 erythrocytes. The effect of each drug concentration was investigated in triplicates. Gametocytocidal activity of drug was recorded as the concentration of drug that inhibited gametocytes by 50% as compared with untreated control.

3. Results

3.1. In vitro antimalarial drug sensitivity of the asexual stage of P. falciparum KT1 and KT3 isolates

Asexual parasites were cultured in the presence of five known antimalarials for 48 h and IC_{50}s of these drugs against *P. falciparum* KT1 and KT3 isolates were determined by measuring uptake of [^{3}H]hypoxanthine compared with K1 strain. Both *P. falciparum* isolates were resistant to chloroquine, pyrimethamine and cycloguanil, but were still sensitive to mefloquine compared with K1 strain (Table 1). The IC_{50}s of the drugs against KT1 isolates were not significantly different from those of KT3 except for that of cycloguanil in KT3 isolate which was approximately six times less than that in KT1 isolate. Primaquine was also able to inhibit asexual parasite growth only at a higher concentration than chloroquine and mefloquine.

Table 1
IC_{50} values of current antimalarials against asexual stages of *P. falciparum* KT1 and KT3 isolates as determined by [^{3}H]hypoxanthine uptake method compared with K1 strain

Drugs	IC_{50} (μM)		
	KT1 isolate	KT3 isolate	K1 strain*
Chloroquine	0.2	0.4	0.23
Mefloquine	0.03	0.01	0.02
Pyrimethamine	34.0	35.5	38.5
Cycloguanil	42.0	7.6	8.5
Primaquine	1.1	2.0	ND

*Chloroquine–pyrimethamine-resistant K1 strain [12]; ND = not determined.

3.2. In vitro activity of pyronaridine and DNA topoisomerase II inhibitors against the asexual stage of P. falciparum KT1 and KT3 isolates

IC_{50}s of pyronaridine and DNA topoisomerase II inhibitors, namely, amsacrine, etoposide and norfloxacin, were determined. All compounds could inhibit parasite growth in vitro and IC_{50}s were found to be between 0.002 and 43 μM (Table 2). Pyronaridine showed the highest activity against the asexual stage of both parasite isolates (IC_{50} = 2 nM). Among the DNA topoisomerase II inhibitors, eukaryotic DNA topoisomerase II inhibitors, amsacrine and etoposide, were more active against both *P. falciparum* isolates than norfloxacin, a prokaryotic DNA topoisomerase II (gyrase) inhibitor.

3.3. Pure gametocyte cultures of P. falciparum KT1 and KT3 isolates

Gametocytes of KT1 and KT3 isolates produced in cultivation could undergo a maturation process and stages I–V identified on the basis of morphology [13]. After sorbitol treatments on day 9, 10 and 11, there was 99% reduction in the

Table 2
IC_{50} values of pyronaridine and DNA topoisomerase II inhibitors against asexual stages of *P. falciparum* KT1 and KT3 isolates compared with K1 strain

Drugs	IC_{50} (μM)		
	KT1 isolate	KT3 isolate	K1 strain[a]
Pyronaridine	0.002	0.002	0.0027
Amsacrine	1.2	1.4	0.5
Etoposide	17.0	21.0	12.5
Norfloxacin	31.5	43.0	ND

[a]Chloroquine-pyrimethamine-resistant K1 strain [12]; ND = not determined.

Table 3
IC_{50} values of pyronaridine, DNA topoisomerase II inhibitors and primaquine against gametocytes of *P. falciparum* KT1 and KT3 isolates

Drugs	IC_{50} (μM)	
	KT1 isolate	KT3 isolate
Pyronaridine	0.006	0.02
Amsacrine	8.0	10.8
Etoposide	97.0	95.0
Norfloxacin	> 100	> 100
Primaquine	0.8	2.1

number of asexual parasites. Pure gametocyte cultures of *P. falciparum* KT1 and KT3 isolates were obtained on day 11 with an average number of gametocytes of 305 and 392 per 10 000 erythrocytes, respectively. These gametocytes consisted of 19% stage II, 60% stage III and 21% stage IV and were used in the drug treatment studies.

3.4. *In vitro gametocytocidal effects of pyronaridine and DNA topoisomerase II inhibitors against P. falciparum KT1 and KT3 isolates*

Gametocytes of *P. falciparum* KT1 and KT3 isolates could be inhibited by pyronaridine and eukaryotic DNA topoisomerase II inhibitors (amsacrine and etoposide) whereas norfloxacin did not have any effect on gametocytes even when the concentration was raised to 100 μM (Table 3). Pyronaridine was the most potent inhibitor against gametocytes in cultures (IC_{50} of 6 and 20 nM against KT1 and KT3, respectively), being approximately 3×10^3–3×10^4 times more effective than amsacrine and etoposide. Moreover, IC_{50} of pyronaridine was lower than IC_{50} of primaquine.

4. Discussion

Gametocyte-producing *P. falciparum* KT1 and KT3 isolates used in this study can be looked upon as multidrug-resistant parasites because of their resistance to chloroquine, pyrimethamine and cycloguanil. Both isolates were still sensitive to mefloquine.

The study of topoisomerases has expanded into the realm of pharmacology and clinical medicine through identification of bacterial topoisomerase II (DNA gyrase) as a target of antibitotics and toxins and of eukaryotic DNA topoisomerase II as a target of a large number of anticancer agents [16]. In vitro activities of pyronaridine and DNA topoisomerase II inhibitors against the asexual stage of recently acquired *P. falciparum* KT1 and KT3 isolates were investigated and the results showed that both prokaryotic and eukaryotic DNA topoisomerase II inhibitors could inhibit asexual parasite growth, similar to previous studies conducted on the established multidrug-resistant *P. falciparum* K1 strain [11]. Pyronaridine was the most potent inhibitor with IC_{50} values for both KT1 and KT3 isolates of 2 nM, not significantly different from that for *P. falciparum* K1 strain (IC_{50} = 2.7 nM) [11]. The present results indicate that chloroquine-, pyrimethamine- and cycloguanil-resistant *P. falciparum* showed no cross resistance to pyronaridine whereas pyronaridine-resistant *P. falciparum* exhibits cross resistance to chloroquine and piperaquine [17].

Divo et al. [18] have reported on the antimalarial activity of fluoroquinolones against asexual stage of chloroquine-sensitive and -resistant *P. falciparum*. Previous study showed that the decatenation activity of *P. falciparum* DNA topoisomerase II is inhibited by fluoroquinolones [19]. Growth inhibition of asexual stages of *P.*

falciparum KT1 and KT3 isolates by norfloxacin is consistent with these observations. Mitochondrial DNA topoisomerase II of *P. falciparum* may be a possible target for DNA gyrase inhibitors.

Gametocytocidal activity of pyronaridine was very much higher than that of the other DNA topoisomerase II inhibitors tested (amsacrine, etoposide and norfloxacin). Since the gametocytes used in this study were predominantly stage III, in which only RNA and protein synthesis occur, it is not surprising that known DNA topoisomerase II inhibitors showed very low gametocytocidal efficacy because their target plays a role in DNA synthesis which occurs only in stage I and II gametocytes.

Although we have shown that pyronaridine can inhibit *P. falciparum* DNA topoisomerase II in vitro, it now appears that DNA topoisomerase II is not the specific target of pyronaridine based on two lines of evidence. Firstly, pyronaridine strongly inhibited gametocyte growth in spite of the lack of DNA synthesis in this stage. Secondly, using an assay for detection of DNA cleavage, we have shown that pyronaridine was not able to inhibit asexual *P. falciparum* topoisomerase II in situ [20]. Pyronaridine has recently been demonstrated to inhibit malaria parasite heme polymerization as well [21].

This is the first report of the gametocytocidal effect of pyronaridine on *P. falciparum*. It is 100 times more effective than primaquine which is the only gametocytocidal antimalarial in clinical use. The dual role of pyronaridine as a schizontocidal and gametocytocidal drug should make it highly attractive for clinical application.

Acknowledgements

We are grateful to Ms Somsri Kajorndechakait and Mr Saiyud Incheng for technical assistance. This work was supported by a grant (RSA/3/2538) from The Thailand Research Fund. P.W. is a Senior Research Scholar of The Thailand Research Fund.

References

[1] World Health Organization. World malaria situation in 1994. WHO Weekly Epidemiol Rec 1997;36:269–276.
[2] Zheng XY, Xia Y, Gao FH, Chen C. Synthesis of 7351, a new antimalarial drug. Acta Pharm Sin 1979;14:736–7.
[3] Zheng XY, Chen C, Gao FH, Zhu PE, Guo HZ. Synthesis of new antimalarial drug pyronaridine and its analogues. Acta Pharm Sin 1982;17:118–25.
[4] Fu S, Bjorkman A, Wahlin B, Ofori-Adjei D, Ericsson O, Sjoqvist F. In vitro activity of chloroquine, the two enantiomers of chloroquine, desethylchloroquine and pyronaridine against *Plasmodium falciparum*. Br J Clin Pharmacol 1986;22:92–6.
[5] Che LG, Huang KG, Yang HL. Determination of susceptibility of chloroquine-resistant *Plasmodium falciparum* to pyronaridine. J Parasitol Parasit Dis 1984;2:280.
[6] Childs GE, Hausler B, Milhous W et al. In vitro activity of pyronaridine against field isolates and reference clones of *Plasmodium falciparum*. Am J Trop Med Hyg 1988;38:24–9.
[7] Chang C, Tang LH, Jantanavivat C. Studies on a new antimalarial compound: pyronaridine. Trans R Soc Trop Med Hyg 1992;86:7–10.
[8] Fu S, Xiao SH. Pyronaridine: a new antimalarial drug. Parasitol Today 1991;7:310–3.
[9] Wu LJ. Ultrastructural study on the effect of pyronaridine on erythrocytic stages of chloroquine-resistant strain of *Plasmodium berghei*. Chin J Parasitol Parasit Dis 1986;4:263–6.
[10] Wu LJ, Rabbege JR, Nagasawa H, Jacobs G, Aikawa M. Morphological effects of pyronaridine on malaria parasites. Am J Trop Med Hyg 1988;38:30–6.
[11] Chavalitshewinkoon P, Wilairat P, Gamage S, Denny W, Figgitt D, Ralph R. Structure–activity relationships and modes of action of 9-anilinoacridines against chloroquine-resistant *Plasmodium falciparum* in vitro. Antimicrob Agents Chemother 1993;37:403–6.
[12] Thaithong S, Beale GH, Chutmongkonkul M. Susceptibility of *Plasmodium falciparum* to five drugs: an in vitro study of isolates mainly from Thailand. Trans R Soc Trop Med Hyg 1983;77:228–31.
[13] Petmitr P, Pongvilairat G, Wilairat P. Development of cultivation technique for pure *Plasmodium falciparum* gametocytes. Southeast Asian J Trop Med Public Health 1995;26:606–10.
[14] Petmitr P, Pongvilairat G, Wilairat P. Large scale culture technique for pure *Plasmodium falciparum* gametocytes. Southeast Asian J Trop Med Public Health 1997;28:18–21.
[15] Lambros C, Vanderberg JP. Synchronization of *Plasmodium falciparum* erythrocytic stage in cultures. J Parasitol 1979;65:418–20.
[16] Wang JC. DNA topoisomerases. Annu Rev Biochem 1996;65:635–92.

[17] Yung HL, Yang PF, Liu DO et al. Sensitivity in vitro of *Plasmodium falciparum* to chloroquine, pyronaridine, artesunate and piperaquine in South Yunnan. Chung Kua Chi Shang Chung Hsueh Yu Chi Sheng Chung Ping Tsa Chih 1992;10:189–200.

[18] Divo AA, Sartorelli AC, Patton CL, Bia FJ. Activity of fluoroquinolone antibiotics against *Plasmodium falciparum* in vitro. Antimicrob Agents Chemother 1988; 32:1182–6.

[19] Chavalitshewinkoon P, Leelaphiwat S, Wilairat P. Partial purification and characterization of DNA topoisomerase II from *Plasmodium falciparum*. Southeast Asian J Trop Med Public Health 1994;25:32–6.

[20] Auparakkitanon S, Wilairat P. Cleavage of DNA induced by 9-anilinoacridine inhibitors of topoisomerase II in malaria parasite, *Plasmodium falciparum*. 8th FAOBMB Congress, November 22–26, abstract C1. Kuala Lumpur, Malaysia, 1998.

[21] Dorn A, Vippagunta SR, Matile H, Jaquet C, Vennerstrom JL, Ridley RG. An assessment of drug–haematin binding as a mechanism for inhibition of haematin polymerization by quinoline antimalarials. Biochem Pharmacol 1998;55:727–36.

MUTATION IN BRIEF

A Novel Splice-Acceptor Site Mutation (IVS13-2A>T) of Polycystic Kidney Disease 1 (*PKD1*) Gene Resulting in an RNA Processing Defect with a 74-Nucleotide Deletion in Exon 14 of the mRNA Transcript

Wanna Thongnoppakhun,[1,2] Nanyawan Rungroj,[1] Prapon Wilairat,[2] Kriengsak Vareesangthip,[3] Chintana Sirinavin,[1,4] and Pa-thai Yenchitsomanus[1,5,*]

[1]Molecular Genetics Unit, Office for Research and Development, Faculty of Medicine-Siriraj Hospital; [2]Department of Biochemistry, Faculty of Science; [3]Renal Unit, Department of Medicine, Faculty of Medicine-Siriraj Hospital; [4]Division of Medical Genetics, Department of Medicine, Faculty of Medicine-Siriraj Hospital; [5]Medical Molecular Biology Unit, Office for Research and Development, Faculty of Medicine-Siriraj Hospital, Mahidol University, Bangkok, Thailand

*Correspondence to Pa-thai Yenchitsomanus, Molecular Genetics Unit, Office for Research and Development, Faculty of Medicine-Siriraj Hospital, Mahidol University, 2 Prannok Road, Bangkok 10700, Thailand. Tel and Fax: +1 662 4184793; E-mail: grpye@mahidol.ac.th

Communicated by Mark H. Paalman

Autosomal dominant polycystic kidney disease (ADPKD) occurs mainly from mutations of polycystic kidney disease 1 (*PKD1*) gene. A novel mutation of the *PKD1* gene due to a nucleotide substitution in splice-acceptor site of IVS13 (AG->TG) was identified by analyses of *PKD1*-cDNA and genomic DNA. The IVS13-2A>T substitution resulted in an inactivation of this splice site and utilization of cryptic splice acceptor site in exon 14, causing a 74-nucleotide deletion of this exon in the *PKD1*-mRNA transcript. The abnormal transcript was present ectopically in the patients' lymphocytes. The partial deletion of *PKD1*-mRNA leads to frameshift translation and introduces a termination signal at codon 1075. The truncated protein with about one quarter of the full-length polycystin-1 is most likely inactive. Thus, the effect of this mutation would be 'loss-of-function' type. Allele specific amplification (ASA) was developed to detect the mutation in DNA samples of other family members. The mutation was present in 11 affected but absent in 13 unaffected family members, corresponding to the results of linkage analysis. In addition, it was not observed in DNA samples of 57 unrelated healthy individuals. © 1999 Wiley-Liss, Inc.

KEY WORDS: Polycystic kidney disease 1; PKD1; long RT-PCR; cryptic splice-site; splicing defect; allele specific amplification; ASA; Thailand

Received 29 July 1999; Revised manuscript accepted 19 October 1999.

INTRODUCTION

Autosomal dominant polycystic kidney disease (ADPKD; MIM# 173900) is one of the most common human inherited disorders worldwide, characterized by the development of multiple abnormal fluid-filled cysts in the kidneys, leading to end stage renal failure (Dalgaard, 1957). At least three genes are responsible for this disease: *PKD1* (MIM# 601313; approved symbol, PKD1) at 16p13.3 (The European Polycystic Kidney Disease Consortium, 1994; Hughes et al., 1995; The International Polycystic Kidney Disease Consortium, 1995), *PKD2* at 4q21-23 (Mochizuki et al., 1996), and the still unmapped, *PKD3* (Daoust et al.,1995). Abnormality of *PKD1* is responsible for about 85% of ADPKD (Peters and Sandkuijl, 1992). *PKD1* has the size of about 54 kb consisting of 46 exons and transcribing 14,148-nt mRNA (The European Polycystic Kidney Disease Consortium, 1994; Burn et al., 1995; Hughes et al., 1995; The International Polycystic Kidney Disease Consortium, 1995).

The existence of at least three *PKD1* homologs which share over 95% identity with *PKD1* on the same chromosome, has made it difficult to characterize *PKD1* mutations (The European Polycystic Kidney Disease Consortium, 1994). This has also resulted in bias of mutation analysis of *PKD1* in which the majority of mutations identified to date fall within its 3' unique region (HGMD; Human Gene Mutation Database: http://www.uwcm.ac.uk/uwcm/mg/search/120293.html). However, the mutations found in this region contribute to only 10-15% of all known cases of PKD1 disease, indicating that most mutations are located in the reiterated region of *PKD1* (Peral et al., 1996). Recently, at least two groups have attempted to identify mutations in the reiterated part of *PKD1* by long-range PCR (LR-PCR) (Watnick et al., 1997; Peral et al., 1997). However, the methods that have been developed could isolate parts of the reiterated sequence of *PKD1*, unable to isolate the sequence beyond exon 15 to the 5' end of the gene. We have recently developed a long RT-PCR method for isolation of the entire coding sequence of *PKD1* from its mRNA transcript (Thongnoppakhun et al., 1999), eliminating the interference from the homologous sequences. In this report, we demonstrate the application of long RT-PCR and LR-PCR methods in identification of *PKD1* mutation in PKD1 patients and report a novel mutation which results in RNA processing defect leading to partial deletion of exon 14 sequence in the *PKD1*-mRNA transcript.

MATERIALS AND METHODS

The PK015 family and linkage study

The proband (IV-6) of the Thai family PK015 (Fig. 2) was firstly referred to see nephrologist with the problems of a mild degree of chronic renal failure (serum creatinine of 4.2 mg/dl), hypertension and gross hematuria. An abdominal ultrasound demonstrated polycystic kidneys and liver. The diagnosis of ADPKD in the patient and other family members was made, based on the demonstration of renal cysts by an abdominal ultrasound (Ravine et al., 1994). Blood samples from the patients and relatives were collected with informed consent. Linkage analysis was performed by detecting 5 polymorphic DNA markers on chromosome 16p including D16S85 (3' HVR) (Reeders et al., 1985), SM7 (Harris et al., 1991), 16AC2.5 (Thompson et al., 1992), SM6 (Peral et al., 1994), and KG8 (Germino et al., 1993).

RNA preparation, long RT-PCR, and nested PCR

The full-length *PKD1*-cDNA was synthesized from RNAs prepared from lymphocytes and then amplified by long PCR, following the protocols as previously described (Thongnoppakhun et al., 1999). The length of PCR product obtained was 13,634 bp. Nested PCRs were carried out by using nested primers (sequences available on request) to generate 9 overlapping fragments of 1,352-1,678 bp by the method as previously described (Thongnoppakhun et al., 1999). A fragment of amplified cDNA (nt 3115-4689) in the region of exons 12-15 (GenBank Accession No. L33243) was digested with either *Bsp1286* I, *Hinf* I, *Pst* I, or *Taq* I (New England Biolabs and Promega) for detailed analysis of deletion observed. Amplification with additional pair of primers covering nt 3254-3538 in exons 13-15 was also performed.

Direct DNA sequencing

PCR products were purified from agarose gel after electrophoresis by QIAquick™ Gel Extraction Kit (Qiagen Gmbh, Hilden, Germany) as instructed by the manufacturer. The purified DNAs were sequenced manually by using fmol® DNA Sequencing System (Promega).

Amplification of genomic DNA

To isolate *PKD1*-specific DNA fragment out of the homologous sequences, a LR-PCR for amplification of genomic DNA (18,099 bp) was carried out by using a primer specific to the unique sequence (Ex34B at nt 44438-44409 in exon 34) coupled with a primer annealing to a region in the reiterated sequence (SI3.1F at nt 26340-26369 in exon 13), and then nested PCRs were performed by using internal pairs of primers. The primers were designed from sequence of *PKD1* gene (GenBank Accession No. L39891). The PCR reaction for a long-range amplification in a total volume of 50 µl contained 200 ng genomic DNA, 200 nM of each primer, 200 µM dNTP mixture, 1 unit ELONGASE Enzyme mix, 10% DMSO, and 1.0 mM MgSO4. The PCR conditions consisted of an initial incubation (hot start) at 95°C for 1 min 30 s, then amplification for 40 cycles at 94°C for 30 s, 61°C for 30 s, 68°C for 20 min, and a final incubation at 70°C for 10 min. The LR-PCR product was diluted up to 1,000 folds depending on its amounts to reduce contamination from genomic DNA and used as template for nested PCRs of the 1,064- and 320-bp products with the primers WT2F/SI3.1B and SI3.2F/SI3.2B, covering the regions of nt 26375-27438 (exon 13-15) and 26717-27036 (IVS 13-14), respectively. Sequences of the nested PCR primers are available on requested. Contamination of homologous sequences has been proven negligible in another similar experiment by the failure to amplify DNA regions outside a LR-PCR product of 12.9 kb, when this product was diluted 1,000 folds and used as template for nested PCRs (data not shown).

Mutation analysis by allele specific amplification (ASA)

Allele specific amplification (ASA), PCR for amplifications of wild-type and mutant alleles with allele-specific primers coupled with a shared primer (Newton et al., 1989), was invented for analysis of the *PKD1* mutation discovered. The wild-type and mutant primers had one different base at their 3' ends, each of which matched to the complementary base at the mutation site in the corresponding allele. Two additional mismatches were also introduced at the third and the ninth nucleotides from the 3'-end of primers to increase discriminating power when they bound across the alleles (Kwok et al., 1990). The sequences of wild-type (13WT) and mutant primers (13MU) are: TTCACTCACTGCGTCCCACCACCCCGACA and TTCACTCACTGCGTCCCACCACCCCGTCT (underlined are nucleotides altered to introduce mismatches), respectively. The sequence of shared primer (SI3.2B) is: GTTGGGGAGGAAGGGGGGCAGCTTGAC.

Each DNA sample was amplified in two separate reactions with a pair of primers for wild-type or mutant allele. A pair of primers (SI7.2F/SI7.2B) amplifying a region of 698-bp in exon 25/intron 26 (nt 38978-39675) of the *PKD1* gene were also added for internal control amplification in both reactions.

RESULTS

Long RT-PCR and nested PCRs of samples from PKD1 patients

A long RT-PCR method (Thongnoppakhun et al., 1999) was performed to study RNA samples prepared from two patients (IV-3 and IV-4) of PK015 family. The full-length *PKD1* cDNA was fractionated into 9 overlapping fragments by nested PCRs. The presence of products with two different sizes (normal 1,575 bp and a shorter fragment of about 1,500 bp) were observed in both patients' samples, using a primer pair amplifying the region between nt 3115 and 4689 (Fig. 1A and 1B). The shorter fragment might have resulted from a partial deletion in the mRNA transcript from the affected allele of *PKD1* in these patients. Restriction endonuclease mapping analyses of the nested PCR product from one patient (IV-3) in comparison with that of a normal individual, by using *Bsp1286* I, *Hinf* I, *Pst* I and *Taq* I, were carried out to localize the area of deletion, which was found to locate between the first sites of *Hinf* I and *Bsp1286* I (nt 3347-3477). A new set of primer pair covering the region of nt 3254-3538 were designed to amplify this region by nested PCR, generating an amplified product of 285 bp in normal samples (Fig. 1A). The samples from the two patients produced both the normal (285 bp) and a shorter (~210 bp) PCR products, as well as a slower migrating band of heteroduplex DNA (Fig. 1C). This data confirmed that there was indeed a deletion in this region of *PKD1* cDNA of both patients. Direct DNA sequencing of the smaller PCR product (~210

bp) from a patient revealed the 74-bp deletion corresponding to nt 3373-3446 in *PKD1* mRNA, the nucleotide positions 1-74 of exon 14 of *PKD1*.

Analysis of genomic DNA

The deletion of 74 nucleotides of exon 14 of the patients *PKD1* mRNA might result from deletion in this region of the gene or from point mutation located near the exon-intron junction producing an abnormally spliced RNA product. A LR-PCR for amplification of *PKD1*-specific sequence, about 18 kb, from genomic DNA was developed to eliminate contamination from sequences of the homologous genes. A pair of nested PCR primers (WT2F and SI3.1B positioned in exons 13 and 15, respectively) amplifying a region covering exon 14 and both flanking introns (1,064 bp) were also used for DNA deletion study in exon 14. The results of DNA analysis in four patients of PK015 family (IV-3, IV-4, IV-11, and V-9) indicated that there was no observable DNA deletion, particularly in the region of exon 14 of *PKD1*.

To identify mutation in exon 14 of *PKD1* precisely, a DNA segment of 320 bp was amplified by using nested PCR primer pair (SI3.2F/SI3.2B) and analysed by DNA sequencing. The result demonstrated a heterozygous A->T substitution at the position 26806 (with respect to the sequence of GenBank Accession No. L39891), which is the first position of the invariable dinucleotides (AG) of the splice acceptor site of intron 13, in *PKD1* of a patient studied. The substitution was confirmed by sequencing of the opposite strand, and it was present in altogether 6 patients examined, most likely to be the PKD1 causative mutation in this family.

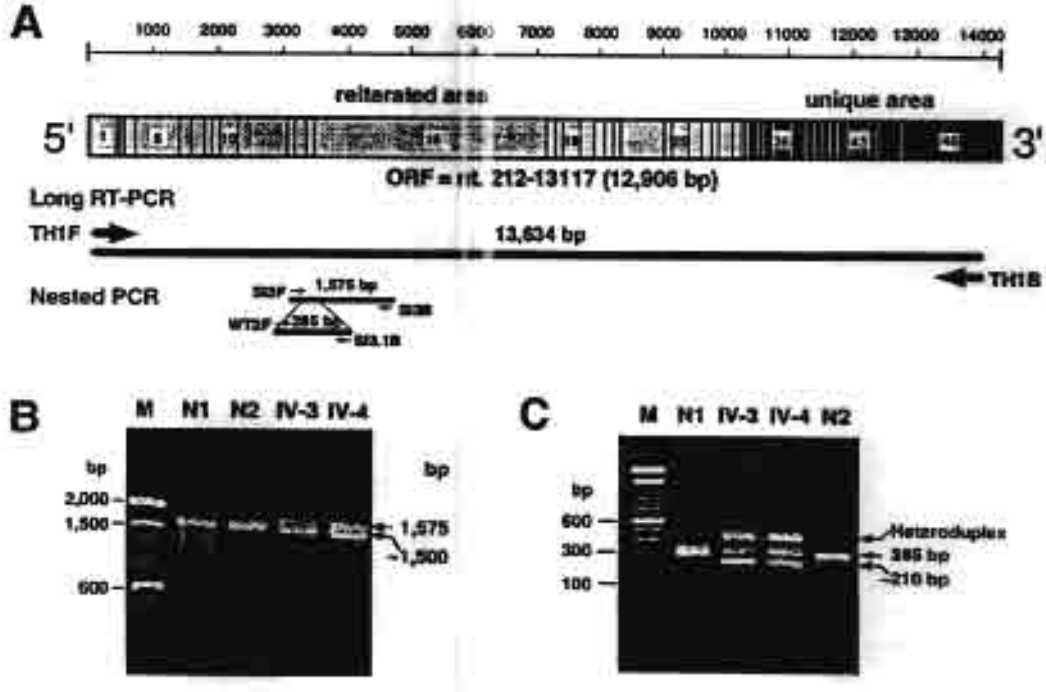

Figure 1 A: Diagrammatic representation of the full-length *PKD1* mRNA (upper), a long RT-PCR product (middle), and nested PCR products (lower). The reiterated region in the *PKD1* mRNA (between exons 1 and 32) is represented by the hatched area and the unique region (between exons 33 and 46) by the blackened area. The relative locations of the primers (TH1F/TH1B, SI3F/SI3B and WT2F/SI3.1B; solid arrows) used for amplifying a long RT-PCR product (long solid horizontal line) and the nested PCR products (short solid horizontal lines) are illustrated. A pair of PCR primers (WT2F/SI3.1B) were made for amplification of 285 bp in the region covering the deleted area (lowest) to confirm the prediction and for further analysis by DNA sequencing. B: Nested PCR products amplified from long *PKD1*-cDNA samples with the SI3F/SI3B primers from two normal individuals (N1 and N2) and from two PKD1 patients (IV-3 and IV-4) of PK015 family. The normal samples showed one fragment of nested PCR product (1,575 bp) whereas the patients' samples demonstrated two fragments (1,575 and ~1,500 bp). Lane M is 100-bp DNA ladder. C: The nested PCR products amplified with the WT2F/SI3.1B primers in the deleted region from the long *PKD1*-cDNA samples of two normal individuals (N1 and N2) and the two patients (IV-3 and IV-4) of the PK015 family. While the normal

samples had only one fragment of 285 bp, the patients' samples contained two fragments of 285 and ~210 bp, as well as a heteroduplex DNA band. Lane M is 100-bp DNA ladder.

Mutation analysis by allele specific amplification (ASA)

Since the mutation observed in PK015 family did not create or abolish the sites of all known restriction endonucleases, the ASA method was employed to detect the mutation in all available members of this family. The genomic DNA sample from each individual was amplified in two separate reactions, with either a pair of wild-type (13WT/SI3.2B) or mutant (13MU/SI3.2B) primers, together with internal control (SI7.2F/SI7.2B) primers in both reactions. Normal and patient DNA samples consistently produced the internal control PCR product of 698 bp. DNA samples from normal individuals produced PCR products with the size of 259 bp only in the reaction containing the wild-type primer pair, whereas those from affected individuals generated PCR products with the size of 259 bp in both reactions.

Analysis by ASA of 24 members of PK015 family revealed 11 individuals with the *PKD1* mutation and 13 individuals without (Fig. 2). The same results were obtained when the LR-PCR products or the genomic DNA samples were used for the ASA analysis, indicating that the homologous sequences normally did not interfere with the reaction. The mutation linked (Fig. 2) and segregated with haplotype A or its variant (A*) defined by the 5 polymorphic DNA markers. By ASA analysis, the mutation could not be detected in DNA samples obtained from 57 unrelated and healthy subjects.

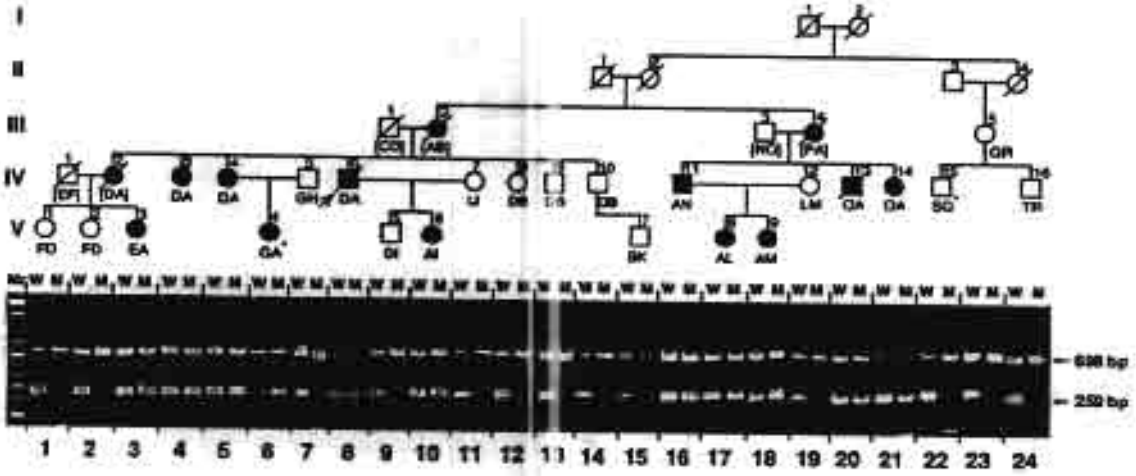

Figure 2 Detection of IVS13-2A>T mutation in *PKD1* by allele specific amplification (ASA) analysis in genomic DNA samples from members of PK015 family. Pedigree of the family is shown and haplotyes (A to T) in *PKD1* region of chromosome 16p13.3 as determined by using 5 polymorphic DNA markers are indicated under the symbols. Filled and blank symbols represent affected and unaffected members, respectively. DNA sample of each member was analyzed both for wild-type (W) allele with 13WT/SI3.2B primers and for mutant (M) allele with 13MU/SI3.2B primers, producing the same PCR-product size of 259 bp. A pair of internal control primers (SI7.2F/SI7.2B) were also added into both reactions, generating the PCR-product size of 698 bp. DNA samples of normal members (nos. 1, 2, 7, 9, 11, 12, 13, 14, 15, 19, 22, 23, and 24) showed only the product of the wild-type allele (259 bp) but those of affected members (nos. 3, 4, 5, 6, 8, 10, 16, 17, 18, 20, and 21) gave the products of both wild-type and mutant alleles, which had the same size (259 bp). Lane Mr is 100-bp DNA ladder. The mutant allele linked and segregated with the designated haplotype A (7.2 kb for 3' HVR, 123 bp for KG8, 121 bp for SM6, 169 bp for 16 AC2.5, and 98 bp for SM7) or its variant, A* (4.0 kb for 3' HVR, 123 bp for KG8, 121 bp for SM6, 169 bp for 16 AC2.5, and 98 bp for SM7) with a possible deletion in the 3' HVR region.

DISCUSSION

We have developed a long RT-PCR method for isolation of the entire *PKD1* coding sequence from its mRNA transcript (Thongnoppakhun et al., 1999) and applied it to study mutation of *PKD1* in patients with ADPKD. A 74-bp deletion of exon 14 in a cDNA fragment amplified from the full-length *PKD1*-cDNA (~13.6 kb) was observed in two PKD1 patients from the same PK015 family. Subsequent sequencing analysis of genomic DNA surrounding

exon 14 region of *PKD1* obtained by LR-PCR and nested PCR procedures revealed that a nucleotide transversion (A->T) had occurred at the position 26806 of *PKD1*. The nucleotide 'A' at this position is the first one in the invariable AG dinucleotide of the splice acceptor site in intron 13. Therefore, this IVS13-2A>T mutation was likely to result in the 74-nt deletion in exon 14 which is brought about by the inactivation of the normal splice acceptor site and utilization of a cryptic splice acceptor site at the nearby AG dinucleotide, located at position 73-74 in exon 14 of the *PKD1* mRNA (Fig. 3A).

When the 3' splice acceptor site is mutated, the effect may be either exon skipping or cryptic splice site utilization. This depends on the presence or absence of the next available legitimate or the next best, albeit illegitimate, splice site in the immediate vicinity (Krawczak et al., 1992). The observed RNA processing defect indicates that the AG dinucleotide at the positions 26880-26881 in exon 14 of *PKD1* is an available cryptic splice acceptor site. In normal splice acceptor sites, a pyrimidine tract is always present preceding the AG dinucleotide (Reed and Maniatis, 1985). A pyrimidine-rich tract, with two purine (GG) substitutions, prior to the AG nucleotide was observed in the cryptic splice acceptor site in exon 14 of *PKD1* (TCCTTCCCGGTTCCAG). The finding that the band intensity of the short cDNA fragment derived from the abnormally spliced mRNA was not reduced compared with that derived from the normally spliced mRNA (Fig. 1B and 1C) indicates that this cryptic splice acceptor site is used as efficiently as the normal splice acceptor site in intron 13. Additionally, the absence of a shorter cDNA fragment lacking entire exon 14 in the same experimental result indicates that exon 14 skipping associated with the IVS13-2A>T mutation did not occur.

Since this abnormal *PKD1*-mRNA was ectopically transcribed in the patients' peripheral blood lymphocytes, it is also highly probably transcribed in the kidneys and in other organs and cells that express polycystin-1. The resulting protein would have a normal amino-acid sequence for the first 1,054 amino acids followed by an abnormal sequence of 20 amino acids introduced by a frameshift (after the nucleotide at position 3373 in codon 1054) before a new stop signal (UGA) at codon 1075 is reached (Fig. 3B). This truncated polycystin-1 lacks the major part of the extracellular domain, all the transmembrane domains, and the cytoplasmic C-terminal portion, which are critical for its predicted function as a signal mediator.

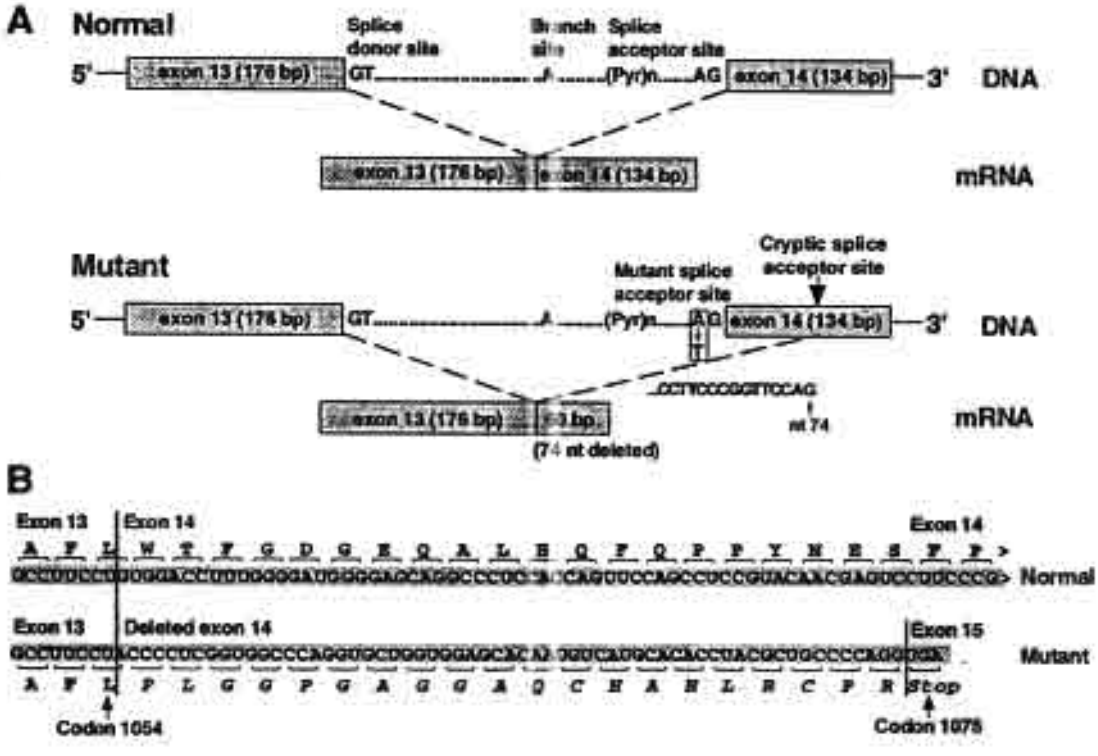

Figure 3 A: Diagram showing normal splicing of intron 13 (upper) and abnormal splicing at a cryptic splice acceptor site in exon 14 (lower) due to IVS13-2A>T mutation in the *PKD1* gene in the patients of PK015 family. The cryptic splice acceptor site has

the sequence of 'CCTTCCCGGTTCCAG', homologous to the native splice acceptor site at the intron 13/exon 14 junction. The abnormal splicing resulted in 74-nt deletion of exon 14, leaving 60 nucleotides of this exon. **B:** Framshift in protein translation from the abnormal *PKD1* mRNA transcript with 74-nt deletion. Parts of protein translations from the normal (upper) and abnormal (lower) mRNA transcripts are compared. Frameshifting translation occurs after codon 1054 in the abnormal mRNA transcript, introducing 20 novel amino acids (italic letters), and prematurely terminates at codon 1075.

Using DNA sequencing, this mutation was found in altogether 6 affected individuals in this family . It was also detected by the ASA method in all 11 available affected members but not in 13 unaffected members. These results corresponded well with linkage analysis using 5 polymorphic DNA markers (Fig. 2). Moreover, the mutation could not be seen in 57 unrelated healthy individuals by using the ASA method. All these evidences support the notion that the *PKD1* mutation identified is the disease-causing gene in this family. The mutation affects *PKD1* by causing 'loss-of-function', which supports the 'two-hit' hypothesis (Qian et al., 1996; Brasier and Henske, 1997) which states that both germline and somatic mutations which would inactivate both alleles of *PKD1* are required.

Application of long RT-PCR and LR-PCR protocols for mutation analysis of *PKD1* in the PKD1 patients will facilitate mutation discoveries, especially in the reiterated region of the gene. Data on *PKD1* mutation spectrum will help us to gain a better understanding of polycystin-1 function, the molecular pathogenesis of PKD1, and phenotypic expression in PKD1 patients.

ACKNOWLEDGMENTS

We thank to Dr. Prida Malasit, Head, Medical Molecular Biology Unit, Office for Research and Development, Faculty of Medicine-Siriraj Hospital, Mahidol University, for allowing to use laboratory facilities; staff of Renal Unit, Department of Medicine, Faculty of Medicine-Siriraj Hospital for collection of patients' blood samples; and all the patients and laboratory personnel who donated the blood samples. This work was partly supported by a grant from the Faculty of Medicine-Siriraj Hospital. P.W. is also a senior research scholar of the Thailand Research Fund.

REFERENCES

Brasier JL, Henske EP (1997) Loss of the polycystic kidney disease (*PKD1*) region of chromosome 16p13 in renal cyst cells supports a loss-of-function model for cyst pathogenesis. J Clin Invest 99:194-199.

Burn TC, Connors TD, Dackowski WR, Petry LR, Van Raay TJ, Millholland JM, Venet M, Miller G, Hakim RM, Landes GM, Klinger KW, Qian F, Onuchic LF, Watnick T, Germino GG, Doggett NA (1995) Analysis of the genomic sequence for the autosomal dominant polycystic kidney disease (*PKD1*) gene predicts the presence of a leucine-rich repeat. Hum Mol Genet 4:575-582

Dalgaard OZ (1957) Bilateral polycystic disease of the kidneys: a follow-up of two hundred and eighty four patients and their families. Acta Med Scand 328:1-255.

Daoust MC, Reynolds DM, Bichet DG, Somlo S (1995) Evidence for a third genetic locus for autosomal dominant polycystic kidney disease. Genomics 25:733-736.

Germino GG, Somlo S, Weinstat-Saslow D, Reeders ST (1993) Positional cloning approach to the dominant polycystic kidney disease gene, *PKD1*. Kidney Int Suppl 39:S20-S25.

Harris PC, Thomas S, Ratcliffe PJ, Breuning MH, Coto E, Lopez LC (1991) Rapid genetic analysis of families with polycystic kidney disease 1 by means of a microsatellite marker. Lancet 338:1484-1487.

Hughes J, Ward CJ, Peral B, Aspinwall R, Clark K, Sanmillan JL, Gamble V, Harris PC (1995) The polycystic kidney disease 1 (*PKD1*) gene encodes a novel protein with multiple cell recognition domains. Nat Genet 10:151-160.

Krawczak M, Reiss J, Cooper DN (1992) The mutational spectrum of single base-pair substitutions in mRNA splice junctions of human genes: causes and consequences. Hum Genet 90:41-54.

Kwok S, Kellogg DE, McKinney N, Spasic D, Goda L, Levenson C, Sninsky JJ (1990) Effects of primer-template mismatches on the polymerase chain reaction: human immunodeficiency virus type I model studies. Nucleic Acids Res 18:999-1005.

Mochizuki T, Wu GQ, Hayashi T, Xenophontos SL, Veldhuisen B, Saris JJ, Reynolds DM, Cai YQ, Gabow PA, Pierides A, Kimberling WJ, Breuning MH, Deltas CC, Peters DJM, Somlo, S (1996) *PKD2*, a gene for polycystic kidney disease that encodes an integral membrane protein. Science 272:1339-1342.

Newton CR, Graham A, Heptinstall LE (1989) Analysis of any point mutation in DNA. The amplification refractory mutation system (ARMS). Nucleic Acids Res 17:2503-2516.

Peral B, Ward CJ, Sanmillan JL, Thomas S, Stallings RL, Moreno F, Harris PC (1994) Evidence of linkage disequilibrium in the spanish polycystic kidney disease I population. Am J Hum Genet 54:899-908.

Peral B, Sanmillan JL, Ong ACM, Gamble V, Ward CJ, Strong C, Harris PC (1996) Screening the 3' region of the polycystic kidney disease 1 (*PKD1*) gene reveals six novel mutations. Am J Hum Genet 58:86-96.

Peral B, Gamble V, Strong C, Ong ACM, Sloanestanley J, Zerres K, Winearls CG, Harris PC (1997) Identification of mutations in the duplicated region of the polycystic kidney disease 1 gene (*PKD1*) by a novel approach. Am J Hum Genet 60:1399-410.

Peters DJM, Sandkuijl LA (1992) Genetic heterogeneity of polycystic kidney disease in Europe. In: Breuning MH, Devoto M, Romeo G (eds) Contributions to nephrology 97: polycystic kidney disease. Basel, Karger, p 128-139.

Qian F, Watnick TJ, Onuchic LF, Germino GG (1996) The molecular basis of focal cyst formation in human autosomal dominant polycystic kidney disease type I. Cell 87:979-987.

Ravine D, Gibson RN, Walker RG, Sheffield LJ, Kincaid-Smith P, Danks DM (1994) Evaluation of ultrasonographic diagnostic criteria for autosomal dominant polycystic kidney disease 1. Lancet 343:824-827.

Reed R, Maniatis T (1985) Intron sequences involved in lariat formation during pre-mRNA splicing. Cell 41:95-105.

Reeders ST, Breuning MH, Davies KE, Nicholls RD, Jarman AP, Higgs DR, Pearson PL, Weatherall DJ (1985) A highly polymorphic DNA marker linked to adult polycystic kidney disease on chromosome 16. Nature 317:542-544.

The European Polycystic Kidney Disease Consortium (1994) The polycystic kidney disease 1 gene encodes a 14 kb transcript and lies within a duplicated region on chromosome 16. Cell 77:881-94.

The International Polycystic Kidney Disease Consortium (1995) Polycystic kidney disease: The complete structure of the *PKD1* gene and its protein. Cell 81:289-298.

Thompson AD, Shen Y, Holman K, Sutherland GR, Callen DF, Richards RI (1992) Isolation and characterisation of (AC)n microsatellite genetic markers from human chromosome 16. Genomics 13:402-408.

Thongnoppakhun W, Wilairat P, Vareesangthip K, Yenchitsomanus P (1999) Long RT-PCR amplification of the entire coding sequence of the polycystic kidney disease 1 (*PKD1*) gene. BioTechniques 26:126-132.

Watnick TJ, Piontek KB, Cordal TM, Weber H, Gandolph MA, Qian F, Lens XM, Neumann HPH, Germino GG (1997) An unusual pattern of mutation in the duplicated portion of *PKD1* is revealed by use of a novel strategy for mutation detection. Hum Mol Genet 6:1473-81.